AN ABSTRACT OF THE THESIS OF

Vichien Tangpanyapinit for the degree of Master of Science in Chemical Engineering presented on November 21, 1995. Title: Catalytic Effect of Recovery Boiler Fume Compounds on NH_3 Oxidation

Redacted for privacy

Abstract approved: _ _____

Kristiina Iisa

The catalytic effect of recovery boiler fume compounds on decomposition of NH_3, oxidation of NH_3 by NO, oxidation of NH_3 by O_2, and oxidation of NH_3 by both O_2 and NO was studied. The effects of two fume species (Na_2CO_3 and Na_2SO_4) were investigated in this study. Fume compounds (90-125 μm in diameter) were pretreated by presintering in a muffle furnace at 780 °C for 0.5 hour to reduce the effect of sintering during the experiments. The experiments were conducted in a fixed bed reactor in the temperature range 550-750 °C. The amount of fume compound used in each run was 0.38-3.0±0.1 g. The inlet concentration of NH_3 was 115-500 ppm for the NH_3 reaction. For the reaction NH_3+NO, the concentrations of NH_3 and NO were 150-400 ppm, and 250-1250 ppm, respectively. For the NH_3+O_2 reaction, 250 ppm and 500 ppm inlet concentrations of NH_3 with 1% O_2 were employed. For the NH_3+O_2+NO reaction, the concentrations of NH_3 and NO were equal at 250 ppm with 1% O_2. The total gas flow rate was 6.3-13.0 cm^3/s at 25 °C. The inlet and outlet concentrations of NH_3 and NO were analyzed by a Fourier Transform Infrared Spectrometer (FT-IR).

No significant reaction over Na_2SO_4 occurred at the conditions studied but Na_2CO_3 catalyzed the reactions at temperatures above 550 °C. The rate of NH_3 consumption was significantly higher when O_2 was present than in the absence of O_2. With 3.0±0.1 g Na_2CO_3, 13.0 cm^3/s gas flow rate at 25 °C, and 500 ppm NH_3, for the reaction NH_3 ,and NH_3+O_2 (with 1% O_2), the highest NH_3 conversion were 26% and almost 100%, respectively, at 750 °C. With the same amount of Na_2CO_3, the same gas flow rate, and 250 ppm NH_3, the highest NH_3 conversion was 30% for the reaction NH_3+NO (with 250 ppm NO), and almost 100% for both NH_3+O_2 (with 1% O_2) and NH_3+O_2+NO (with 250 ppm NO and 1% O_2) at 750 °C. In the NH_3+NO reaction, the rate of NH_3 disappearance was almost independent of NO concentration but the rate of NO disappearance depended highly on NH_3 concentration. The highest NO conversions for the reaction were 15-18% at 750 °C. The NO production from the reaction of NH_3+O_2 ranged from 28-38% inlet NH_3. For the reaction of NH_3+O_2+NO, the highest NO conversions of 12-17% were found at 650-700 °C. For the rate of NH_3 consumption, reaction orders of 0.53 with respect to NH_3 were obtained by differential reactor analysis for the reactions NH_3 and NH_3+NO with activation energies of 98±3 kJ/mol. By integral reactor analysis, the reactions of NH_3+O_2 and NH_3+O_2+NO were found to be first order reactions with respect to NH_3 with activation energies of 170±23 kJ/mol and 185±42 kJ/mol, respectively. The kinetics of NH_3 oxidation over Na_2CO_3 were used to estimate the importance of the reactions in recovery boilers. The prediction indicated that approximately 29% of NH_3 produced during black liquor pyrolysis was consumed by the reaction.

Catalytic Effect of Recovery Boiler Fume Compounds on NH_3 Oxidation

by

Vichien Tangpanyapinit

A THESIS

submitted to

Oregon State University

in partial fulfillment of
the requirement for the
degree of

Master of Science

Completed November 21, 1995
Commencement June 1996

Master of Science thesis of Vichien Tangpanyapinit presented on November 21, 1995

APPROVED:

Redacted for privacy

Major Professor, representing Chemical Engineering

Redacted for privacy

Chair of Department of Chemical Engineering

Redacted for privacy

Dean of Graduate School

I understand that my thesis will become part of the permanent collection of Oregon State University libraries. My signature below authorizes release of my thesis to any reader upon request.

Redacted for privacy

Vichien Tangpanyapinit, Author

ACKNOWLEDGMENTS

I would like to express my heartfelt gratefulness to the following people:

Dr. Kristiina Iisa, my advisor, who gave many helpful suggestions and comments for the study, without her support this work could never have been completed.

Dr. William James Frederick who provided useful suggestions and the knowledge of recovery boiler.

Dr. Gregory Rorrer who allowed me to use the BET equipment and Kravinet Lourvanij who instructed me during the measurements.

All the professors in Chemical Engineering department and Industrial engineering department who gave me the valuable knowledge during studying at Oregon State University.

My devoted family

All my dear friends here, particularly, Viboon Sricharoenchaikul.

This research is being sponsored by the US Department of Energy, ABB Combustion Engineering, Ahlestrom Recovery Inc., and Gotaverken Energy Systems.

TABLE OF CONTENTS

TABLE OF CONTENTS (Continued)

LIST OF FIGURES

LIST OF FIGURES (continued)

LIST OF FIGURES (continued)

LIST OF TABLES

LIST OF APPENDICES

LIST OF APPENDIX FIGURES

NOMENCLATURE

A_c = cross sectional area of reactor, cm^2

C_{NH3} = concentration of NH_3, mol/cm^3

$C_{NH3,ave}$ = average gas concentration of NH_3, mol/cm^3

$C_{NH3,cyd.}$ = the standard concentration of NH_3 in gas cylinder, ppm

$C_{NH3,o}$ = bulk gas concentration of NH_3, mol/cm^3

$C_{NH3,s}$ = concentration of NH_3 at the external surface area of particle, mol/cm^3

C_{NO} = bulk gas concentration of NO, mol/cm^3

$C_{NO,ave}$ = average gas concentration of NO, mol/cm^3

ΔC_{NH3} = absolute error of NH_3 concentration, ppm

$C'_{NH3,o}$ = inlet concentration of NH_3, ppm

C'_{NH3} = outlet concentration of NH_3, ppm

C_{wp} = Weisz-Prater criterion number

d_p = diameter of particle,cm

d_r = diameter of the reactor, cm

Dp = Droplet diameter (m)

D_V = Gas diffusivity (m^2/s)

$D_{NH3\text{-}He}$ = diffusion coefficient, cm^2/s

$D_{NH3\text{-}K}$ = Knudsen diffusion coefficient, cm^2/s

$D_{NH3\text{-}eff}$ = effective diffusion coefficient, cm^2/s

E = activation energy, kJ/mol

NOMENCLATURE (continued)

$F_{NH3,o}$ = NH_3 feed rate, mol/s

F_{NH3} = flow rate of NH_3, mol/s

h_r = the length of the reactor which has the uniform temperature, cm

k_c = mass transfer coefficient, cm/s

k_{empty} = rate constant of empty bed reaction, unit depend on reaction order

k' = reaction rate constant based on weigth of catalyst, unit depend on reaction order

$k'_{,obs}$ = observed reaction rate constant, cm^3/s

k'_{total} = observed reaction rate constant, $(cm^3)^n/mol^{(n-1)}g.s$

k" = reaction rate constant based on surface of catalyst, unit depend on reaction order

L = characteristic length of particle, cm

M_{NH3} = molecular weight of NH_3, g/mol

M_{He} = molecular weight of He, g/mol

n = reaction order

P = Total pressure, atm

R = particle radius, cm

ΔR_n = absolute error of gas flow rate caused by the rotameter used, cm^3/min

Re = Reynolds number

Re' = Reynolds number in packed bed

R = ideal gas constant = 82.05 cm^3.atm/(mol.K)

r_e= average pore radius, cm

NOMENCLATURE (continued)

$-r'_{NH3}$ = rate of disappearance of NH_3 based on mass of catalyst, mol/g.s

$-r'_{NH3,ave}$ = average rate of reaction of NH_3, mol/g

$-r'_{NH3,obs}$ = observed reaction rate of NH_3 , mol/gs

$-r'_{NO}$ = rate of disappearance of NO based on mass of catalyst, mol/g.s

$-r'_{NO,ave}$ = average rate of reaction of NO, mol/g

Sh = Sherwood number

Sh' = Sherwood number in packed bed

Sc = Schmidt number

S_{Na2CO3} = total surface area of Na_2CO_3, cm^2

s_D = surface area of BL droplet, cm^2/droplet

T = temperature, K

t_{ave} = average residence time in the reaction zone, s

U = superficial velocity of gas flow in packed bed, cm/s

V = volume through the reactor, cm^3

V_F = total volume of flue gas, cm^3/s

V_o = total volumetric gas flow rate, cm^3/s

V_{zone} = volume of gas phase reaction zone, cm^3

v_D = volume of BL droplet cm^3/droplet

W = weight of catalyst, g

w_{Na2CO3} = weight per droplet of Na_2CO_3, g/droplet

NOMENCLATURE (continued)

X_{NH3} = NH_3 conversion

X_{NO} = NO conversion

Z = distance through reactor, cm

Greek symbols

ε_a = total void fraction in packed bed

ε_b = macro void fraction of packed bed

ε_{NH3} = the energy of molecular interaction for NH_3 or Lennard-Jones energy, J

ε_{He} = the energy of molecular interaction for He or Lennard-Jones energy, J

$\varepsilon_{NH3\text{-}He}$ = the energy of molecular interaction for NH_3-He or Lennard-Jones energy, J

σ_{NH3} = collision diameter or Lennard-Jones length, Å

σ_{He} = collision diameter or Lennard-Jones length, Å

$\sigma_{NH3\text{-}He}$ = collision diameter or Lennard-Jones length, Å

κ = Boltzmann constant = $1.38*10^{-23}$ J/K

ρ_b = bulk density of packed bed, g/cm^3

ρ_p = density of the particle, g/cm^3

ρ_{Na2CO3} = density of molten Na_2CO_3, g/cm^3

ρ_{He} = bulk density of gas, g/cm^3

Ω_D = collision integral*

τ_m = average for the tortuosity of pores of variety of size

NOMENCLATURE (continued)

γ = shape factor

μ_{He} = viscosity of gas, g/cms

Catalytic Effect of Recovery Boiler Fume Compounds on NH_3 Oxidation

CHAPTER 1
INTRODUCTION

1.1 Kraft Pulping and Recovery Process

Kraft pulping is a semimechanical process which yields a higher quality pulp than that made by mechanical or thermomechanical processes. This process is commonly referred to as the sulfate process because sodium sulfate is used as a make-up chemical for the cooking liquor. Most of the pulping processes consume large quantities of chemicals and energy in production so it is necessary to have a chemical and fuel recovery unit included in the production process. The recovery unit also reduces the amount of pollutants generated in the system. The process diagram of kraft pulping and recovery is shown in Figure 1.1.

First, wood chips are mixed with white liquor, which contains the major inorganic chemicals NaOH and Na_2S, which are the active pulping reagents. This is the so called pulping process. Next in the washing process, pulp (cellulose fibers) is excluded from the spent pulping liquor. The remaining liquor, known as weak black liquor (with 12-15% solids content, Adams and Frederick, 1988) consists of dissolved wood, and spent pulping chemicals. The solid content in weak black liquor is increased by evaporation in multiple effect evaporators. The product from this process is called

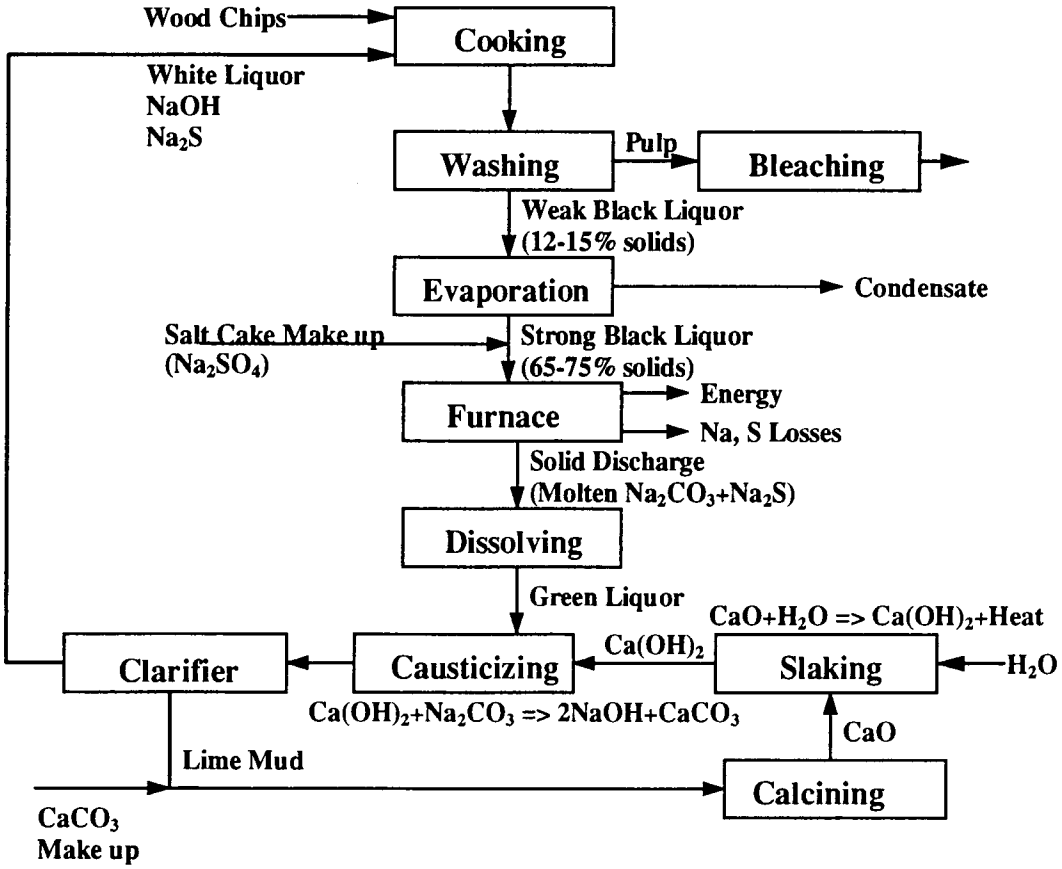

Figure 1.1 The process diagram of kraft pulping and recovery (Austin, 1984)

Table 1.1 Sample analysis of kraft black liquor solids (concentrator product) (Adams and Frederick, 1988)

Element		**wt.% Black Liquor Solids**
carbon	C	39.0%
hydrogen	H	3.8%
oxygen	O	33.0%
sodium	Na	18.6%
potassium	K	1.2%
sulfur	S	3.6%
chloride	Cl	0.6%
inerts	Si, Al, Fe, Ca, etc.	0.2%
Total solids	**BLS**	**65%**

strong black liquor (65-75% solids, Adams and Frederick, 1988). An analysis of a typical sample liquor solids is shown in Table 1.1. The strong black liquor is then mixed with make-up salt cake (Na_2SO_4) and recycle dust before being sprayed into a recovery boiler for combustion. The main functions of recovery boiler are to recover the inorganic cooking chemicals used in the pulping process and to generate energy as steam for the mill. Figure 1.2 shows the schematic diagram of a recovery boiler. The details of how black liquor is burnt in the recovery boiler will be given in the next section.

The products from recovery boiler are liquid smelt, and flue gas with solid particles (carryover and fume). The smelt consists of about two-thirds Na_2CO_3 and one-third Na_2S, with a small quantity of Na_2SO_4, other sodium/sulfur compounds, and unburned carbon. The smelt is removed from the recovery boiler and dissolved to form green liquor which is then treated with lime and causticized to be reused as white liquor. Solid particles which are separated from the flue gas by the economizer hopper and electrostatic precipitator, can be classified into two categories, fume and carryover. The chemical and physical properties, and the mechanism of formation of the two types of solid particles are different. Fume is in the form of sub-micron particles and consists of condensed volatile sodium and potassium compounds. Carryover whose particle size is distinctively larger than that of fume, consists of black liquor and char material. Since this paper focuses on reactions catalyzed by fume compounds, the mechanisms of fume formation in recovery boiler is covered briefly in the literature review chapter.

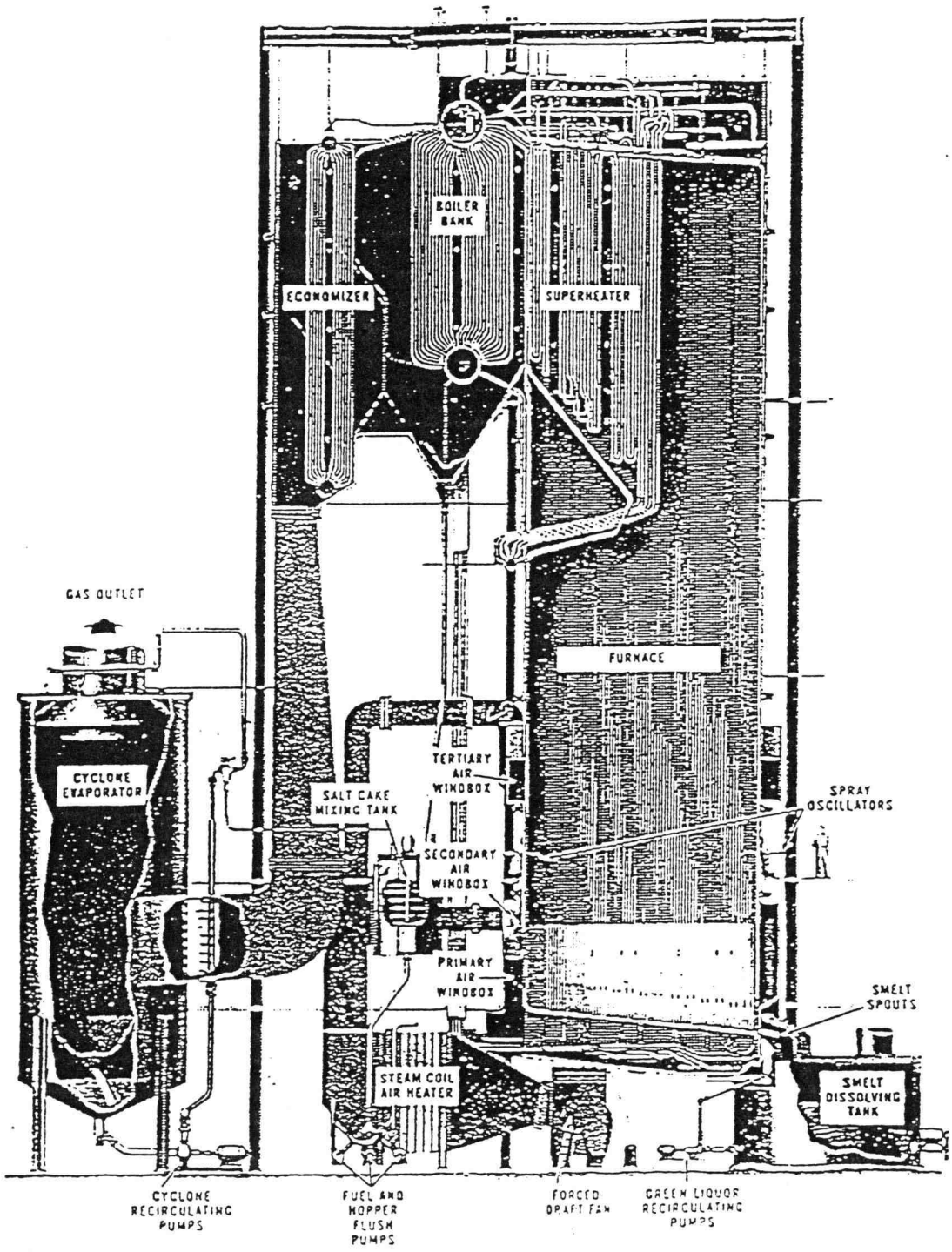

Figure 1.2 A schematic diagram of kraft recovery boiler (Adams Frederick, 1988)

1.2 Black Liquor Combustion in Recovery Boilers

In the recovery boiler, black liquor droplet combustion process generally follows four sequential stages : drying, devolatilization, char burning, and smelt coalescence. A diagram of the stages is shown in Figure 1.3.

The drying stage begins as black liquor droplets (size range from 0.5-5 mm in diameter) enter the furnace. Most of the water in the droplet is evaporated. The droplet swells and its surface ruptures as a result of boiling. The second stage, devolatilization, includes two sub-stages, pyrolysis and the combustion of volatiles. Pyrolysis begins when the organic substance in the black liquor droplet is degraded into volatiles by rapid particle heating. The volatiles include CO, CO_2, H_2O, light hydrocarbons, tars, H_2S, and reduced sulfur compounds. The combustion of the volatile gases occurs when they get into contact with O_2. During this stage, the black liquor droplet also swells significantly to several times its initial volume.

The residual of the droplet at the end of devolatilization is recognized as black liquor char. Char has a porous structure and consists of residual organic carbon along with inorganics mainly in the form of sodium based salts. In the char burning stage, heterogeneous combustion reactions between carbon in the char and O_2 occur yielding CO and CO_2. During this stage, char burning raises the particle temperature high enough to melt the sodium based salts in the char particles, and the remaining sodium sulfate is reduced to sodium sulfide. Fume particles are also formed mainly in this stage by sodium volatilization above the char surface. Smelt coalescence occurs as the final stage in

which the inorganic smelt coalesces into a smelt bead, composed of mainly Na_2CO_3, Na_2S, and Na_2SO_4.

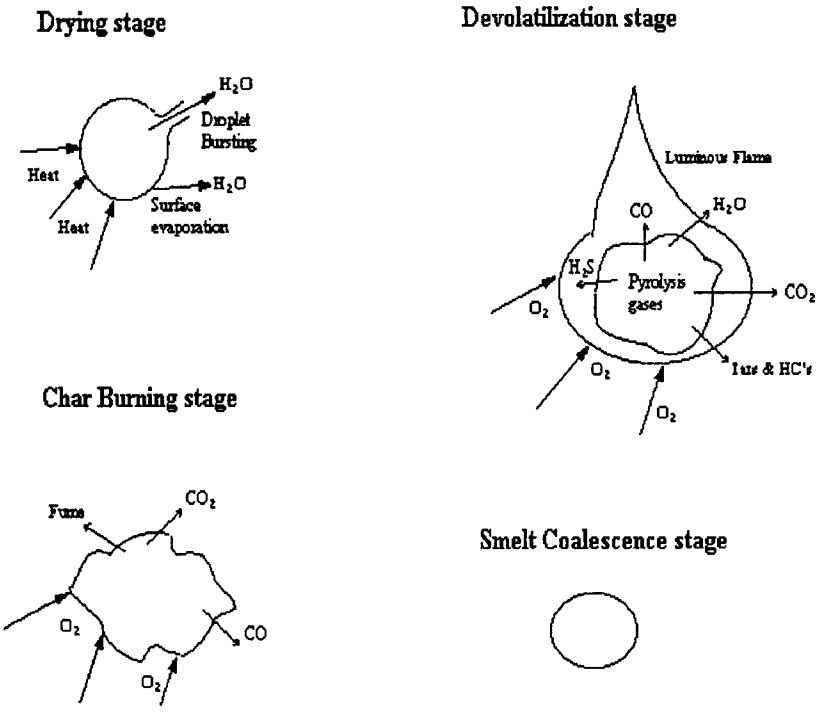

Figure 1.3 Diagram of black liquor combustion stages (Adams and Frederick, 1988)

1.3 Nitrogen Oxides

1.3.1 Sources and fate of nitrogen oxides in atmosphere

The principal nitrogen oxides which are all considered air pollutants are nitric oxide (NO), nitrogen dioxide(NO_2), and nitrous oxide(N_2O). Nitrogen oxides are important in relation to photochemical reactions, the formation of acid rain precursors,

the destruction of ozone in the stratosphere, global warming, and their known effects on health (Bowman, 1991). Figure 1.4 summarizes the nitrogen cycle for nitrogen containing compounds in air pollution.

N_2O is emitted almost totally by natural sources, by bacterial action in the soil and by reactions of N_2 with O and O_2 in the upper atmosphere (Seinfield, 1974). NO and NO_2, called by the composition formula NO_X, are emitted by both natural and human sources. The significant part of increased emissions, however, is due to human activities. Table 1.2 shows an estimation of the comparative importance of human and natural sources for NO_X and N_2O emissions on a global basis.

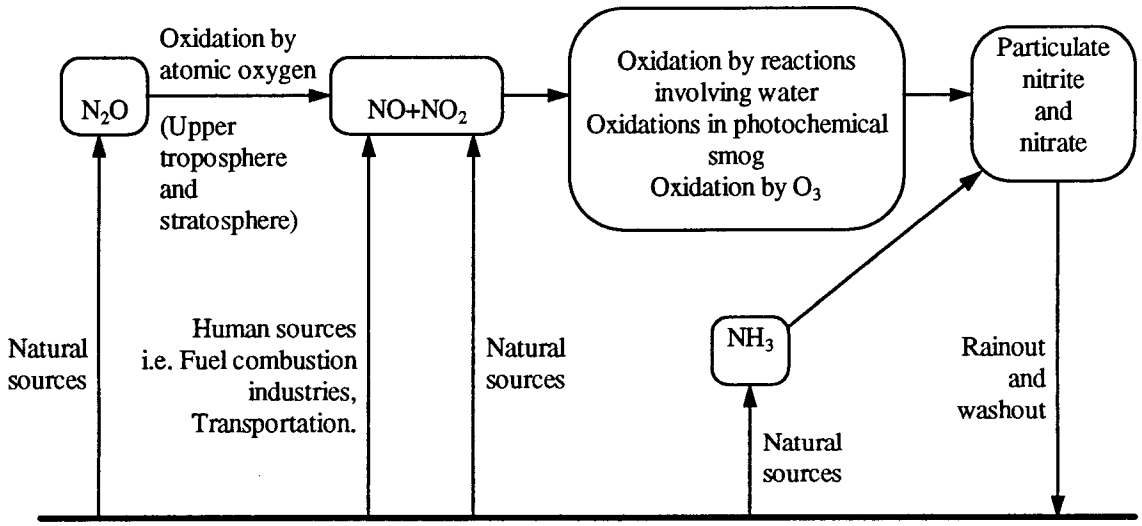

Figure 1.4 Nitrogen cycle for the nitrogen-containing compounds in air pollution (Seinfeld, 1974)

Although there are large uncertainties in these estimates, it is found that combustion is the major direct source of NO_X and a relatively minor source of N_2O (Bowman, 1991).

Fossil fuel combustion is the primary human source of NO_X, more than 50 % of this is due to transportation, industrial processes, and solid waste disposal (Wark and Warner, 1981). The vast majority of NO_X in combustion flue gases is NO with only a small fraction appearing as NO_2. Examples of stationary source emitters include power plants, internal combustion engineers, industrial boilers, process heaters, and gas turbines.

1.3.2 Nitrogen oxides formation mechanisms in combustion process

There are three primary formation mechanisms of NO_X during combustion which are thermal NO_X, fuel NO_X, and prompt NO_X.

Thermal NO_X is formed by the oxidation of nitrogen in the combustion air at high temperatures. The reactions involved in thermal NO_X are recognized as the extended Zeldovich mechanism and are presented by the following three reaction steps :

$$N_2 + O \quad <=> \quad NO + N \qquad (1)$$

$$N + O_2 \quad <=> \quad NO + O \qquad (2)$$

$$N + OH \quad <=> \quad NO + H \qquad (3)$$

(Bowman, 1991)

Reaction (1), the rate limiting step, has a high activation energy which causes a high temperature sensitivity. Thermal NO_X is the dominant emission source for combustion of fuels which contain very low levels of chemically bound nitrogen such as natural gas and gasoline. The reaction mechanism and kinetic data show that the key factor of the extent of thermal NO_X is depend on temperature, residence time, and O_2 concentration.

Table 1.2 Estimation of emissions of NO_X and N_2O from global sources (Bowman, 1991)

Source	NO_X (percentage)	N_2O (percentage)
Human sources		
Fossil fuel combustion		
Stationary sources	24	3
Mobile sources	15	-
Biomass burning	22	<8
Agriculture	9	<8
Sub-total	**70**	**19**
Natural sources		
Soils	15	41
Lightning	15	-
Oceans	-	16
Others	-	24
Sub-total	**30**	**81**
Total	**100**	**100**

Fuel NO_X is formed by the oxidation of organic nitrogen bound in the fuel. Presently, the complete mechanism of fuel NO_X formation is not completely known, but the general concept that the mechanism includes many intermediate reaction steps is accepted. During the combustion process, part of fuel nitrogen is released as volatile nitrogen, while the rest remains in char and it is called char nitrogen. Volatile nitrogen is rapidly converted to HCN through an initial reaction pathway (Bowman, 1991). This ignites several continuing homogeneous reactions which convert HCN into other nitrogen containing intermediates and radicals such as CN, NH_i, and N. These

intermediates are converted to NO by reactions with oxygen containing species or to N_2 by reaction with NO itself. Char nitrogen can be released as NO by heterogeneous oxidation reaction and NO may be further reduced to N_2. The overall NO formation pathways are illustrated in Figure 1.5. Fuel NO_X mechanism is not highly temperature sensitive but fuel NO_X formation depends on the nitrogen level in fuel, the fuel-air ratio, the rate of volatilization of nitrogen, and slightly operation temperature.

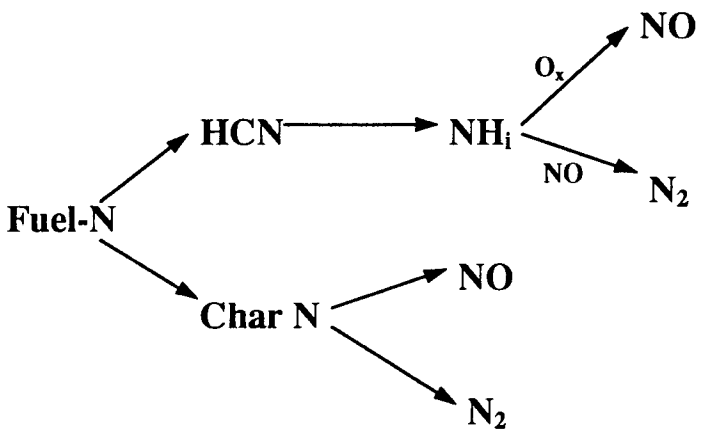

Figure 1.5 Overall reaction pathway of fuel NO_X formation in combustion processes (Sarofim, 1979)

Prompt NO_X formation is described by the Fenimore prompt-NO mechanism. The mechanism starts when hydrocarbon free radicals react with molecular nitrogen to form the intermediate HCN. HCN is rapidly oxidized to form N_2 or NO with the same reaction pathways as that of fuel NO_X formation. Because the rate of prompt NO_X formation is slow, compared to that of NO_X formation by fuel oxidation, this type of NO_X is neglected in most combustion process (Flagan and Seinfeld, 1988).

1.3.3 NO_X formation in kraft recovery boiler

The emissions of NO_X from recovery boilers are typically 40-100 ppm (Aho et al., 1994). These values are considerably lower than the uncontrolled NO_X emissions from fossil fuel combustion, however, with more stringent regulations it has become important to reduce NO_X emission from recovery as well. It is suggested that the majority of NO_X emissions in recovery furnaces may arise from fuel NO_X (Nichols et al., 1993), (Aho et al., 1994), (Forssen et al., 1995), (Veverka et al., 1993), (Martin et al., 1994), (NCASI, 1992). Two mechanisms of NO_X , which are considered to contribute to NO_X emission from recovery boilers, are thermal NO_X and fuel NO_X. Considering the thermal NO_X formation theory, the temperature resulting from black liquor combustion is not high enough to produce significant amounts of thermal NO_X and thermal NO_X is found to be a minor constituent of NO_X emission from recovery boilers (Nichols et al., 1993, Adams et al., 1993). Fuel NO_X formation, on the other hand, depends on fuel nitrogen content and concentration of oxygen in the combustion gas but it is relatively an temperature insensitive. Pianpucktr (1995) suggested that prompt NO_X may also contribute to NO_X formation.

A significant fraction of N in black liquor is released during the pyrolysis stage (Aho et al, 1994, Forssen et al., 1995, Carangal, 1994). The major volatile N intermediate is NH_3 (Aho et al, 1994, Forssen et al, 1995). The additional NO is formed during the char combustion stage (Forssen et al, 1995, Pianpucktr, 1995).

CHAPTER 2
OBJECTIVES OF THE STUDY

NO_X emissions from recovery boilers are considered to be an important environmental issue in the coming years. There are several ongoing research projects regarding NO_X formation and reduction in kraft recovery boilers whose aim is to predict the NO emissions. The reactive intermediate NH_3, which is found during the pyrolysis of black liquor in recovery boilers as the volatile nitrogen compound, could be oxidized to NO or N_2 by many possible reactions. Fume compounds which are produced during the process of black liquor combustion are considered to be potential catalysts for reactions of NO_X formation and reduction, these catalytic reactions may take place while fume particles are entrained in surrounding gases from the char bed surface to the upper part of the furnace.

This research studies the importance of catalytic NH_3 oxidation by fume compounds in recovery boilers. Na_2CO_3 and Na_2SO_4, the two main constituents in fume, are used as catalysts in a fixed bed reactor in this study.

The objectives of this thesis are:

1. To study the rate of NH_3 destruction and oxidation by fume species.
2. To investigate the effect of NO on NH_3 oxidation in fume catalytic reactions.
3. To compare the catalytic activity of the two fume at the experimental conditions
4. To obtain global kinetic expressions for the important reactions
5. To estimate the importance of the reactions in recovery boilers.

CHAPTER 3
LITERATURE REVIEW

3.1 NH_3 Formation during Black Liquor Combustion

Typically, nitrogen contents found in black liquors range from 0.04 to 0.26 weight percent of dry black liquor solids, with an average of 0.11 wt.% (Nichols et al., 1993). During combustion of black liquor in recovery boilers, fuel nitrogen is released as fixed nitrogen compounds (all nitrogen species except N_2) and N_2. The fixed nitrogen compounds such as NH_3 and HCN are reactive intermediates which may be oxidized to be NO. As described in section 1.2 in Chapter 1, the combustion of black liquor is composed of four sequential stages which are drying, devolatilization, char burning, and smelt coalescence. It is believed that part of fuel nitrogen is released as fixed nitrogen compounds and molecular nitrogen (N_2) during the degradation of black liquor into gases and light hydrocarbons (the black liquor pyrolysis).

Aho et al.(1994) conducted experiments of black liquor droplet pyrolysis in a tube furnace in argon in the temperature range 300- 950 °C. The black liquor samples studied were from different laboratories and mills, with a nitrogen content range from 0.106 to 0.478% of dry solids. In each run, a single droplet of liquor was suspended on a platinum hook, lowered into the reactor and removed after 300 seconds as argon flowed downward past the droplet and into a gas analyzer. The fixed nitrogen compounds, NH_3, HCN and NO, released during the experiments were measured. A significant part of fuel nitrogen was found to be released during pyrolysis at the temperatures studied, while

only a minor part of fuel nitrogen was released during drying. The total amount of fuel nitrogen released in pyrolysis was studied by heating black liquor for 1 hour at 400 °C. Depending on the liquor approximately 20-60% of the original fuel nitrogen in black liquor was volatilized in pyrolysis. NH_3 was found to be the main product fixed nitrogen compounds during devolatilization of black liquor combustion in the experiments. Small amounts of nitrogen oxide (1-2% of fuel nitrogen) were also present in pyrolysis gases. The rest was assumed to be molecular nitrogen. About 10-30% of fuel nitrogen was released as fixed nitrogen, NH_3 and NO in the pyrolysis gases. In the temperature range 600-800 °C, a maximum in the level of fixed nitrogen release during pyrolysis was obtained. At temperatures higher than 800 °C, the total amount fixed nitrogen decreased. The explanation was that reactions of fixed nitrogen species might occur to form molecular nitrogen in the pyrolysis gas stream. With higher temperature, the rate of release of fixed nitrogen increased. The conversion of fuel nitrogen to fixed nitrogen also increased with increasing nitrogen content of liquor. Other important information obtained from the study was that typical NO_X emissions from recovery boiler are in the same range as obtained if the total amount of NH_3 released during pyrolysis was oxidized to NO. The suggested behavior of fuel nitrogen during black liquor pyrolysis in recovery boilers is summarized in Figure 3.1.

Iisa et al. (1994) studied fuel nitrogen evolution during black liquor pyrolysis as well. The experiments were conducted at temperatures 600-1100 °C using a laminar entrained-flow reactor. The black liquor in the study was a southern pine liquor

containing 0.11 wt.% nitrogen. Black liquor particles were introduced into the top of the reactor through a water-cooled injector in a primary gas stream. A movable reactor

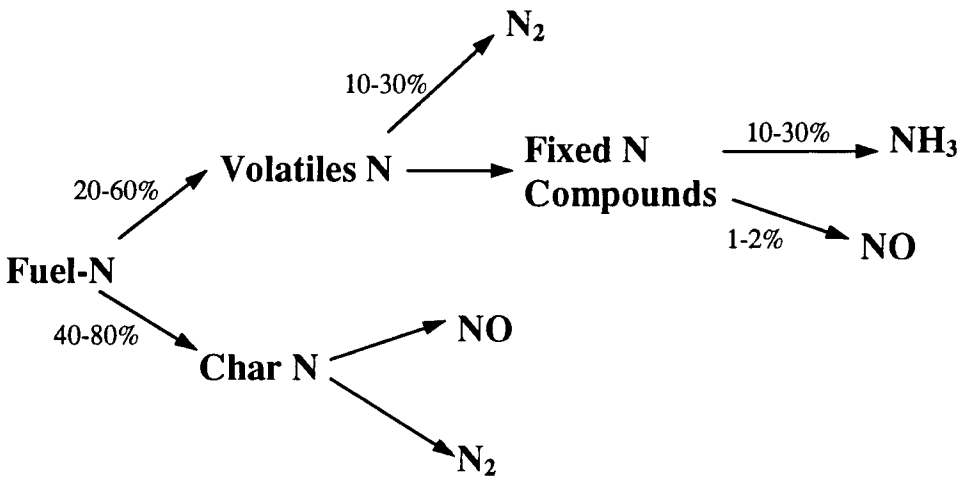

Figure 3.1 Suggested behavior of fuel nitrogen during black liquor pyrolysis in recovery boilers (Aho et al., 1994)

collector was used to collect the pyrolysis products. The gaseous products NH_3 and NO were monitored during black liquor pyrolysis at residence times of 0.3-1.7s. It was found that about 35-65% of fuel nitrogen was volatilized and the fraction of fuel nitrogen volatilized increased along with increasing temperature at the same residence time. Most of the N was released at short residence time(< 0.2 s). About 0-20% of fuel nitrogen was NO depending upon temperature and residence time, while up to 6% of the fuel nitrogen was detected as NH_3. However, the NH_3 data were not believed to be accurate due to problems in the NH_3 measurement system. It was also possible that, during the

experiments, part of NH_3 which was the reactive intermediate formed from volatile nitrogen was already oxidized to NO. The fraction amount of fuel nitrogen released during pyrolysis seemed to be in accordance with the result of Aho et al.(1994) but there were differences regarding how much of each of the nitrogen intermediate compounds were formed during black liquor pyrolysis. For example, the approximate fraction of NO formed in the study of Iisa et al. (1995) (0-20% of fuel nitrogen) is considerably higher than that of Aho et al. (1994) (1-2% of fuel nitrogen). The causes of the different outcomes might be dissimilar experimental conditions (residence time, gas atmosphere, for example) and types of reactor used.

3.2 Fuming in Kraft Recovery Boiler

Fume is produced during black liquor combustion process in recovery boilers. It is composed of submicron-sized aerosol particles which are formed by condensation of vaporized sodium, potassium and chloride species. About 10% of the sodium in the black liquor burnt in the furnace becomes fume (Adams and Frederick, 1988). The primary chemical components of fume are Na_2SO_4, Na_2CO_3, potassium salts, and chlorides. Fume composition depends on combustion conditions and changes due to chemical reactions when fume is transported from the lower part of a recovery boiler (char bed) to the upper part (convective section). An advantage of fume in recovery boiler is that it reacts with oxidized sulfur compounds in flue gas, so the level of SO_2 and SO_3 released to the atmosphere becomes less. The resulting fume (Na_2SO_4) which is collected by electrostatic precipitator is returned to the system by mixing with feed black

liquor, thus reducing the loss of sulfur from the recovery cycle. On the contrary, fume causes deposition problems in the convective heat transfer sections and also pluggage of the economizer. The presence of fume requires expensive flue gas cleaning systems. The recycled dust from the precipitator reduces the heating value of black liquor which is fired into the boiler (Adams and Frederick, 1988).

The fume formation process includes two steps, sodium and potassium salts vaporization, and homogeneous reactions of fume with flue gases after vaporization. It is widely believed that fuming is present mainly during char combustion (Adams and Frederick, 1988).

Frederick and Hupa (1991), on the other hand, proposed that the most significant source of fume in industrial recovery boilers was sodium release from black liquor during devolatilization. They explained that the amount of sodium mass loss during single-drop pyrolysis experiments was an order of magnitude higher than that during char burning and smelt oxidation. Verrill et al.(1994) however argued that all the sodium weight loss did not necessarily contribute to fume, since the form of sodium loss was unidentified.

Verrill and Nichols (1994) studied inorganic aerosol formation during black liquor droplet combustion. The amounts of fume products, during the different stages of black liquor droplet combustion, were measured. The experiments were performed in a drop tube furnace at the temperature of 750 °C with N_2 and O_2 flowing through the reactor. The results showed that the sodium mass loss of liquor droplets during pyrolysis stage ranged from 20 to 30%. The sodium mass loss was at least 7 to 9% during the

combustion of single droplets of liquor in 92.5% N_2 with 7.5% O_2 at 750 °C. The highest range of sodium deposition rate in the collector of system was observed during char burning and smelt oxidation The field data of Borg et al.(1974) had shown that approximately 9% of the sodium content in black liquor was collected as fume in the electrostatic precipitator. The conclusion was drawn from these results that the majority of fume formation probably occurred during the char burning and smelt oxidation stages of combustion.

With the consideration of vapor pressure data available (shown in Figure 3.2), elemental Na, NaOH, and NaCl are the most likely to vaporize in the temperature region of kraft char combustion of about 1000 to 1300 °C (Adams and Frederick, 1988).

The fundamental mechanisms of fume formation including the effect of the recovery boiler conditions on fume formation were studied in the studies of Cameron and Cameron et al., (1985, 1988). Fuming during char burning in kraft recovery boilers can occur either under reducing conditions in the char bed or under Na_2S oxidation condition.

3.2.1 Fuming under reducing condition

The process occurs when Na_2CO_3 in the smelt reacts with CO, H_2 or C in a reduction reaction, and elemental Na is released to an environment of inert gases such as N_2, etc. The limitation of this reaction pathway is that it is inhibited by the presence of sulfate in smelt which will react with CO, or C to form CO_2 and sulfide instead. In

recovery boilers, it is found that the fuming under reducing condition is less important than the fuming during Na_2S oxidation (Cameron et al., 1985).

3.2.2 Fuming during Na_2S oxidation

First, Na_2S is oxidized to Na_2SO_4 by Na_2CO_3 in the smelt and volatile elemental sodium is released near the smelt surface. The concentration of sodium in the vapor phase above the smelt depends on the equilibrium of the reaction shown in equation 3.1 (Cameron, 1988).

$$Na_2CO_3 + 1/4\ Na_2S \ <=>\ 1/4\ Na_2SO_4 + 2\ Na + CO_2 \qquad (3.1)$$

The information obtained from equation 3.1 is its stoichiometry but it is not necessarily representative of the mechanism of fume formation.

Second, the elemental Na vapor diffuses away from the char surface and undergoes gas-vapor reactions. Rapid reactions between the surrounding gas and Na vapor increase the rate of vapor diffusion, resulting in a high fuming rate . The explanation of this event is that Na vapor is used up by reactions with O_2, CO_2 and SO_2 near the char surface during its diffusion through the boundary layer. So the diffusion pathway is shortened, causing the concentration gradient of Na vapor to be steeper which finally increases the vaporization rate. This mechanism was found to be insensitive to smelt composition and to gas phase composition. The rate of fuming could be fitted by an Arrhenius expression with an activation energy of about 86 kJ/mole (Cameron, 1985).

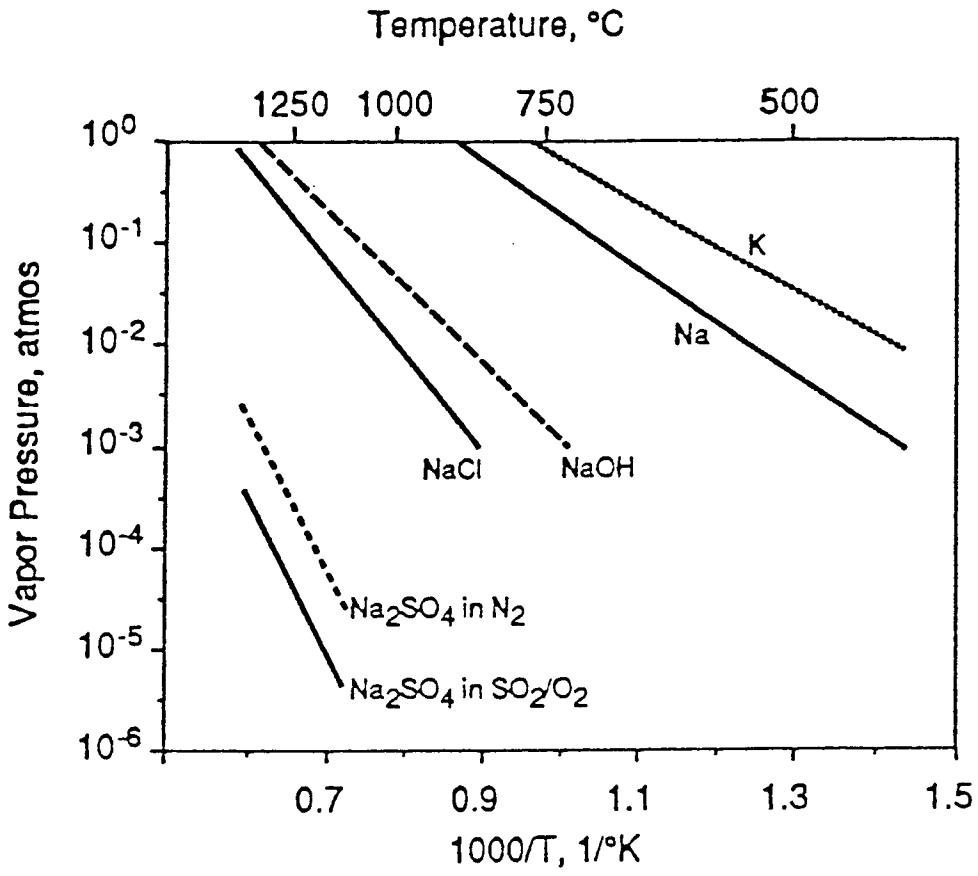

Figure 3.2 Vapor pressure for sodium salts and potassium (Adams and Frederick, 1988)

3.2.3 Gas phase reactions

The reactions in the gas phase between the elemental sodium vapor released from the char bed and various surrounding gaseous compounds determine the final composition of fume in the recovery boiler. The study of Grace, Cameron, and Clay (1985) showed that with solely O_2, and N_2 present above the smelt, the major component of fume is Na_2CO_3. On the other hand, if SO_2 is also available, the major

fume compound is Na_2SO_4. Table 3.1 summarizes the effects of different gaseous species and different components of smelt on the final fume composition. The

Table 3.1 Effect of gas and smelt or char compositions on fume compositions (Grace et al., 1985)

Melt Components	**Gas Components**	**Carbon present?**	**Fume Components**
Na_2CO_3, Na_2S, Na_2SO_4	O_2, N_2	No	>92% Na_2CO_3 the rest Na_2SO_4
Na_2CO_3, Na_2S, Na_2SO_4	H_2O, O_2, N_2	No	70% Na_2CO_3, 30% Na_2SO_4
Na_2CO_3, Na_2S, Na_2SO_4	O_2, N_2	Yes	70% Na_2CO_3, 30% Na_2SO_4
Na_2CO_3, Na_2S, Na_2SO_4	SO_2, O_2, N_2	No	Na_2SO_4
Na_2S, Na_2SO_4	O_2, N_2	No	Na_2SO_4

composition of fume varies with location in the recovery boiler. Fume which is collected by the electrostatic precipitator is primarily composed of Na_2SO_4, with some potassium and chloride salts and small amounts of Na_2CO_3 (Adams and Frederick, 1988), while Na_2CO_3 is found to be the major chemical compound in fume above the molten salts (Grace et al., 1985). This is supported by the study of Borg and coworkers (1974) which indicated that CO_2, O_2, and H_2O which are the gaseous species with high concentration above the smelt, cause the elemental sodium vapor rapidly to convert to Na_2CO_3. Na_2CO_3 is then slowly converted to Na_2SO_4 as it is transported from the char bed to the upper section of recovery boiler (Borg et al., 1974). Rizhinshvili and Kaplun (1983) reported that Na_2SO_4 content in fume particles was 64% at the tertiary air level while at

the furnace outlet it was 96%. Backman et al. (1985) studied the rate of conversion of Na_2CO_3 to Na_2SO_4 in an atmosphere containing SO_2 and O_2 at temperature below 650 °C. They found that the rate of reaction was proportional to SO_2 partial pressure but not to O_2 partial pressure in the system. The intrinsic rate of reaction had an activation energy of 65 kJ/mol. Boonsongsup et al. (1993) showed that the rate of Na_2CO_3 conversion to Na_2SO_4 in the solid state is too low to be important and does not occur fast enough to relate with the disappearance of SO_2 in recovery boilers.

CHAPTER 4
EXPERIMENTAL PROCEDURE

4.1 Experimental Materials and Apparatus

4.1.1 Materials

Fume compounds: Na_2CO_3 and Na_2SO_4 (fume species) were used as the catalysts in this study. Both chemicals are anhydrous granulars from Mallinckrodt company with the purity of 99.62% for Na_2CO_3, and 99.49% for Na_2SO_4. Both fume compounds were presintered and sieved to collect the preferred size range to be ready to be used in the experiments.

Presintering method of the sodium compounds (Na_2CO_3 and Na_2SO_4): when studying the kinetics of sulfation of Na_2CO_3 in artificial flue gases in the temperature range 300 °C to 700 °C, Backman et al. (1985) showed that the available surface area of Na_2CO_3 decreased due to sintering. To reduce the effect of sintering during the experiments, it was suggested that the compounds should be presintered before use. In this study, each sodium compound was sieved and the particle size 90 to 125 μm in diameter was collected, and treated in a ceramic crucible in a muffle furnace at 780 °C, 1 atm for ½ hour. After cooling down, the presintered sodium compounds were sieved once again and the same range of particle sizes (90 to 125 μm) was collected. Both untreated sodium compound and presintered sodium compound were analyzed for BET surface area. The BET surface area of untreated Na_2CO_3 was 0.26 m^2/g and that of presintered Na_2CO_3 was 0.18 m^2/g, analysis gas was N_2.

Gases: NH_3, NO, and air were used as the reactant gases in the experiments with the following concentrations.

NH_3 : 476-514 ppm in He (differences of NH_3 concentrations according to different gas cylinders used)

NO : 2050 ppm in He (with other oxides of N <20 ppm)

Air : 21% O_2 in N_2

He : 99.99% (grade 5 high purity)

Helium was used as inert gas to dilute the concentration of other reactant gases and also as purge gas to clean residual gases in the experimental system.

4.1.2 Apparatus

Reactor: the fixed bed reactor used in the experiment was made of quartz glass. It had a 1.3 cm inside diameter and a length of 95 cm. A fritted quartz glass plate was used to support the fixed bed particles (Na_2CO_3 and Na_2SO_4) and it was located in the center of the reactor. Quartz wool was placed between the fixed bed particles and the fritted quartz glass to avoid direct contact of these two materials. This prevented the catalyst particles from a depositing in the fritted glass pores which might have caused errors in the subsequent experiments in particular, for empty bed tests or for experiments with the other catalyst. Na salts may have also reacted with the fritted quartz.

Thermocouple: two thermocouples were operated in the experimental system. The thermocouple used to monitor the bed temperature was an OMEGA K type stainless steel thermocouple, with a temperature range -200 to 1250 °C, located inside

the reactor at the center of the fixed bed. The other one which was used for the temperature controller was an OMEGA K type with a thermocouple ceramic fibre-insulated probe. The maximum operating temperature of the probe is 1400 °C.

Temperature controller: the temperature controller for the furnace was a micro processor based controller (OMEGA CN 76000) with solid state relay output.

Furnace: an electric single zone furnace from Hevi Duty Electric Co. was used to heat the reactor. Its working temperature limit is 1010 °C. In the experiments, the highest operating temperature was 750 °C.

Thermometer: a digital thermometer of OMEGA HH81, for type K or J thermocouples was used to monitor temperature inside the fixed bed reactor during the experiments. The measured temperature range is valid from -160 °C to 1372 °C.

Rotameter: the rotameters (N062-01 and N112-02) in the experimental system were standard 150 mm flow meters with standard valves from Cole-Parmer company. The floating material in all of them was stainless steel 316. For the flows of He, NH_3 in He, and NO in He, the flow rate range of the rotameters (N112-02) is 48-1290 ml/min at standard conditions (1 atm, 70 °F). For the flow of air (N062-01), the flow rate range of the rotameter is 21-243 ml/min at standard conditions. The accuracy of the rotameters is ±2% of full scale. Calibration curves of the rotameters were prepared once before all the studied experiments (shown in Appendix A).

Tubing: the type of tubing used in the experiments was Teflon PTFE semiflexible tube. Its outside diameter is 1/4" and inside diameter is 3/16". It can resist temperature of -240 to 260°C.

Gas sampling bag: a Teflon FEP gas sampling bag was used to collect the outlet gas from the reactor and to supply it to a FT-IR for gas analysis. The 30x30cm bag has 5 mm wall-thickness with a nickel-plated brass on/off valve which accepts 1/4" I.D. flexible tubing. Its capacity is 4.7 liters.

Heating tape and input controller: the heating tapes used in the experiments was Thermolyne flexible heating tape which can resist temperatures up to 250 °C. The input controller was a Thermolyne type 45500 input controller which control power input to the heating tape. At the gas line entering the reactor, the heating tape was used for preheating the inlet gas flow to the reactor, and at the sampling line, it was used to reduce NH_3 loss by adsorption on the gas lines because the outlet concentrations of NH_3 from the reactor were already low. Temperature set points at both locations were the same, about 70 °C.

4.2 Experimental Set Up

The experimental equipment was set up according to the schematic diagram shown in Figure 4.1. Reactant gases flowed through rotameters, and were mixed. The mixed gas was led to the two-way valve which was used to select the path between by-pass or reactor. The by-pass was selected when the initial concentrations of the reactants in the mixed gas were to be analyzed. In the reactor path, the mixed gas flowed downward through the heated fixed bed reactor which contained a known amount of the catalyst. The gas lines from the reactor and from the by-pass were joined and connected to the other two-way valve which was used to select between exhaust line or sampling

line. The sampling line was connected with the gas sampling bag to collect the outlet gas for analysis. The part of filled-up sampling bag was connected to the FT-IR to detect gas species and their concentrations.

4.3 Experimental Method

A predetermined amount of the presintered Na_2CO_3 or Na_2SO_4 was placed on quartz wool which was held by a fritted quartz glass at the center of the reactor. Both ends of the reactor were connected to the gas lines. The fixed bed reactor was set to be at the center of the cylinder-shell furnace in both vertical and radial directions. The furnace was heated up to the lowest experimental temperature (550 °C) at the rate of about 10 °C/min. During the heating process, there was a He flow of 13.0 cm^3/sec (25 °C, 1 atm) through the reactor to purge the system. Before the temperature reached the set point (at approximately 500 °C), the gas was switched to by-pass. Then the selected flows of the gas reactants were allowed to flow through the by-pass for about 5 minutes, after which the outlet gas was switched to the sampling line, which was connected to the gas sampling bag, to begin collecting the gaseous sample. When the sampling bag was nearly filled up to its full capacity (4.7 liters), the increase of gas pressure in the sampling bag caused the gas flow rates to decrease. To reduce the problem, the sampling bag was filled with the outlet gas less than to its capacity but enough for gas analysis each time. The sample was immediately brought to the Fourier Transform Infrared Spectrometer (FT-IR) for analysis. Two samplings were conducted for one gas analysis. The first sampling was used to flush the gas chamber of the FT-IR, and the second sampling was

used for gas analysis by the FT-IR. At least two samples were made at each experimental condition and the average value of the gas concentrations was calculated. After each sample collection, the sampling bag was vacuumed to be ready for being used again. Next the gas was switched back to flow through the reactor. The same reactant gas flow rates were used as when the samples of the by-pass gas were collected. After the reactant gases had flowed for about 10 minutes through the reactor, the outlet gas was collected and analyzed by the FT-IR. The flows of the reactant gases were switched off and He was used to purge the system again, while the temperature in the reactor was increased to the next set point. The same steps of experiment were repeated.

4.4 Fourier Transform Infrared Spectrometer (FT-IR) for Gas Analysis

In this study, a FT-IR was used for the quantitative analysis of nitrogen compounds (NH_3 and NO) in the reactants and the gaseous products. The FT-IR can be used to analyze infrared active gaseous species, this excludes all homonuclear diatomic molecules species such as N_2, etc. Different gaseous species have their unique IR absorption characteristics so infrared spectrometer (IR) makes it possible to identify all the interesting infrared active gases. The advantages of using FT-IR over using other gas analyzers such as gas chromatography (GC), for example (Sricharoenchaikul, 1995):

- High resolution (ppb concentration can be detected in some cases).

- Each gas species can be identified from others by its unique characteristic peak shape.

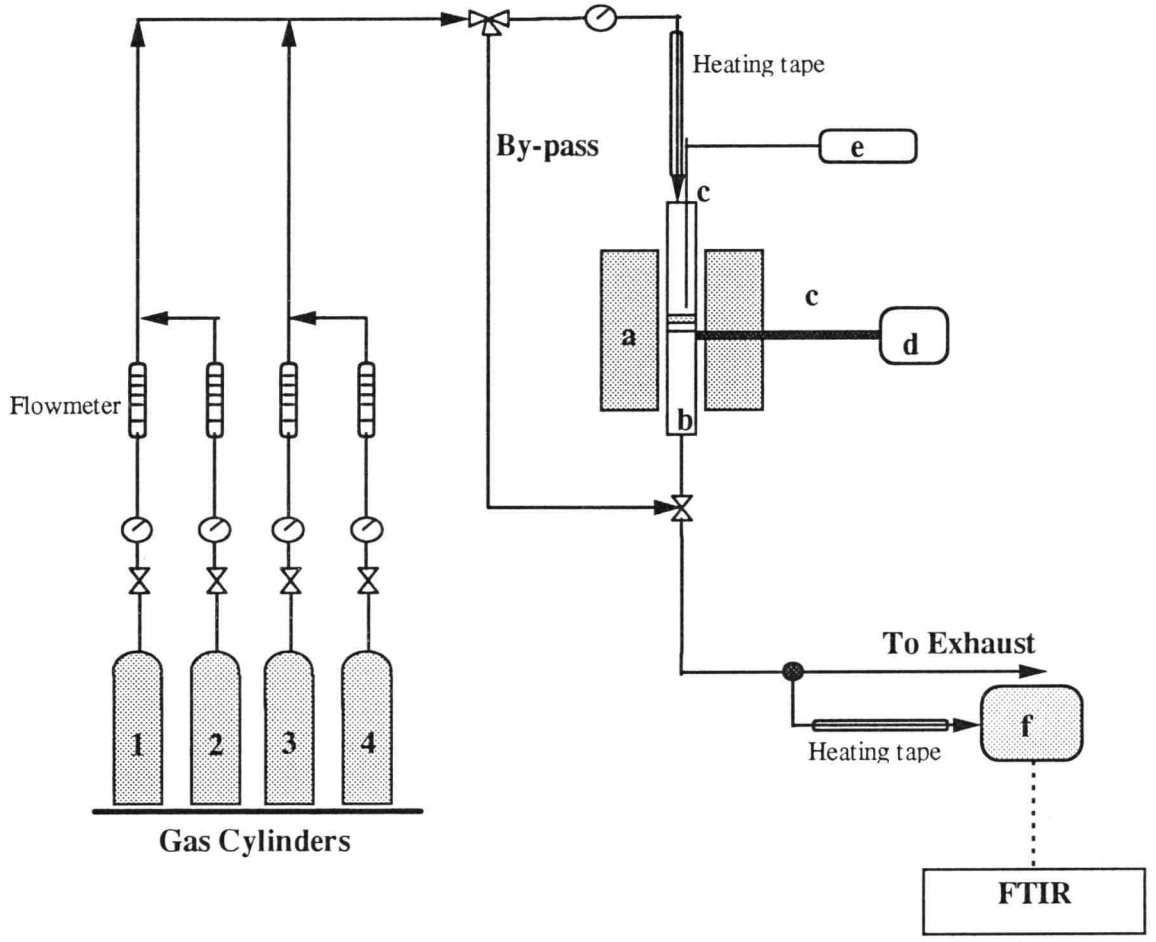

a : Electric furnace	**b : Fixed-bed reactor**
c : Thermocouples	**d : Temperature controller**
e : Digital Thermometer	**f : Gas sampling bag**
1 : He gas cylinder	**2 : NO in He gas cylinder**
3 : NH_3 in He gas cylinder	**4 : Air (21% O_2, 79% N_2) cylinder**

Figure 4.1 Schematic diagram of the experimental equipment setup

- With only one gas sampling, FT-IR can detect most of the gas species components.

- The operation condition is simpler to control than that of GC: no need to select column type, set injection and column temperature, for example.

The spectrometer used in these experiments was a Bomem MB100 mid IR FT-IR with a 7 meter pathlength gas cell. A simplified optical representation of the spectrometer is illustrated in Figure 4.2. The on-line data acquisition software used was Lab Calc™ of Galactic Industries Corporation.

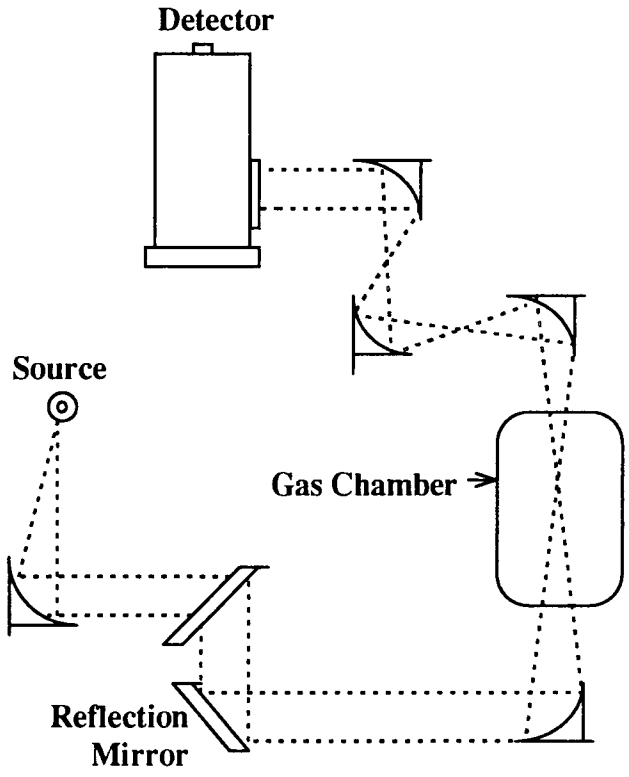

Figure 4.2 Schematic diagram of FT-IR spectrometer (Sricharoenchaikul, 1995)

The operating specification for the analysis of the gaseous species using FT-IR are shown in Table 4.1.

Table 4.1 Operating specification for FT-IR

Resolution	1 cm^{-1}
Number of scans	32
Path length	7 meters
Type of scan	absorbance

A concentration calibration curve of each interesting gaseous species (NH_3 and NO) was prepared before doing all the quantitative analysis (shown in Appendix B). The wavelengths used for the NH_3 analysis were 980-900 cm^{-1}, while wavelengths used for NO were 1970-1780 cm^{-1}. The peak characteristics of NH_3 and NO are shown in Figure 4.3 and Figure 4.4, respectively. An average reproducibility of the measurements was less than 3%.

Procedure: first, the FT-IR detector was filled with liquid nitrogen. The gas sampling chamber was preheated by electrical heating to above 70 °C to prevent gas adsorption from the sample on the gas chamber wall. Before starting the sampling, He was used to flush the gas chamber for at least five minutes to purge all undesired gas residual from inside the chamber. Then the sampling chamber was evacuated and the inlet gas line was connected to the gas sampling bag. The gas chamber was flushed with the sample gas with almost its volume capacity (about 1.2 liters) and was evacuated. For the measurement, the inlet valve was left open to let the gas flow into the chamber until the pressure in the chamber was at atmospheric pressure. The flushing step and the gas measurement step used two gas sampling. After finishing the scanning, the chamber was evacuated and was prepared by the same steps to be ready for the next analysis.

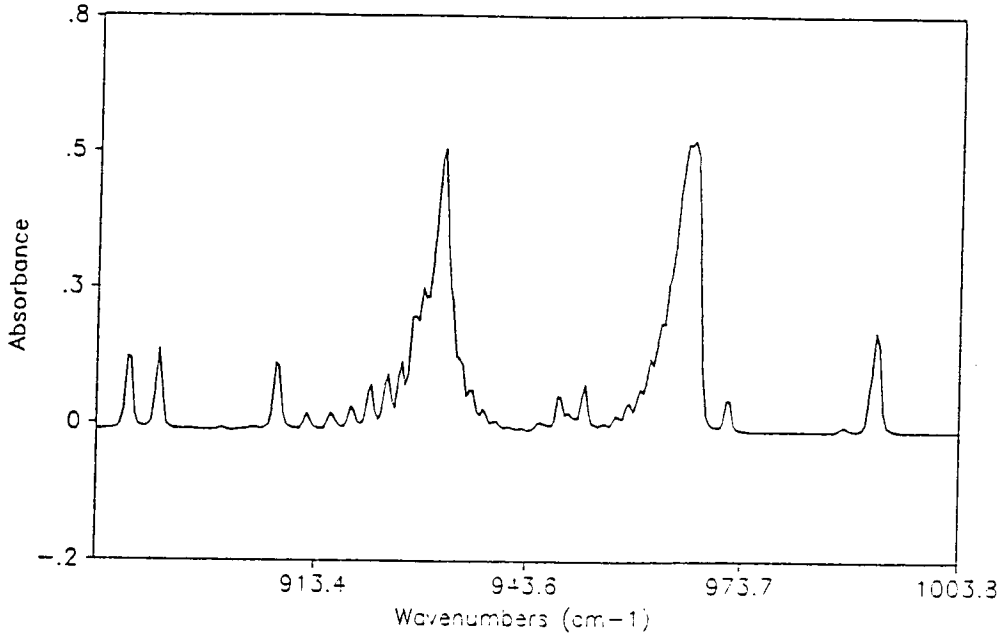

Figure 4.3 NH_3 spectrogram from FT-IR analysis

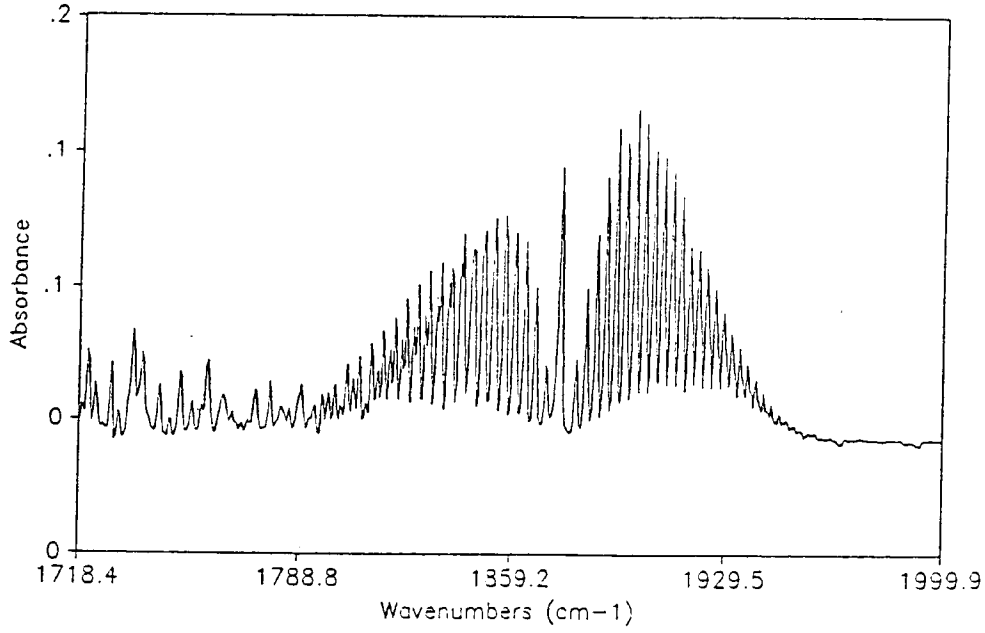

Figure 4.4 NO spectrogram from FT-IR analysis

4.5 Experimental Conditions for NH_3 Oxidation by Fume Species

4.5.1 Investigation of transport processes resistances

The importance of external mass transfer (film diffusion) effect was tested by experiments at the same residence time but with different gas flow rates and different weights of catalyst at the highest temperature studied (750 °C). The rate data obtained were also used in calculations of film mass transfer by comparing to the Mears' criterion (Fogler, 1992). The importance of internal mass transfer (pore diffusion) effect, was justified by the Weisz-Prater criterion (Fogler, 1992).

4.5.2 Investigation of the kinetics of the reactions by fume compounds

In order to obtain the rate constants and the activation energy values of the four reactions (NH_3, NH_3 + NO, NH_3 + O_2, and NH_3 + O_2 + NO) by the fume compounds, each reaction was studied at five different temperatures, 550, 600, ..., 750. Two initial concentrations of NH_3, 250 and 500 ppm, were used in these tests. In order to obtain the reaction order, the analysis method was determined first. For differential reactor, only the inlet concentration of NH_3 was varied in the experiments (Levenspiel, 1972). For integral analysis reactor, the ratio between the weight of the catalyst and the volumetric gas flow rate was varied in the experiments (Levenspiel, 1972). A summary of all the experimental conditions is shown in Table 4.2.

Table 4.2 The experimental conditions studied

Na_2CO_3 (particle size 90-125 μm)	0.38-3.0±0.1 g			
Test/Reaction studied	**Temp., °C**	**NO inlet, ppm**	**NH_3 inlet, ppm**	**Flow rate, cm^3/s**
NH_3	550-750	-	115-500	13.0
NH_3+NO	550-750	250-1250	150-400	13.0
NH_3+O_2 (1% O_2)	550-750	-	250,500	6.3, 13.0
NH_3+O_2+NO (1% O_2)	550-750	250	250	13.0
Na_2SO_4 (particle size 90-125 μm)	3.0±0.1 g			
NH_3	550-750	-	500	13.0
NH_3+NO	550-750	250	250	13.0
NH_3+O_2 (1% O_2)	550-750	-	500	13.0
NH_3+O_2+NO (1% O_2)	550-750	250	250	13.0

4.6 Interpretation of the Experimental Data

A reactor which contains solid catalyst particles, and operates with a flow of the fluid phase, is considered a fixed bed reactor. The assumption was employed that the solid particles remained unchanged during the reaction. Since the inlet concentrations of the reactants were small, any volume change during the reaction was ignored. Further assumptions are as follows:

Plug flow: the assumption for plug-flow is that the contents of the reactor are completely mixed in the radial direction, while no mixing occurs in the axial direction (direction of the flow) while the reacting stream flows through a reactor (Holland and Anthony, 1979). If the height of the fixed bed is large relative to a particle diameter,the

plug flow assumption is valid for flow in a tubular fixed bed reactor (Kubota and Ikeda, 1963). In the experiments, the height of the reactor was nearby 28-230 times the diameter of the packed bed particle, so this requirement was closely met in the experiments.

Uniform temperature in the reactor bed: in the experiments the fixed bed was located in the center of the reactor in the furnace, was shallow catalyst bed heights varying from 0.30 to 2.5 cm depending on the amount of catalyst used. Further, the concentrations of the reactants were low (the highest was 500 ppm). Thus the effects of the heat of the reactions and the furnace temperature profile could be disregarded, and the assumption of a uniform temperature profile could be employed.

Figure 4.5 shows a diagram of a fixed bed with notations used in developing the performance equations.

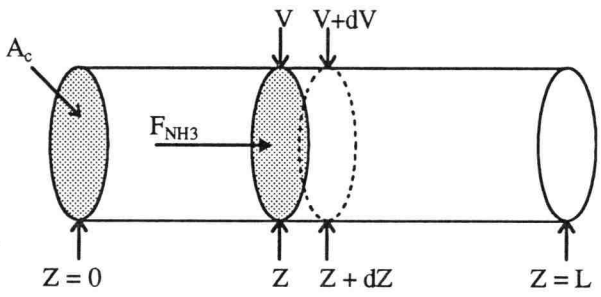

Figure 4.5 Diagram of fixed bed reactor

where: $C_{NH3,o}$ = bulk gas concentration of NH_3, mol/cm^3

F_{NH3} = flow rate of NH_3, mol/s

$-r'_{NH3}$ = rate of disappearance of NH_3 by reaction per mass of catalyst, mol/g.s

W = weight of catalyst, g

A_c = cross sectional area of reactor, cm^2

Z = distance through reactor, cm

V = volume through the reactor, cm^3

$= A_c .Z$

ρ_b = bulk density of catalyst bed, g/cm^3

Material balance of NH_3 for a differential element of reactor volume ($A_c dZ$) for a steady state system :

Input of NH_3 - Output of NH_3 = Disappearance of NH_3 by reaction

$F_{NH3}|_V \quad - F_{NH3}|_{V+dV} \quad = -r'_{NH3}\rho_b dV$

Dividing all term with dV and taking the limit as dV goes to zero results

$$-\frac{dF_{NH3}}{dV} = -r'_{NH3}\rho_b$$
$$\frac{F_{NH3,o}dX_{NH3}}{A_c dZ} = -r'_{NH3}\rho_b \qquad (4.1)$$

For an n^{th} order irreversible reaction, and no limitation of mass transfer effects (the assumption is tested in Section 5.3.2), the following differential equation can be obtained from Equation (4.1):

$$\frac{F_{NH3,o}dX_{NH3}}{A_c dZ} = k' C^n_{NH3}\rho_b \qquad (4.2)$$

(n=any number)

4.6.1 Integral reactor

This method of analysis accounts for the variation in the reaction rate within reactor. For all other isothermal reactions except zero order reactions, there is significant variation in the reaction rate when there is a significant change in the reactant concentration through the reactor. In this study, integral reactor analysis will be used for reactions with the highest conversion of NH_3 higher than 45 %. The differential equation (4.2) for the n^{th} order reaction, can simply be integrated to get the performance equation as follows:

$$k' \frac{W}{F_{NH3,o}} = \{\frac{1}{(1-n)} - \frac{1}{(1-n)}.(1-X_{NH3})^{(1-n)}\} \frac{1}{C^n_{NH3,o}} \qquad (4.3)$$

(n = any number except 1)

$$k' \frac{W}{F_{NH3,o}} = -\ln(1-X_{NH3}) \frac{1}{C_{NH3,o}} \qquad (4.4)$$

(n = 1)

With the boundary condition at the entrance of the reactor used:

$$X_{NH3} = 0 \text{ at } Z = 0$$

4.6.2 Differential reactor

When the variation of the reaction rate within the reactor is small, an average rate of the reaction can be assumed to be constant through out the reactor with little error. In this study, for reactions with the highest conversion of NH_3 lower than 45 %, differential reactor analysis will be used.

From equation (4.1), change $-r'_{NH3}$ to be $-r'_{NH3,ave}$ which is constant at all points within the reactor. For the n^{th} order reaction, the following performance equation is obtained:

$$\frac{F_{NH3,o} \cdot X_{NH3}}{W} = k' C^{n}_{NH3,ave} \qquad (4.5)$$

$$-r'_{NH3,ave} = k' C^{n}_{NH3,ave}$$

$$\ln(-r'_{NH3,ave}) = \ln k' + n \ln(C_{NH3,ave}) \qquad (4.6)$$

(n=any number)

With the boundary condition at the entrance of the reactor:

$$X_{NH3} = 0 \text{ at } Z = 0$$

CHAPTER 5
RESULTS AND DISCUSSION

In this thesis, four catalytic reactions were studied in the temperature range from 550 °C to 750 °C. They were decomposition of NH_3, oxidation of NH_3 by NO, oxidation of NH_3 by O_2, and oxidation of NH_3 by both O_2 and NO. Two species of fume compounds (Na_2CO_3, and Na_2SO_4) were used in the experiments as the catalysts. All the experiments were conducted in a fixed bed reactor. The inlet and outlet concentration of NH_3 and also those of NO, were measured in each experiment.

5.1 Reactions in an Empty Bed

The purpose of the experimental runs in the empty bed was to test whether there were gas phase reactions or catalytic effects of the reactor materials on the NH_3 oxidation reactions. If the effects were significant, the empty bed reaction kinetics would be used to correct with the kinetic data obtained for the fume catalytic reactions.

All reactor materials (quartz wool, and fritted quartz glass), except fume compounds were the same as in the fume catalytic experiments. Reactions of NH_3 (with inlet NH_3 = 500 ppm), NH_3+NO (with inlet NH_3 = 250 ppm, NO = 250 ppm), NH_3+O_2 (with inlet NH_3 = 500 ppm, 1% O_2), and NH_3+O_2+NO (with inlet NH_3 = 250 ppm, NO = 250 ppm, 1% O_2) were tested at 550 °C, 650 °C, 700 °C and 750 °C at the same total gas flow rate of 13 cm^3/s. Figure 5.1 shows the NH_3 conversions of all the reactions in the empty bed in the range of temperature studied. At the temperature of 650 °C and

lower, there was no NH_3 conversion detected for any of the reactions studied. At the highest temperature studied (750 °C), for the reactions NH_3, and NH_3+O_2 the conversions of NH_3 were 5%, and 8%, respectively, and no NO was detected. For the reactions NH_3+NO, and NH_3+O_2+NO at 750 °C, the conversion of NH_3 were 10%, and 15%, respectively. The outlet NO concentrations in both reactions were unchanged from the inlet concentrations.

5.2 Conversion Data of Catalytic Reactions in Fixed Bed

For the convenience of the analysis later, the catalyzed reactions of NH_3 and NH_3+NO are grouped together when showing the data from the experiments. Also, the other two reactions data of NH_3+O_2, and NH_3+O_2+NO are displayed together.

5.2.1 The reactions with Na_2CO_3 as a catalyst in the fixed bed

5.2.1.1 NH_3 and NH_3+NO reactions

The conversion of NH_3 as a function of temperature is shown in Figure 5.2 for the reactions of NH_3, and NH_3+NO with Na_2CO_3 as the catalyst in the reactor bed. The inlet concentration of NH_3 was 500 ppm for the decomposition of NH_3 experiments. For the oxidation of NH_3 by NO, the concentration of NH_3 and that of NO were equal (250 ppm). In each run, the total gas flow rate was 13 cm^3/s at 25 °C and the amount of Na_2CO_3 used was 3.0 ± 0.1 g. For both NH_3 reaction and NH_3+NO reaction,

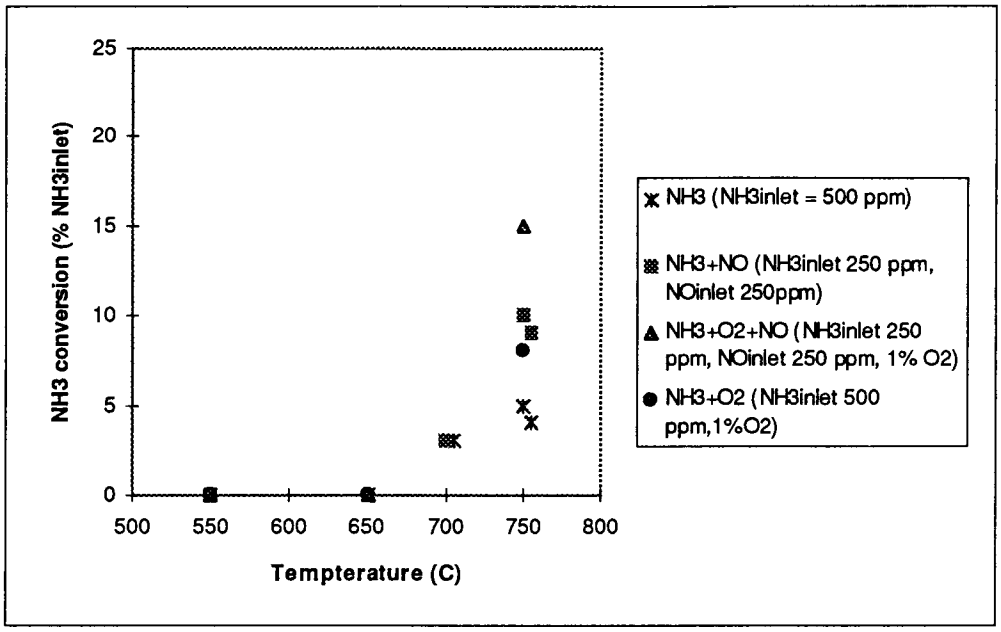

Figure 5.1 NH_3 conversions as a function of temperature in the empty bed experiments

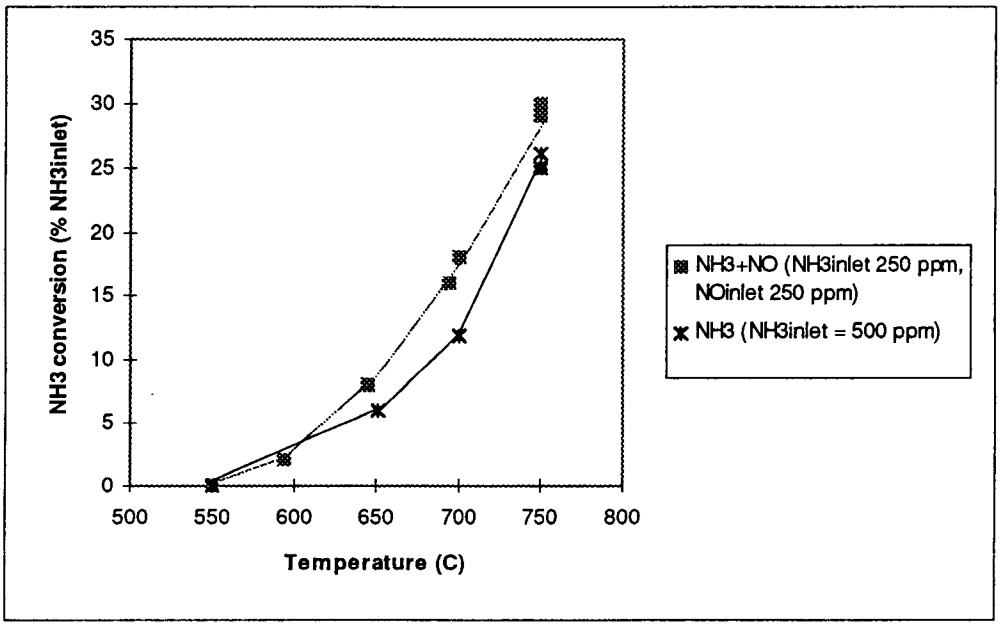

Figure 5.2 NH_3 conversions as a function of temperature of the catalytic reactions NH_3, and NH_3+NO with 3.0 ± 0.1 g Na_2CO_3 and a total flow rate of 13 cm^3/s at 25 °C.

there were conversions of NH_3 less than 5% at 600 °C or below. The conversions of NH_3 at 750 °C were 25-26% (reaction of NH_3) and 25-30% (reaction of NH_3+NO). For both reactions, the conversion of NH_3 increased with increasing temperature. At the condition studied, NO conversion is shown in Figure 5.3. The NO conversion of the reaction NH_3+NO was less than 5% at 600 °C or below and was up to 18% at 750 °C.

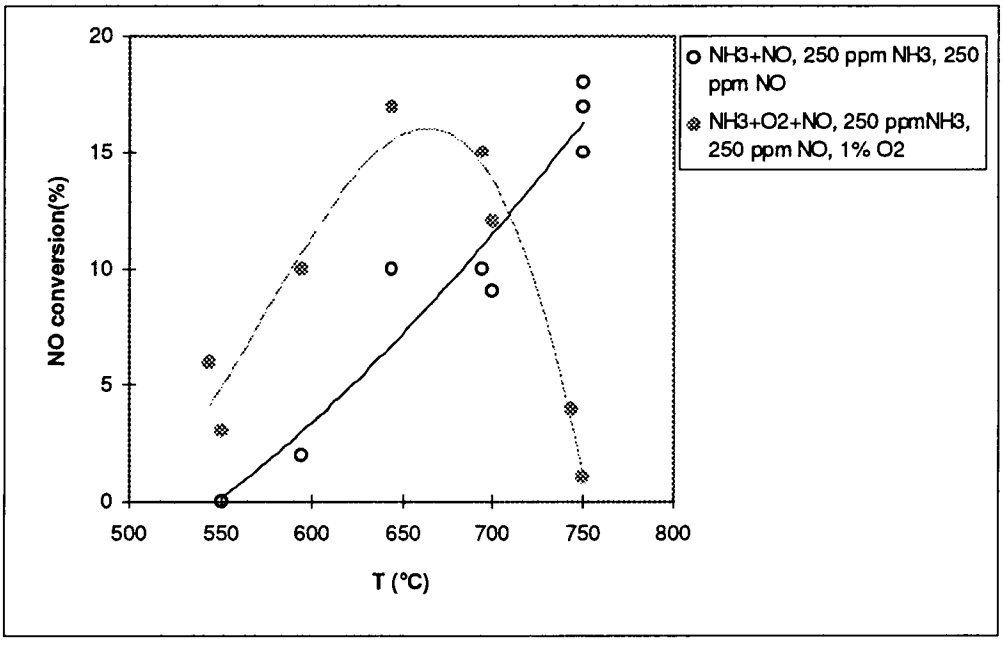

Figure 5.3 NO conversions as a function of temperature of the reactions NH_3+NO and NH_3+O_2+NO, 3.0 ± 0.1 g Na_2CO_3 at a total flow rate of 13 cm^3/s at 25 °C.

5.2.1.2 NH_3+O_2 and NH_3+O_2+NO reactions

Figure 5.4 illustrates the conversion of NH_3 in the reactions of NH_3+O_2 and NH_3+O_2+NO with 3.0 g ± 0.1 g Na_2CO_3 in the bed as a function of temperature. For the reaction of NH_3+O_2 (1% O_2), two different inlet concentrations of NH_3 (250 ppm and

500 ppm) with the same total flow rate of 13 cm^3/s at 25 °C were tested. The NH_3 conversions were significant at temperatures higher than 550 °C and were

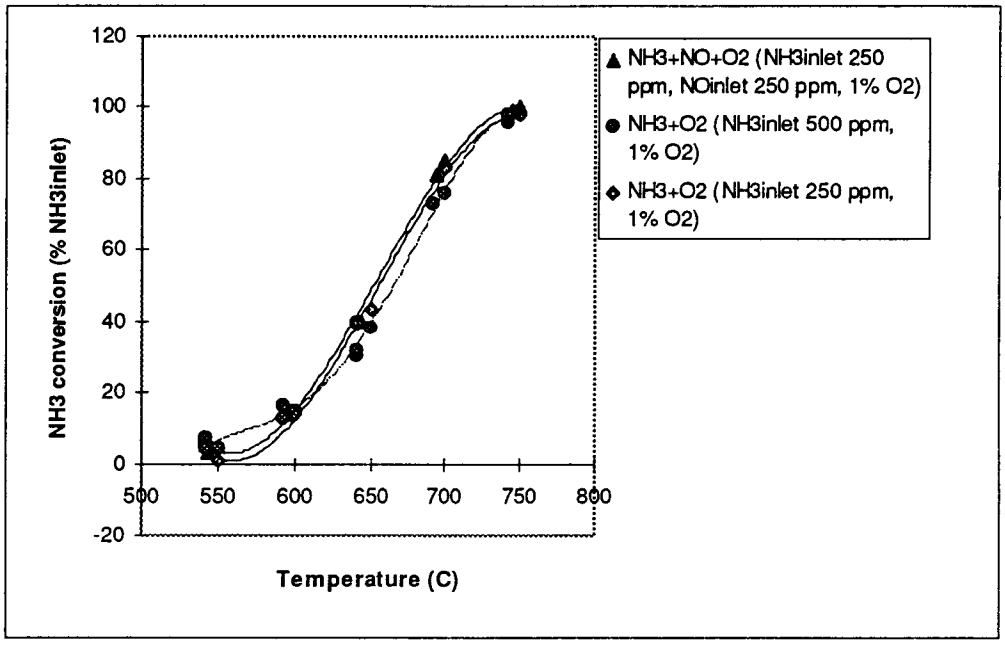

Figure 5.4 NH_3 conversions as a function of temperature of the catalytic reactions NH_3+O_2 and NH_3+O_2+NO, 3.0 ± 0.1 g Na_2CO_3 at a total flow rate of 13 cm^3/s at 25 °C.

almost 100% at 750 °C. For the reaction NH_3+O_2, the conversions of NH_3 with the lower inlet NH_3 concentration (250 ppm) were slightly higher than those in the experiment with the higher inlet NH_3 concentration (500 ppm) at 650 °C (5 percentage points higher) and 700 °C (7 percentage points higher). At other temperatures, there were no differences in the NH_3 conversions between the two sets of experiments. In the reaction NH_3+O_2, NO was found as one of the products. Figure 5.5 shows NO production based on inlet concentration of NH_3 as a function of temperature for the

NH_3+O_2 reaction. The maximum NO detected ranged from 28% to 37% of inlet NH_3 at 750 °C with 500 ppm NH_3 and 1% O_2 and 3.0±0.1 g Na_2CO_3. With 250 ppm NH_3, the maximum NO conversion found at 750 °C was 38% of the inlet NH_3. From the figure,

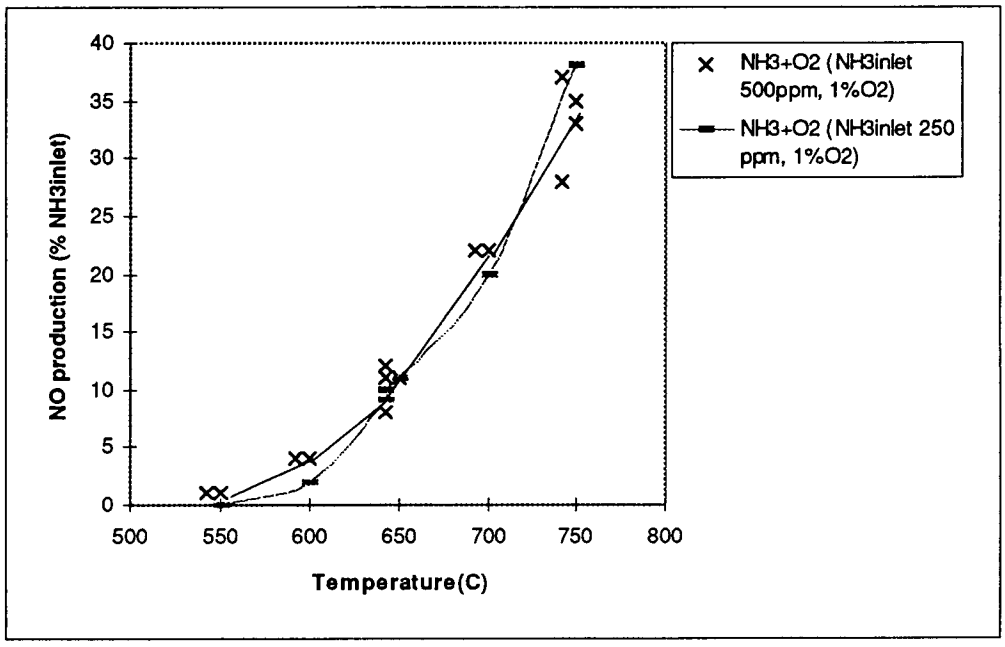

Figure 5.5 NO production as a function of temperature of NH_3+O_2 reactions with two different NH_3 inlets (500 ppm and 250 ppm), Na_2CO_3 3.0 ± 0.1 g at a total flow rate of 13 cm^3/s at 25 °C.

NO productions with both NH_3 inlet experiments yielded almost the same fraction at each temperature. The NO concentrations produced from the 500 ppm inlet of NH_3 were approximately twice those produced from the 250 ppm inlet of NH_3 at each temperature. The highest concentration of NO produced was range from 140 to 184 ppm at 750 °C for the 500 ppm inlet of NH_3, while it was 96 ppm for the 250 ppm inlet of NH_3. The amounts of NO produced were not equal to the amounts of NH_3 converted

since NH_3 could be consumed by other reactions ($NH_3 \rightarrow H_2+N_2$ or $NH_3+NO \rightarrow H_2O+N_2$, for example) and NO could be reduced by NH_3 or the products of NH_3 destruction. Figure 5.6 shows the fraction of moles NO produced per mole of NH_3 reacted. The data from the plot seemed to have higher variation than the data of NO produced based on NH_3 inlet. The possible explanation was that values of the variation were magnified by the smaller values of denominators (NH_3 reacted < NH_3 inlet).

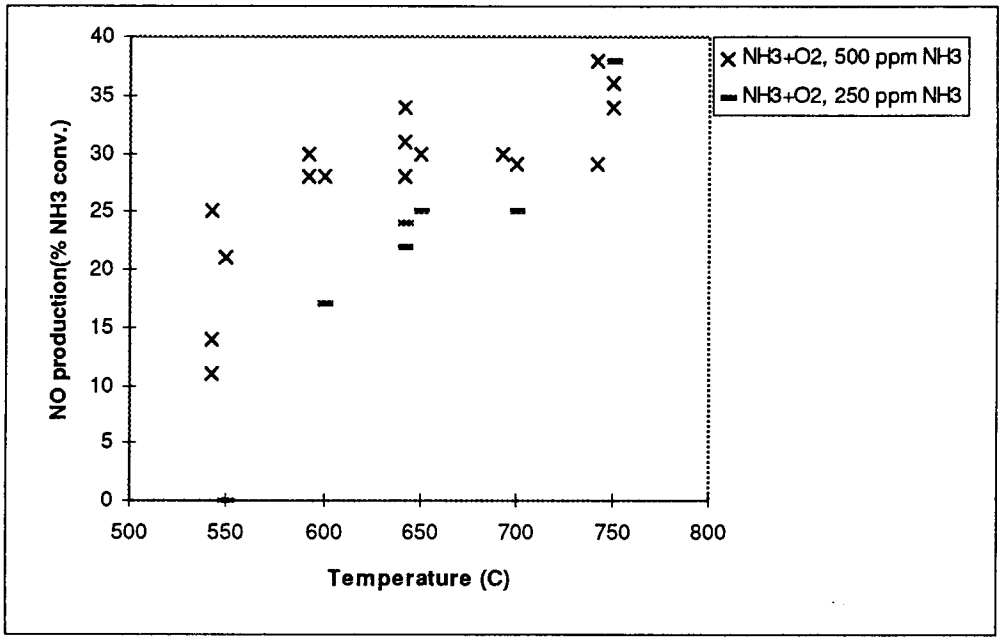

Figure 5.6 Moles NO production per mole NH_3 reacted as a function of temperature of NH_3+O_2 reactions with two different NH_3 inlets (500 ppm and 250 ppm), Na_2CO_3 3.0 ± 0.1 g at a total flow rate of 13 cm^3/s at 25 °C.

However the fractions of moles of NO produced per mole of NH_3 reacted seemed to be constant (average 0.28) at the temperature range 600-700 °C and increase (average 0.35) at 750 °C.

For the reaction of NH_3+O_2+NO, NH_3 inlet concentration and NO inlet concentration were equal at 250 ppm with 1% of O_2 at a total flow rate(13 cm^3/s at 25 °C). At temperatures higher than 550 °C, the conversion of NH_3 was above 10%, and, similar to that of NH_3+O_2 reaction, the highest NH_3 conversion was almost 100% at 750 °C. At other temperatures, the NH_3 conversions were close to those of NH_3+O_2 with inlet NH_3 250 ppm. The NO conversions based on NO inlet (or NH_3 inlet) was shown in Figure 5.3. NO concentration was found to decrease at 550-750 °C. NO conversion, increased at 550-650 °C, was highest (12-17%) at 650-700 °C and decreased at higher temperatures. The possible reason is that, at temperatures higher than 650 °C, the rate of NO reduction was balanced by the rate of NH_3 oxidation to produce NO.

5.2.2 The reactions with Na_2SO_4 as a catalyst in the fixed bed

The amount of Na_2SO_4 used in each experiment was 3.0 ± 0.1 g. All other conditions were the same as in experiments with Na_2CO_3.

5.2.2.1 NH_3 and NH_3+NO reactions

Figure 5.7 shows the NH_3 conversion as a function of temperature for the NH_3 reaction, and that of NH_3+NO. The highest conversion of NH_3 in the decomposition reaction was less than 5%, while for the reaction of NH_3+NO, the highest conversion was 7% at 750 °C. The conversions in the empty bed experiments were 5% for NH_3 and 10% for NH_3+NO. For the NH_3+NO reaction, the outlet concentration of NO did not

change from the inlet concentration at any temperatures studied, which is the same result as in the empty bed. The results indicated that the decomposition of NH_3 or the oxidation of NH_3 by NO were not catalyzed by Na_2SO_4 at the conditions studied.

5.2.2.2 NH_3+O_2 and NH_3+O_2+NO reactions

For the reactions of NH_3+O_2, and NH_3+O_2+NO, the graphs between NH_3 conversion and temperature are shown in Figure 5.8. Only one inlet NH_3 concentration, 500 ppm, was used in the experiments with Na_2SO_4 for the reaction of NH_3+O_2. For

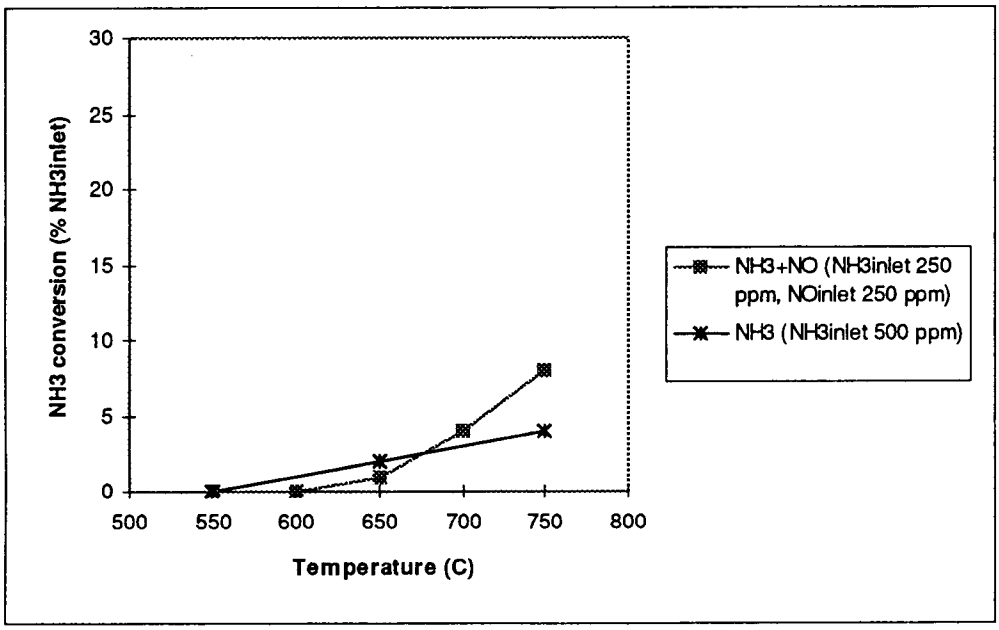

Figure 5.7 NH_3 conversions as a function of temperature for the catalytic reactions of NH_3 and NH_3+NO, 3.0 ± 0.1 g Na_2SO_4, at a total flow rate of 13 cm^3/s at 25 °C.

NH_3+O_2 reaction, the NH_3 conversions were less than 10% and no NO was produced at 700 °C or below. The highest conversion of NH_3 was 17% and the highest NO outlet concentration was 6 ppm (1% of NH_3 inlet) which were higher than the values in the empty bed experiments (8% NH_3 conversion, and no NO produced) at 750 °C. For the reaction NH_3+O_2+NO, 10% of NH_3 inlet or less was converted at 700 °C or below. At 750 °C, the NH_3 conversion was 22% which was higher than the conversion in

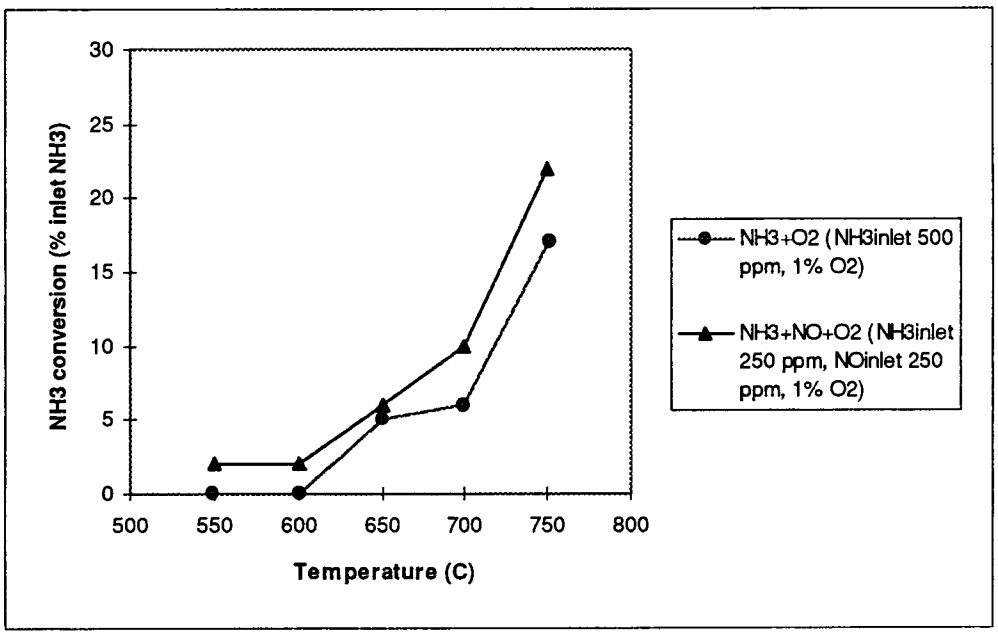

Figure 5.8 NH_3 conversions as a function of temperature for the catalytic reactions NH_3+O_2, and NH_3+O_2+NO, Na_2SO_4 3.0 ± 0.1 g, at a total flow rate of 13 cm^3/s at 25 °C.

the empty bed experiment (15%). The outlet NO concentration was approximately equal to the inlet NO concentration throughout the temperature range (the maximum difference was 3% of NO inlet at 750 °C).

5.2.3 Summary of initial tests

The NH_3 conversion data of the reactions in empty bed indicated that the gas phase reactions or the catalytic effect of the reactor materials could be ignored at 700 °C or below. For the NH_3 and NH_3+NO reactions, the NH_3 conversions in the empty bed were about 25% to 30% of the conversions in the Na_2CO_3 bed and were equal to the conversions in the Na_2SO_4 bed. For the reactions of NH_3+O_2 and NH_3+O_2+NO, the NH_3 conversions in the empty bed were 8% to 15% of the conversions in the Na_2CO_3 bed and were 50% to 70% of the conversions in the Na_2SO_4 bed at 750 °C.

For the experiments in the Na_2CO_3 bed, the reactions of NH_3+O_2 and NH_3+O_2+NO had considerably higher NH_3 consumptions than those of NH_3 and NH_3+NO at temperatures above 550 °C. For the first two reactions, the highest conversions were approximately 100% at 750 °C, while for the latters were 25-30% at 750 °C at the conditions studied. The kinetic data of all the reactions in the Na_2CO_3 bed should be corrected with the empty bed data at 750 °C.

For the experiments in the Na_2SO_4 bed, the reactions of NH_3+O_2 and NH_3+O_2+NO also had higher NH_3 consumptions than those of NH_3 and NH_3+NO at temperatures above 550 °C. For the first two reactions, the highest conversions were 17-22% at 750 °C, while for the latter, the highest conversions were 4-7% at 750 °C. The comparison with the empty bed data suggested that there was no catalytic effect of Na_2SO_4 on the NH_3 and NH_3+NO reactions at any temperature studied, while the catalytic effect on the reactions of NH_3+O_2 and NH_3+O_2+NO initially showed at 750 °C, they were insignificant, comparing to those occurred in the Na_2CO_3 bed.

In conclusion, the data of the NH_3 conversions over fume compound beds, indicated that Na_2CO_3 had higher catalytic effect than Na_2SO_4 did on the reactions at the conditions. So, the kinetics of the reactions in the Na_2CO_3 bed were to be studied.

5.3 Global Catalytic Reaction Rate of NH_3

Kinetic data for each interesting catalytic reaction (all the reactions over Na_2CO_3) was obtained by either differential reactor or integral reactor analysis. The maximum conversion of NH_3 for each reaction was considered the main factor in selecting the interpretation method. Different experiments were used for differential reactor and integral reactor analysis to obtain data for the determination of the reaction orders and the rate constants.

For the reaction of NH_3 and the reaction of NH_3+NO for which the highest percent conversions of NH_3 at the studied experimental conditions were less than 45%, the differential reactor analysis was accepted. The following equation was derived from the NH_3 mole balance in a fixed bed reactor to interpret the experimental data, assuming steady state of the system. The derivation of the equation was shown in Section 4.6 of Chapter 4.

$$\frac{F_{NH3,o} \cdot X_{NH3}}{W} = k' C_{NH3,ave}^{n} \qquad (4.5)$$

$$-r'_{NH3,ave} = k' C_{NH3,ave}^{n}$$

$$\ln(-r'_{NH3,ave}) = \ln k' + n \ln(C_{NH3,ave}) \qquad (4.6)$$

(n= any number)

Equation (4.6) yields the relationship between the average rate of reaction of NH_3 ($-r'_{NH3,ave}$), the average concentration of NH_3 ($C_{NH3,ave}$), the reaction order, and the rate constant for a differential reactor. The experiments were conducted by varying only $C_{NH3,in}$. The experimental results yielded a set of different NH_3 conversions which were used to calculated $-r'_{NH3,ave}$. A graph between $\ln(-r'_{NH3,ave})$ as Y-values and $\ln(C_{NH3,ave})$ as X-values should give a straight line which the slope value equals to the reaction order (n) and the Y-interception can be used to determine the rate constant (k').

For the reaction of NH_3+O_2 and the reaction of NH_3+O_2+NO, the highest percent conversions of NH_3 were almost 100% at the experimental conditions studied. Integral analysis of the integral reactor was used for these reactions. The following equations derived in Section 4.6 in Chapter 4 were used for this analysis method in the interpretation of the experimental data

$$k'\frac{W}{F_{NH3,o}} = \{\frac{1}{(1-n)} - \frac{1}{(1-n)}.(1-X_{NH3})^{(1-n)}\}\frac{1}{C_{NH3,o}^{n}} \qquad (4.3)$$

$$\text{Define } Y_{nth} = \{\frac{1}{(1-n)} - \frac{1}{(1-n)}.(1-X_{NH3})^{(1-n)}\}\frac{1}{C_{NH3,o}^{n}}$$

(n= any number except 1)

$$k'\frac{W}{F_{NH3,o}} = -\ln(1-X_{NH3})\frac{1}{C_{NH3,o}} \qquad (4.4)$$

$$\text{Define } Y_{1st} = -\ln(1-X_{NH3})\frac{1}{C_{NH3,o}}$$

(n= 1)

Equations (4.3) and (4.4) relate the conversion of NH_3, the reaction order, the rate constant, and other experimental variables such as weight of catalyst used in the reactor

(W), feed rate of NH_3 ($F_{NH3,o}$), etc., for the integral analysis of integral reactor. The experiments were performed by varying W, while other experimental variables were kept constant. The experimental results yielded a set of different NH_3 conversions which were used to calculated the right hand sides of Equation (4.3) with an input value of the n^{th} order and of Equation (4.4) defined as Y_{nth} and Y_{1st}, respectively. For the n^{th} order reaction, a plot of Y_{nth} as Y-values and $W/F_{NH3,o}$ as X-values should give a straight line going through the origin which the slope equals to the rate constant (k'). For the 1^{st} order reaction, a plot of Y_{1st} as Y-values and $W/F_{NH3,o}$ as X-values also yields the same line as characteristics.

5.3.1 Reaction order test

5.3.1.1 Reaction of NH_3

The experiments to find the reaction order were performed by varying the inlet concentration of NH_3 from 115 to 500 ppm for the same total flow rate (13.0 cm^3/s at 25 °C). The reactor temperature was set at 750 °C. The amount of Na_2CO_3 used was 3.0 g. The data of the NH_3 conversions from the different NH_3 inlet concentrations are shown in Table 5.1. It was found that the NH_3 conversions depended on the inlet concentrations of NH_3. The lower the concentration of NH_3, the higher the conversion of NH_3 was. This implied that the reaction order was lower than first order. The plot of $\ln(-r'_{NH3,ave})$ and $\ln(C_{NH3,ave})$ according to Equation (4.6) for the differential reactor

analysis is shown in Figure 5.9. The reaction order value obtained is 0.53 with respect to NH_3 concentration.

Table 5.1 Results of NH_3 conversions from the different NH_3 inlets with 3.0±0.1 g, Na_2CO_3 total flow of 13.0 cm^3/s 25 °C, at reactor temperature 750 °C

NH_3 inlet concentration (ppm)	NH_3 conversion (%)
455	26
453	25
274	27
243	34
115	45

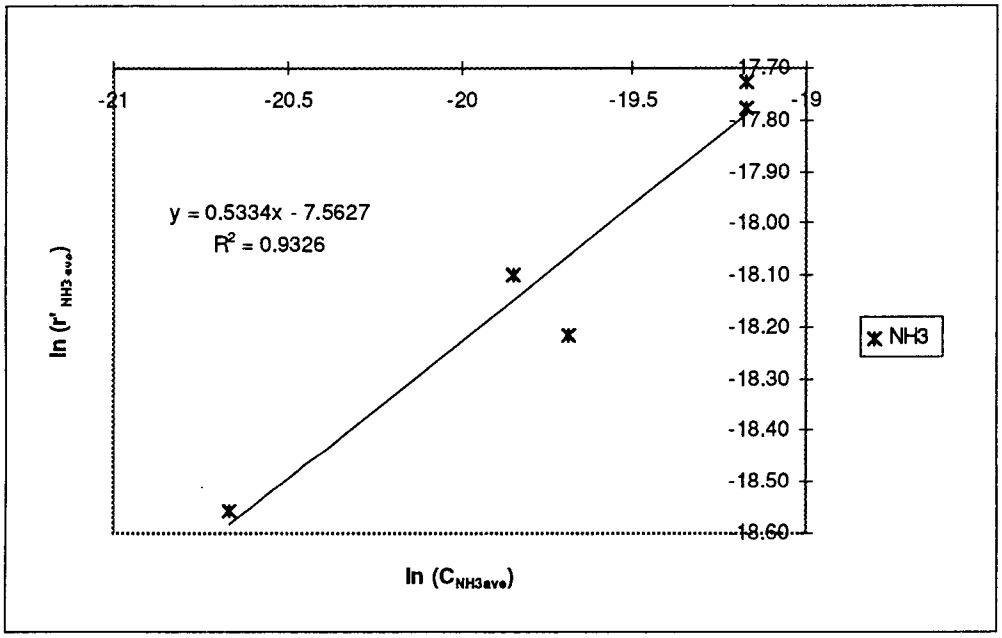

Figure 5.9 Differential reactor analysis of the NH_3 reaction with NH_3 = 115 to 500 ppm, and 3.0 ± 0.1 g Na_2CO_3, total flow 13.0 cm^3/s 25 °C at 750 °C.

5.3.1.2 Reaction of NH_3+NO

The effect of NO on the NH_3 conversions was tested by varying the inlet concentration of NO from 0 to 1253 ppm, while the inlet concentration of NH_3 was kept constant at 250 ppm. The total flow rate was 13 cm^3/s at 25 °C and the experimental temperature was 750 °C. The amount of Na_2CO_3 used was 3.0±0.1 g. Figure 5.10.1 shows the relationship between NH_3 conversion, and NO conversion and the inlet concentration of NO used in the experiments. The NH_3 conversion varied from 28% (average point at 250 ppm NO) to 34% (the conversion dropped initially from 34 to 28% when NO concentration was changed from 0 to 250 ppm). As the concentration was further increased from 250 to 1250 ppm, the NH_3 conversion increased from 28-34%. One possible explanation for this behavior is that, initially, when NO is added, the rate of NO disappearance decrease because NO occupies catalytic sites and prevent NH_3 from adsorbing on them. As NO concentration is further increased, the rate of the reaction NH_3+NO increases and the overall effect is that the rate of NH_3 disappearance increases. For the purpose of this work, however, it seemed that the effect of NO on the NH_3 conversion was insignificant. So the global rate of NH_3+NO obtained was based on only NH_3 concentration. The NO conversion is shown in the same figure. The moles of NO consumed per mole of NH_3 consumed varied from 0.58-0.93, being the highest at high NO concentration. The explanation of the effect of NO on NO conversion is given in the section of NO analysis in the reaction NH_3+NO (Section 5.4).

Experiments in which the inlet concentration of NH_3 was varied, were conducted at the same condition (750 °C). The NH_3 inlet concentration was varied from 150 to 400

ppm while the inlet concentration of NO was constant at 250 ppm. Figure 5.10.2 shows the relationship between NH_3 conversion and NO conversion, and the inlet concentration of NH_3 used in the experiments. It is found for this reaction as well that the conversion of NH_3 depended on the inlet concentration of NH_3. The NH_3 conversion was lower when the inlet concentration of NH_3 was higher. This suggests a reaction order which is

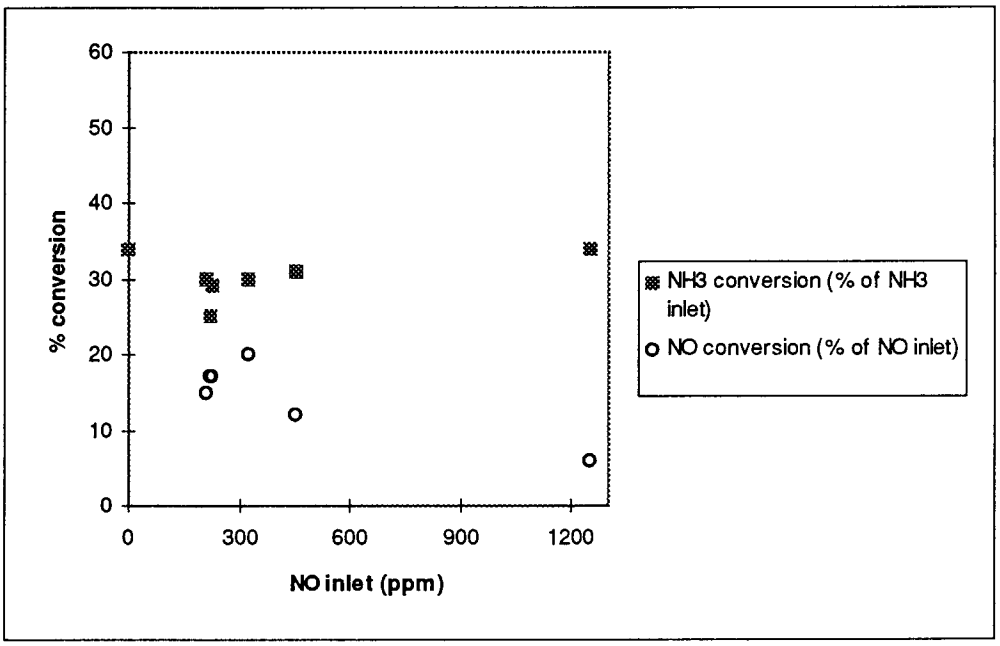

Figure 5.10.1 Effect of NO inlet on NH_3 conversion and NO conversion of the NH_3+NO with 0-1250 ppm NO, 250 ppm NH_3, and 3.0±0.1g Na_2CO_3, flow rate 13 cm^3/s at 25 °C at 750 °C

lower than first order. The relationship between $-r'_{NH3,ave}$ and $C_{NH3,ave}$ according to Equation (4.6) is illustrated in Figure 5.11. The global reaction order from the plot in Figure 5.11 is 0.48 with respect to NH_3 concentration. The reaction order found seemed

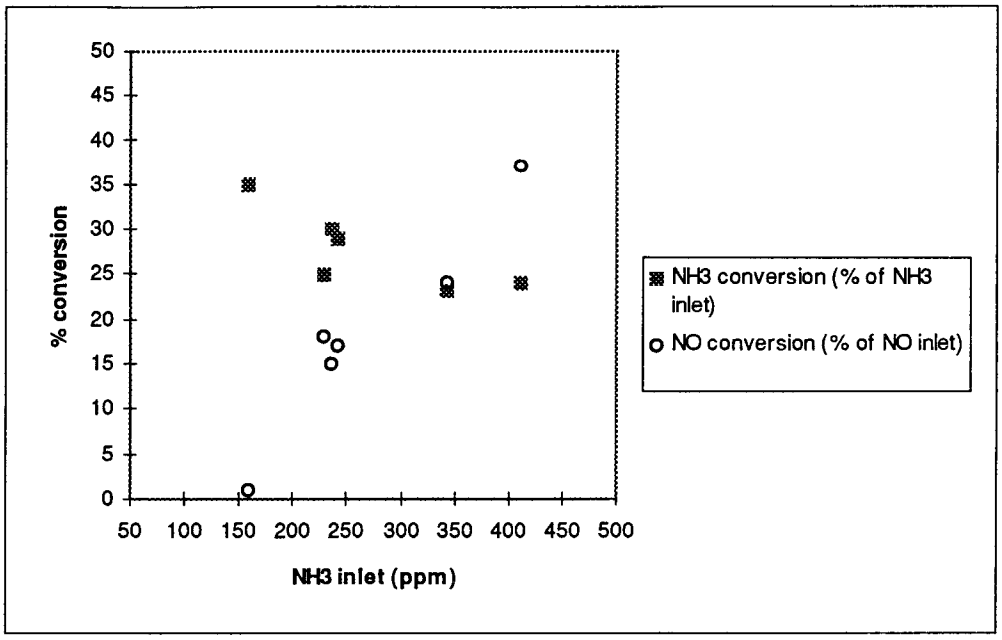

Figure 5.10.2 Effect of NH_3 inlet on NH_3 conversion and NO conversion of the NH_3+NO with 150-400 ppm NH_3, 250 ppm NO, and 3.0±0.1g Na_2CO_3, flow rate 13 cm^3/s at 25 °C at 750 °C

to be insignificantly different from that of the reaction NH_3, thus the reaction order of NH_3+NO was accepted to be 0.53 for the purpose of reaction rate comparison.

5.3.1.3 Reaction of NH_3+O_2

According to Equation (4.3) and (4.4), the kinetics of the NH_3+O_2 were obtained by the experiments in which the amount of Na_2CO_3 (W) was varied. The weight ranged from 0.38 to 1.53 g. The inlet concentration of NH_3 used was 500 ppm with 1% O_2 at a total flow rate of 13.0 cm^3/s at 25 °C for all runs. The temperature was 750 °C. The method of trial and error was used for the n^{th} order reaction to find the order of reaction

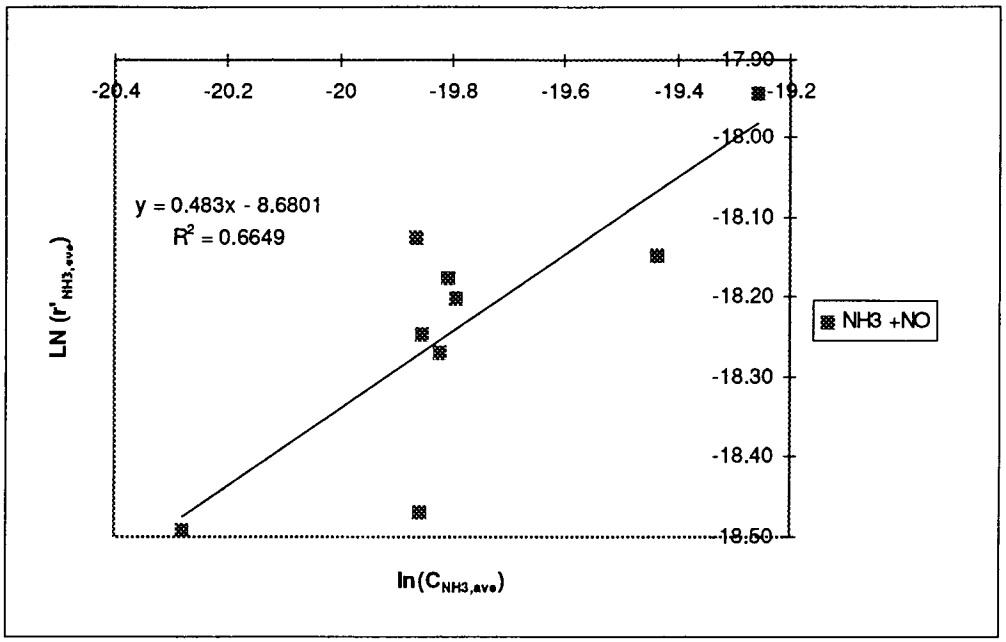

Figure 5.11 Differential reactor analysis of the NH_3+NO reaction with 115-400 ppm NH_3, 250-1250 ppm NO, and 3.0±0.1g Na_2CO_3, flow rate 13 cm^3/s at 25 °C at 750 °C

(n) which gave the highest value of R^2 for a straight line through origin for a plot between Y_{nth} and $W/F_{NH3,o}$ (shown in Figure 5.12). The order of 1.27 with respect to NH_3 was found. However for the first order reaction plot, R^2 is not significantly different from that for the 1.27^{th} reaction order(shown in Figure 5.13). Within the uncertainty of the data, the first order reaction with respect to NH_3 seems to be acceptable.

5.3.1.4 Reaction of NH_3+O_2+NO

The experiments were similarly performed by varying the amount of Na_2CO_3 from 0.38 to 1.53 g, while the inlet concentration of NH_3 and that of NO were equal to 250 ppm with 1% O_2 at a total flow rate of 13.0 cm^3/s at 25 °C. The temperature of the

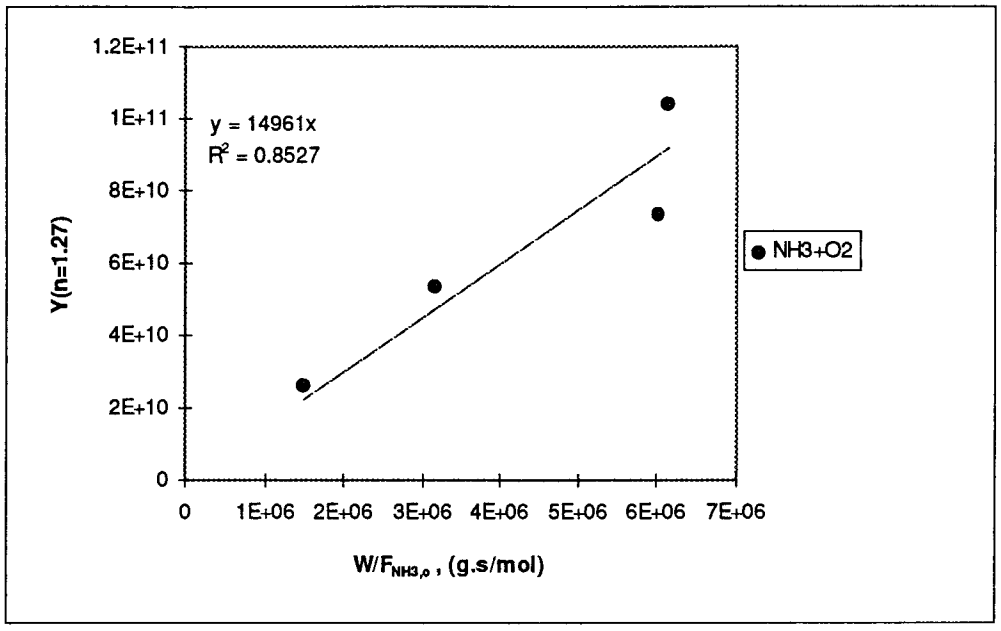

Figure 5.12 Integral analysis of the NH_3+O_2 reaction (n=1.27) with 500 ppm NH_3, 1%O_2 0.38-1.53 g Na_2CO_3, 13 cm^3/s (25 °C), at 750 °C

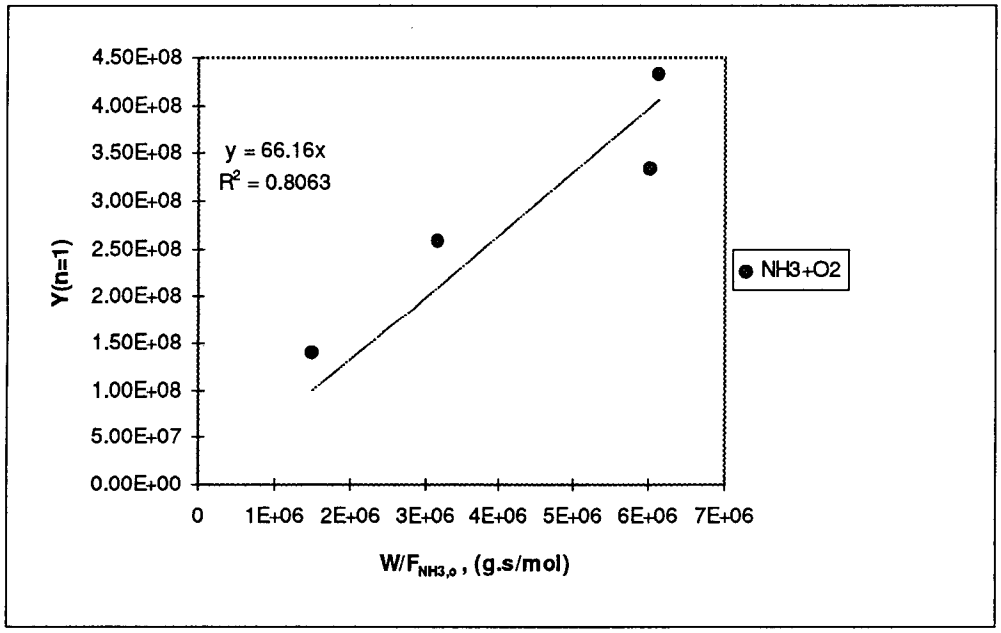

Figure 5.13 Integral analysis of the NH_3+O_2 reaction (n=1) with 500 ppm NH_3, 1%O_2 0.38-1.53 g Na_2CO_3, 13 cm^3/s (25 °C), at 750 °C

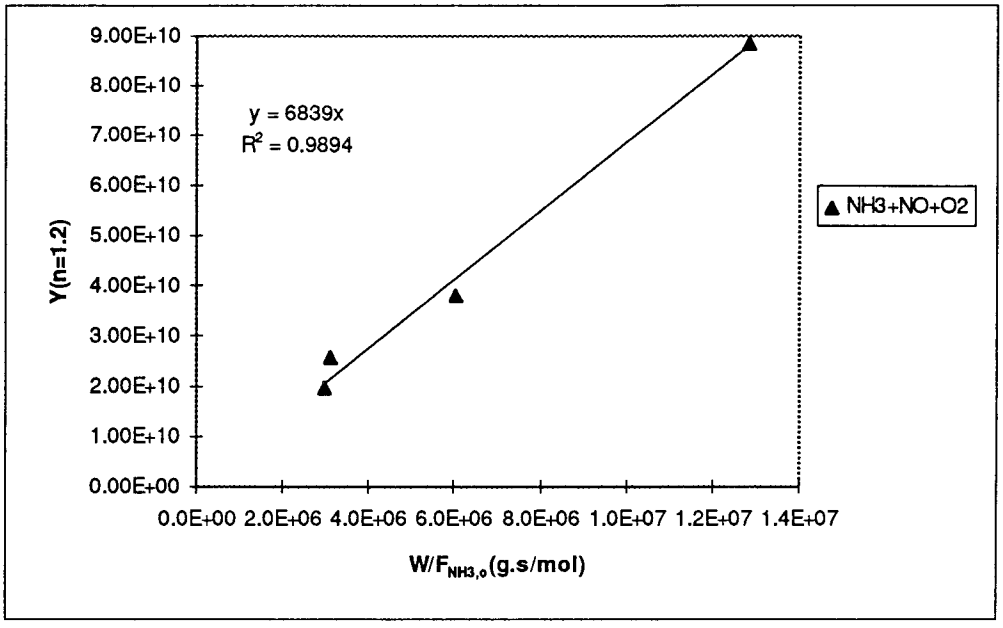

Figure 5.14 Integral analysis of the NH_3+O_2+NO reaction (n=1.2),with NH_3 = 250 ppm NO = 250 ppm, 1% O_2, 3.0±0.1g Na_2CO_3, 13 cm^3/s (25 °C), at 750 °C

reactor was 750 °C. The method of trial and error for the n^{th} order reaction was used. Figure 5.14 shows the result for the reaction order of 1.2 with respect to NH_3 which gave the best fit to the experimental data (highest value of R^2). The fit of the first order reaction expression (shown in Figure 5.15) did not give a R^2 value significantly different from that of the 1.2^{th} reaction order. Within the uncertainty of the data, the first order reaction with respect to NH_3 is acceptable.

5.3.2 Examination of mass transfer effects on the global reaction rate

An intrinsic rate of reaction can be obtained when the chemical kinetic rate controls the overall rate of reaction. Two types of mass transfer processes which may

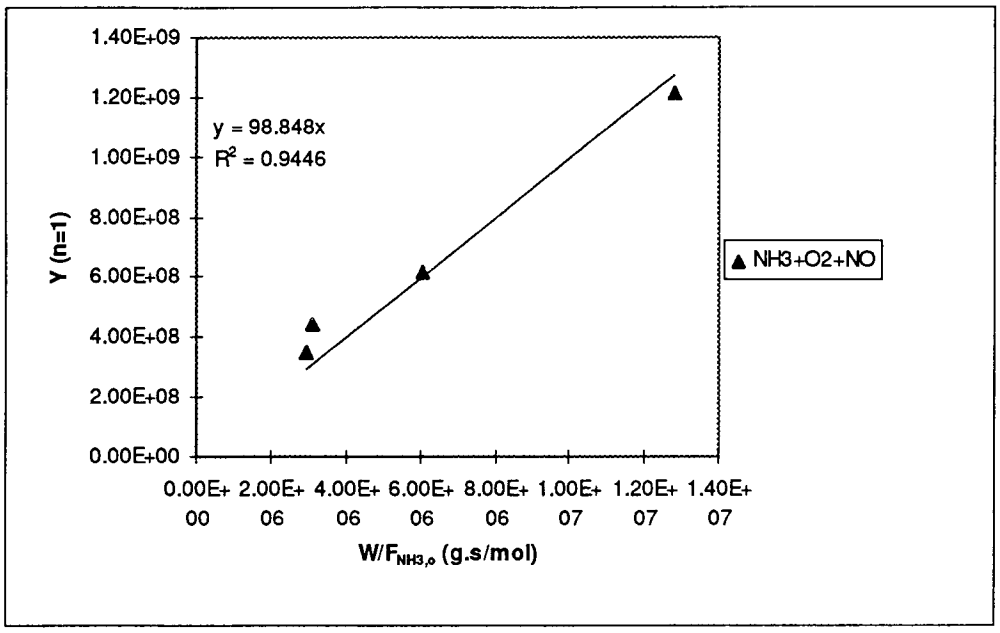

Figure 5.15 Integral analysis of the NH_3+O_2+NO reaction (n=1), with NH_3 = 250 ppm NO = 250 ppm, 1% O_2, 3.0±0.1g Na_2CO_3, 13 cm^3/s (25 °C), at 750 °C.

affect the reaction rate in a porous solid catalyst, are film mass transfer and pore diffusion. In this study, the effect of film mass transfer process was investigated by both experiments and a theoretical criterion (Mears' criterion, Fogler, 1992). The tests were conducted at the temperature which yielded the highest rates of reaction (750 °C). The amount of catalyst and the total flow rate were reduced to half of the values used in the kinetic data experiment. This condition yielded the same residence time but a differentgas velocity. The reaction NH_3+O_2 was chosen for the test of the film mass transfer effect. Other reactions studied were investigated by using the rate of reactions from the experimental data to evaluate the Mears' criterion. The effect of pore diffusion

was examined by the Weisz-Prater criterion (Fogler, 1992). The experimental data of all the studied reactions were used to evaluate the satisfaction of the Weisz-Prater criterion.

The results of the test for the mass transfer effect and the calculations are shown in Table 5.2. For the film mass transfer resistance test of the NH_3+O_2 reaction, the higher gas velocity gave a higher NH_3 conversion (2-4 percentage points higher). The

Table 5.2 The evaluation of mass transfer effects of the reactions at 750 °C

Reaction	$Weight_{cat.}$ W, g	Total Flow rate, cm^3/s	NH_3 ,ppm inlet	% NH_3 converse.	Mears' criterion	Weisz-Prater criterion
NH_3+O_2	1.53	6.3	488	94	0.0042	0.039
	1.53	6.3	488	96	0.0042	0.039
	3.09	12.3	475	98	0.0028	0.037
NH_3+O_2+NO	3.05	13.2	241	99	0.0041	0.055
NH_3	3.07	12.7	451	25	0.0001	0.002
NH_3+NO	3.09	12.5	236	30	0.0001	0.002

the Mears' criterion < 0.15, no film mass transfer limitation
the Weisz-Prater criterion << 1, no pore diffusion limitation

variation in the NH_3 conversions could have been caused by the effect of mass transfer or the uncertainty in the data since the difference was of the same order as the uncertainty in the measurement (Section 5.6). However, the Mears' criterion was satisfied for all the reactions studied at 750 °C. For the investigation of pore diffusion control, the Weisz-Prater criterion was satisfied for all the reactions studied at 750 °C. In conclusion the mass transfer effects could be ignored at 750 °C. For the conditions at temperatures lower than 750 °C, the reaction rates are slower, which causes the mass

transfer effects to be less important, too. So, it can be concluded that neither film transfer control nor pore diffusion control are important at the experimental conditions studied.

The calculation of Mears' criterion and the Weisz-Prater criterion are shown in Appendix E and Appendix F, respectively.

5.3.3 Kinetic rate constants and Arrhenius plots

The experiments in the empty bed showed the possibility of gas phase reactions occurring at 750 °C. So the rate constants obtained from the performance equations are the total rate constant (k'_{total}) which should be correlated with the rate constants of the gas phase reactions (k_{empty}) for the data points at 750 °C. With the assumption that the reactions in the gas phase have the same reaction order as the catalytic reactions, Equation (5.1) shows the correlation of the rate constant as described.

$$k'_{total} = k' + V_{zone}/W * k_{empty} \qquad (5.1)$$

where

k'_{total} = observed kinetic rate constant, $(cm^3)^n/mol^{(n-1)}.g.s$

k' = kinetic rate constant of the catalytic reaction, $(cm^3)^n/mol^{(n-1)}.g.s$

k_{empty} = kinetic rate constant of the gas phase reaction, $(cm^3/mol)^{(n-1)}/s$

where

n = reaction order

V_{zone} = volume of the gas phase reaction zone, cm^3

$= \pi*(d_r/2)^2*h_r = 31\ cm^3$

d_r = diameter of reactor, cm = 1.3 cm

h_r = the length of reactor which has uniform temperature, cm = 23 cm

W = weight of catalyst used in the catalytic reaction, g

The values of k_{empty} for each reaction are calculated from the reaction rate equation of homogeneous reaction with differential reactor analysis. The equations are shown here:

$$-r'_{NH3,ave} = k_{empty}*(C_{NH3,ave})^n \quad , mol/cm^3.s$$

$$F_{NH3,o}*X_{NH3}/V_{zone} = k_{empty}*(C_{NH3,ave})^n \quad (5.2)$$

The value of k_{empty} of the reactions at 750 °C are shown in Table 5.3. At other temperatures, the reaction in the empty bed reaction was insignificant.

Table 5.3 k_{empty} of the reactions at 750 °C

Reaction	k_{empty}
NH_3 (n=0.53)	$1.00*10^{-5}$, $(mol/cm^3)^{(0.47)}/s$
NH_3+NO (n=0.53)	$1.30*10^{-5}$, $(mol/cm^3)^{(0.47)}/s$
NH_3+O_2 (n=1)	0.12 , 1/s
NH_3+O_2+NO (n=1)	0.23 , 1/s

5.3.3.1 Reactions NH_3 and NH_3+NO

Since differential analysis according to Equation (4.6) was used for both reactions, the method of calculation of the kinetic rate constant is the same. The reaction orders of the reactions (n = 0.53 for the NH_3 and the NH_3+NO) which were derived at

750 °C, are assumed to be valid at other temperatures studied (550-700 °C). At each temperature, the data from the experiments are directly inserted into the correlation equation (4.6), and the rate constants (k') are calculated. Except at 750 °C, the value of rate constant obtained is the total rate constant (k'_{total}). Once k'_{total} is known, k' can be calculated from Equation (5.1). Both the rates of reaction and rates constant used in this study are based on weight of catalyst. The units of the reaction rate and the rate constant are the same for all reactions (mol/g.s), according to the same reaction order. The temperature dependencies of the reaction rate coefficients according to Arrhenius' law can be illustrated by a plot between ln(k') and 1/T. The slope contains the term of the activation energy of the reaction (E, kJ/mol). Figure 5.16 shows the Arrhenius plot of both reactions.

The results shows that the activation energy of the decomposition of NH_3 is 98±3 kJ/mol (95% confidence interval), while the activation energy of the NH_3 oxidation by NO is 103±6 kJ/mol (95% confidence interval) in the temperature range studied. Since the kinetic data of the reactions indicates that neither the n^{th} orders nor the activation energies are significantly different, the change of the reaction order of the NH_3+NO to be the same as that of the NH_3 would make no critical error. The average reaction rate constants at each temperature studied are shown in Table 5.4. The reaction rate constant data shows that the rate of NH_3 decomposition is slightly faster than the rate of the reaction NH_3+NO at the temperatures studied.

The kinetic data of the reactions can be summarized as follows: the reaction orders with respect to NH_3 and the activation energy values are apparently the same

(0.53^{th} order with E = 98±3 kJ/mol for the decomposition of NH_3 and the NH_3 oxidation by NO). NO consumption in the reaction NH_3+NO was also present but the rate of NH_3 disappearance was independent of the NO concentration. One explanation is that NO

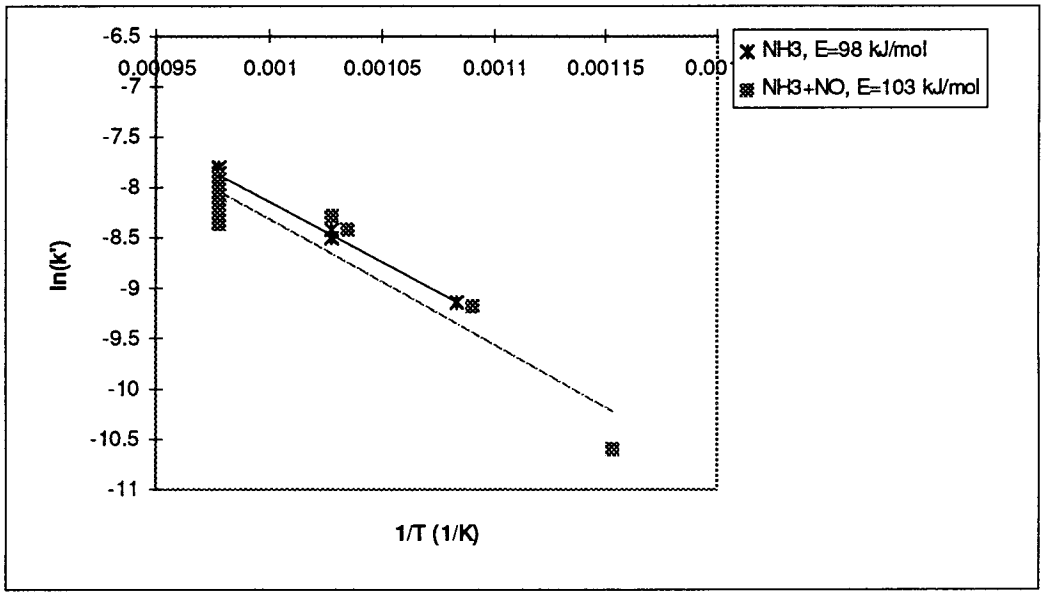

Figure 5.16 The temperature dependencies of the rate constants according to Arrhenius' Law for the NH_3 reaction (n=0.53), at NH_3 = 500 ppm, and the NH_3+NO reaction (n=0.53), at NH_3 = 150-400 ppm, NO = 250 to 1250 ppm, in the studied temperature ranges

Table 5.4 The average reaction rate constants of the NH_3 reaction and the NH_3+NO reaction with Na_2CO_3 at temperatures studied

Temperature, °C	**Reaction of NH_3 k', $(mol^{0.47} (cm^3)^{0.53}/g.s)$**	**Reaction of NH_3+NO k', $(mol^{0.47}(cm^3)^{0.53}/g.s)$**
550	-*	-*
600	-*	$3.90*10^{-5}$
650	$1.08*10^{-4}$	$8.40*10^{-5}$
700	$2.09*10^{-4}$	$1.67*10^{-4}$
750	$3.80*10^{-4}$	$3.11*10^{-4}$

Note: (*) no reaction observed at the temperature

may be reduced by the products of NH_3 decomposition (H_2).The details of a rate of NO reduction in the NH_3+NO are illustrated and discussed in the NO analysis in the NH_3+NO in Section 5.4.

5.3.3.2 Reactions NH_3+O_2 and NH_3+O_2+NO

The rate constants of the two reactions can be obtained by Equation (4.5) for first order reaction in an integral reaction. The experimental data at each temperatures are used to calculate the rate constants separately. At 750 °C, the total rate constant (k'_{total}) is used to calculate the catalytic rate constants (k') from Equation (5.1). The temperature dependencies of the rate constants according to Arrhenius' law are shown in Figure 5.17. The rate constants of both reactions at different temperatures are exhibited in Table 5.5. In the Arrhenius plot, the two reactions seem to be almost indistinguishable. The activation energy value of NH_3+O_2 is 170±23 kJ/mol and that of NH_3+O_2+NO is 185±42 kJ/mol. Considering from the reaction rate constant, the reaction rates of NH_3+O_2+NO at NO inlet 250 ppm are slightly higher than those of NH_3+O_2 at temperatures above 600 °C.

5.4 Analysis of NO in the Reaction NH_3+NO

Nitric oxide (NO) is the other interesting species in this study as one of the reactants and/or the products of NH_3 oxidation.

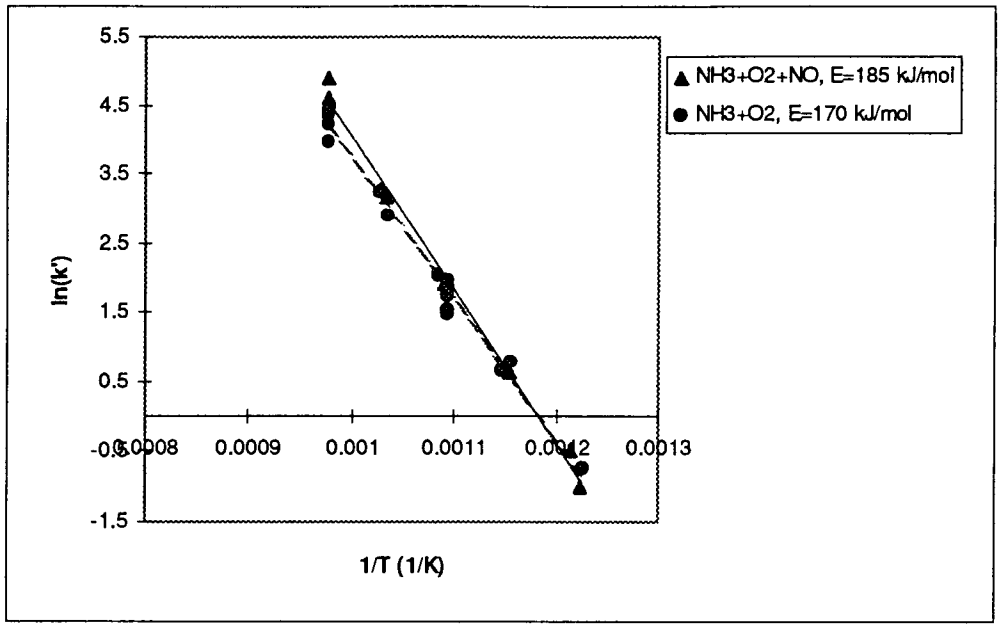

Figure 5.17 The reaction rate constants of the NH_3+O_2 reaction (n=1), at 500 ppm and 250 ppm NH_3 with 1% O_2, and the NH_3+O_2 +NO reaction (n=1), at NH_3 250 ppm, NO 250 ppm and 1% O_2, with Na_2CO_3 at temperatures studied

Table 5.5 The reaction rate constants of the NH_3+O_2 reaction and the NH_3+O_2+NO reaction at NO inlet 250 ppm with Na_2CO_3 at temperatures studied

Temperature, °C	**Reaction of NH_3+O_2 k', $(cm^3)/g.s$**	**Reaction of NH_3+O_2+NO k', $(cm^3)/g.s$**
550	0.498	0.483
600	2.06	2.27
650	7.30	9.02
700	22.7	31.1
750	63.3	95.0

The results of NO conversion shown in Figure 5.10.1 and Figure 5.10.2 indicated that the NO conversion was increased by an increase in NH_3 inlet concentration and was

decreased by an increase in NO inlet concentration at 750 °C (with the exception of the measurement at 322 ppm NO). With 250 ppm NH_3 and 250 ppm NO, the highest NO conversion was 18% at 750 °C. This makes NO reduction in the presence of NH_3 over Na_2CO_3 interesting.

The kinetics of the rate of NO consumption was found by differential analysis (Equation 4.5) since the highest NO conversion was less than 45%. The method was the same as that for the rate of NH_3 consumption. First, the reaction order of NO reduction with respect to NH_3 concentration was studied by experiments in which NO was kept constant at 250 ppm and NH_3 was varied from 150 to 400 ppm with 3.0±0.1 g Na_2CO_3

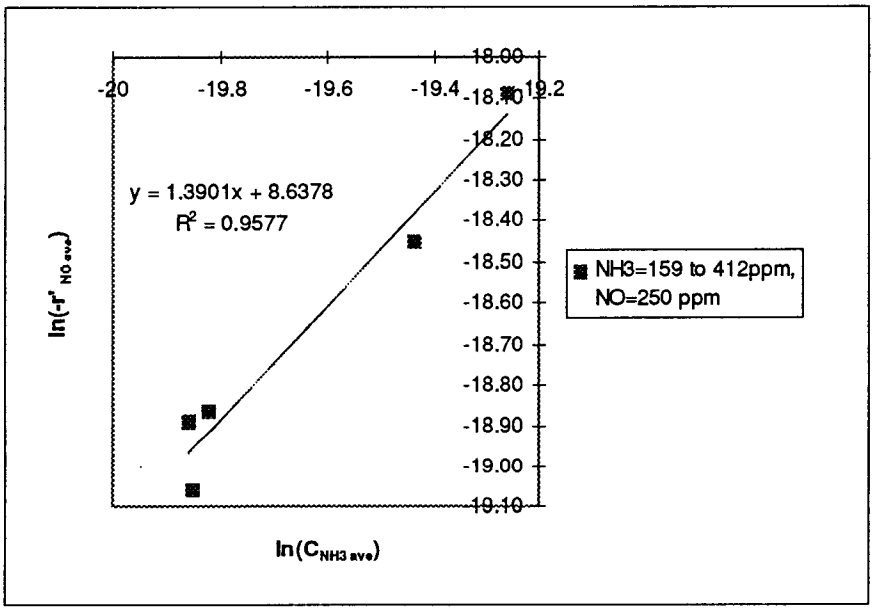

Figure 5.18.1 The plot to find the reaction order with respect to NH_3 concentration for the reaction NH_3+NO with 150-400 ppm NH_3, 250 ppm NO, and 3.0 g Na_2CO_3 at 750 °C.

at 750 °C. The slope of a plot between $\ln(-r'_{NO,ave})$ and $\ln(C_{NH3,ave})$ is equal to the reaction order (n th) with respect to NH_3 inlet concentration (shown in Figure 5.18.1). The order with respect to NH_3 was found to be 1.4. The reaction order of NO reductionwith respect to NO was tested by experiments in which NH_3 was constant at 250 ppm and NO was varied from 250 to 1250 ppm with 3.0±0.1 g Na_2CO_3 at 750 °C. The plot between $\ln(-r'_{NO,ave})$ and $\ln(C_{NO,ave})$ yields the slope as the value of reaction order (n th) with respect to NO inlet concentration (shown in Figure 5.18.2). The order with respect to NO was found to be 0.4. The reaction rate constants at different temperatures were found from the reaction rate equation:

$$-r'_{NO,ave} = k' (C_{NH3,ave})^{1.4} (C_{NO,ave})^{0.4} \qquad (5.3)$$

where $-r'_{NO,ave}$ = average rate of reduction of NO, mol/g.s

k' = reaction rate constant of NO reduction, $(cm^3)^{1.8}/mol^{0.8}.g.s$

$C_{NH3,ave}$ = average concentration of NH_3, mol/cm^3

$C_{NO,ave}$ = average concentration of NO, mol/cm^3

The rate constant obtained at 750 °C did not need to be corrected by k_{empty} because no NO consumption occurred in the empty bed experiments. The temperature dependency according to Arrhenius' law is shown in Figure 5.19. The activation energy from the plot is 100±24 kJ/mol (95% confidence interval). The activation energy found was close to that of the rate of NH_3 disappearance in the reaction NH_3+NO (103±6 kJ/mol). The average rate constants at different temperature are shown in Table 5.6. The result of kinetics indicates that the NO consumption rate depends more on the NH_3 than the NO concentration.

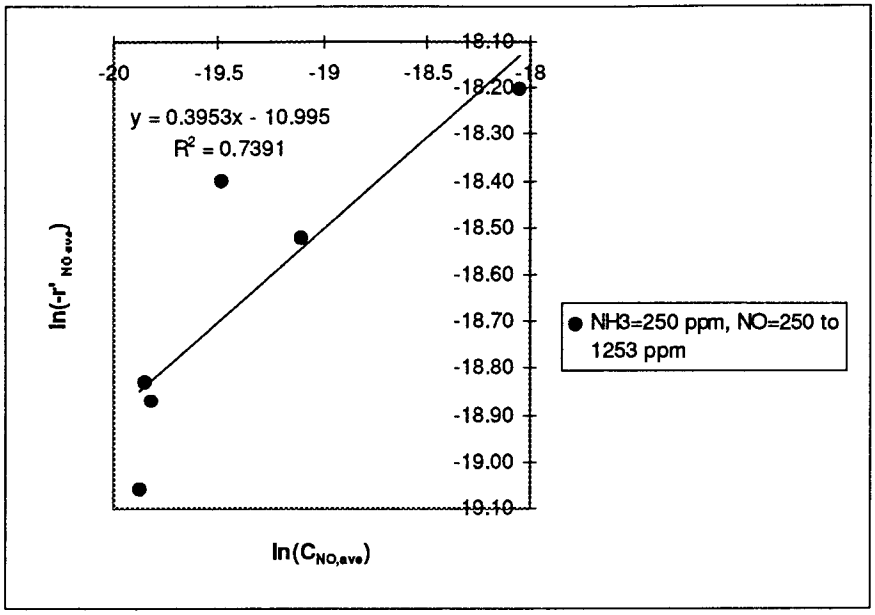

Figure 5.18.2 The plot to find the reaction order with respect to NO concentration for the reaction NH_3+NO with 250 ppm NH_3, 250-1250 ppm NO, and 3.0 g Na_2CO_3 at 750 °C.

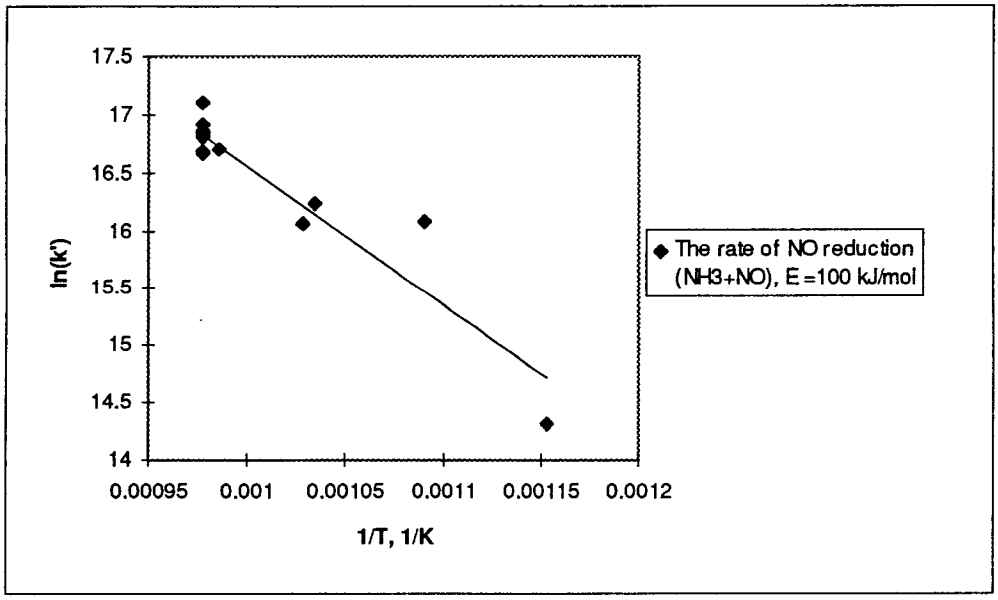

Figure 5.19 Temperature dependency of the rate of NO reduction according to Arrhenius' law for the reaction NH_3+NO at the temperatures studied.

Table 5.6 The NO reaction rate constants of the NH_3+NO reaction with NH_3 150 to 400 ppm, NO 250 to 1250 ppm and 3.0± 0.1 g Na_2CO_3 at temperatures studied

Temperature, °C	**Reaction of NH_3 +NO k', $(cm^3)^{1.8}/g.s.mol^{1.8}$**
550	-
600	$2.74*10^6$
650	$5.79*10^6$
700	$1.13*10^7$
750	$2.07*10^7$

5.5 Prediction of the Importance of NH_3 Oxidation Catalyzed by Fume Species in a Recovery Boiler

In this section, data of a typical recovery boiler were combined with laboratory data to roughly estimate the importance of NH_3 oxidation by fume species in a recovery boiler. The detailed calculations to estimate the fraction of NH_3 oxidized by fume compounds in a recovery boiler are shown in Appendix G. The recovery boiler data used are shown in Table G.1. The estimation was limited to the data set shown only.

First, a potential reaction zone of NH_3 oxidation by fume compounds in a recovery boiler was defined. The experimental results indicated that the catalytic activity of Na_2CO_3 was substantially higher than that of Na_2SO_4 in promoting NH_3 oxidation at the temperatures studied (600 to 750 °C), while the oxidation data were insignificant over both Na_2CO_3 and Na_2SO_4 at 550 °C. If it is assumed that the reaction mechanisms were the same at higher temperatures (> 750 °C), the possible reaction zone could be the location in the boiler where fume particles are primarily composed of Na_2CO_3 and the

temperature is higher than 550 °C. It has been found that the fraction of Na_2SO_4 in submicron fume particles increases as the furnace height increases, as referenced in Section 3.2 in Chapter 3. Na_2CO_3 was almost the only component in fume particles found above the char bed surface, while Na_2SO_4 was the major component of fume at the outlet of the boiler. The Na_2SO_4 content in fume particles was 64% at the tertiary air level while at the furnace outlet it was 96% Na_2SO_4 (Rizhinshvili and Kaplun, 1983). The gas phase above the char bed contains mostly N_2, CO_2, O_2, and H_2O with only a small amount of SO_2 (1 ppm) and thus very little Na_2SO_4 is formed (Borg et al., 1974). The concentration of SO_2 in the gas phase increases significantly near the tertiary air level and is enough to convert Na_2CO_3 to Na_2SO_4 gradually. The average furnace gas temperature is about 1100 °C in the lower furnace (for black liquor loading of 0.18 $kg/s.m^2$) (Adams and Frederick, 1985). Thus the possible reaction zone was defined to be from the char bed surface to the tertiary air level. The average residence time in this reaction zone was 1.3 s for a black liquor loading of 0.18 $kg/s.m^2$.

Second, each fume particle was assumed to be a spherical liquid droplet. The temperature of the flue gases in the reaction zone (1100 °C) was higher than the melting point of Na_2CO_3 (850 °C). In fact, the fume may be molten at lower temperatures as well because of eutectics formed with other fume species. Mikkanen et al.(1994) studied particle size and chemical species distributions of aerosols generated during kraft black liquor pyrolysis and combustion. In experiments conducted in a recovery boiler with two different black liquor sources (hardwood, and softwood), the dominant fume particle size was 0.7 μm on an average. The diameter of the fume droplets in the boiler was

assumed to be 0.7 μm. The rate of fume generation in recovery boilers is not known. Borg et al. (1974) reported that, on average, 9% of Na fed into the boiler becomes fume. The average 68% of the fume was taken to be Na_2CO_3 within the reaction zone. This gave 391 g/s as the total amount of Na_2CO_3 generated in a boiler with the firing rate 14.22 kg BLS/s which also yielded the total surface area of $1.8*10^7$ cm^2/s.

The amount of NH_3 released during black liquor combustion in a recovery boiler was estimated based on the study of Aho et al.(1993). The study suggested that depending on the type of liquor, 10-30% of fuel nitrogen in black liquor was released as NH_3. The average nitrogen content of kraft black liquors is about 0.11% weight of dry solids (Nichols et al., 1993). The total amount of the flue gas generated is 664 kg/ 100 kg BLS with 15% excess air (Adams and Frederick, 1988) and the average flow rate corresponding to the amount of flue gas is 390 m^3/s. In accordance with these data, the NH_3 concentration is 33-99 ppm. Pianpucktr (1995) reported that the nitrogen release during black liquor pyrolysis in a laminar entrained flow reactor was 58% of fuel nitrogen at the shortest residence time 0.3 s, at the temperature 1100 °C and that little N was released after this. So it could be assumed that all NH_3 had already been produced at the beginning of the residence time in reaction zone.

The NH_3 consumption was calculated by the rate equation of NH_3+O_2 catalyzed by Na_2CO_3. The rate of reaction based on weight of Na_2CO_3 was changed to be based on Na_2CO_3 surface area by dividing it with the BET surface area. The rate obtained is shown below:

$$-r''_{NH3} = 1.62*10^7 \text{ cm/s}* \text{EXP}((-20400 \text{ K})/T) *C_{NH3} \quad (5.4)$$

It was assumed that the fume droplets and the flue gas had the same velocity (i.e. that the terminal velocity of the fume particles was zero), perfect radial mixing and no axial mixing. It was further assumed that all fume and NH_3 were produced instantaneously at the base of the reaction zone, and the structure and composition of fume were unchanged.

Integrating the rate equation yields NH_3 conversion as a function of temperature, total surface area of Na_2CO_3 (S_{Na2CO3}, cm^2/s), total flue gas flow rate (V_F, cm^3/s), and average residence time(t_{avg} , sec).

$$1.62*10^7 \text{ cm/s}* \text{EXP}((-20400 \text{ K})/T)\ S_{Na2CO3}\ t_{avg}\ /V_F = -\ln(1-X_{NH3}) \qquad (5.5)$$

The oxidation of NH_3 over Na_2CO_3 was found to consume 29% of NH_3 at the average residence time from char bed to the tertiary air port (1.3 s). The conversion obtained indicates that the rate of NH_3 oxidation catalyzed by fume compounds even though leading to a measured conversion may not be fast enough to account for the conversion of NH_3 in recovery boilers. In fact, most of NH_3 is believed to be converted to other N compounds rapidly in the lower part of a recovery boiler. So this suggests that there could be other dominant reactions to efficiently consume NH_3 in a recovery boiler.

This rough estimation may be useful for a comparison of the importance of NH_3 with other possible reactions. Examples of competing reactions are char catalyzed reactions, and gas phase reactions.

The validity of the estimation is discussed in the following paragraph. A significant source of uncertainty in the model is the extrapolation of the kinetic data from 750 ° to 1100 °C. The mechanism of the reaction and thus the rate may be considerably

different at 1100 °C. Fume is solid at 750 °C and molten at 1100 °C which make a possible change in the reaction mechanism. The conditions in the boiler were assumed to be constant with respect to temperature, gas flow, and fume amount and composition, All of these vary with the location in the boiler. For reaction rate estimation, the use of an average temperature often leads to serious errors, because of the exponential temperature depending of the reaction rates. The assumptions of an average fume amount and composition may not be as detrimental to the estimation. The location of NH_3 release in the boiler may neither be as important. The validity of the assumption of the gas flow and patterns in the boiler are also essential for the accuracy of the estimation.

So to make this estimation more realistic a computational fluid dynamics model preferably including fume and generation models should be used, such model are currently developed (Grace, 1995). A study of the reaction over molten fume is also needed to give the real kinetic data.

5.6 Sources of Error

The measurement of NH_3 concentration was the major source of error in these experiments. One reason was that NH_3 can easily be adsorbed on the surface of gas lines or sampling system. Even though heating tape was used to warm part of the lines, some of NH_3 might have been lost in the experimental system. The other reason was a use of a different path of gas flow when the inlet and outlet concentration of NH_3 were measured (flow through by-pass or reactor). Due to the flow rotameter inaccuracies, and

the difficulty of adjustments of the constant flow. The inlet concentrations with gas flows through the by-pass and the reactor may not have been the same. In most cases, the calculation and the measured inlet concentration were within 10%.

Errors in the values of NH_3 concentration caused variations in the conversion data (X_{NH3}) which were used to obtain the reaction kinetics. The estimation of these errors is shown in Appendix H. The relative error of X_{NH3} is related to the absolute error of the inlet concentration of NH_3 ($\Delta C_{NH3,o}$) and that of the outlet concentration of NH_3(ΔC_{NH3}). The value of $\Delta C_{NH3,o}$ is depend on the absolute errors of the rotameters (5% of the flow rate in the rotameter) and that of the concentration in the gas cylinder used (1% of the concentration in cylinder). The value of ΔC_{NH3} depends on the absolute error of the NH_3 measurement (5% of outlet NH_3 concentration).

The reaction in which more rotameters were used have larger errors in conversion data. In the reaction of NH_3, only one rotameter was used, in the NH_3+O_2 two rotameters, in the NH_3+NO three rotameters, and in the NH_3+O_2+NO four of them. For the reaction of NH_3, the highest relative error in X_{NH3} was 100% found at the lowest X_{NH3} (6%), and the lowest relative error was 20% at the highest X_{NH3} (25%). For the reaction of NH_3+O_2, the highest relative error of X_{NH3} was 150% at the lowest X_{NH3} (4%), and the lowest relative error found at the highest X_{NH3} (92%) was 1%. For the reaction of NH_3+NO, the highest relative error found was 550% at NH_3 conversion of 2%, and the lowest relative error found was 27% at 30% NH_3 conversion. For the NH_3+O_2+NO, the highest relative error found was 220% at 5% conversion of NH_3,

while the lowest was 1% found at the 96% NH_3 conversion. The calculation results suggested that there were high relative errors at low NH_3 conversion.

CHAPTER 6
CONCLUSIONS AND RECOMMENDATIONS FOR FUTURE WORK

6.1 Conclusions

The catalytic effect of recovery boiler fume compounds on NH_3 decomposition, NH_3 oxidation by NO, NH_3 oxidation by O_2, and NH_3 oxidation by O_2 and NO were studied in the temperature range 550-750 °C. The gas inlet were NH_3 115-500 ppm for the NH_3 reaction, NH_3 150-400 ppm and NO 250-1250 ppm for the NH_3+NO reaction, NH_3 250 ppm and 500 ppm with 1% O_2 for the NH_3+O_2 reaction, NH_3 250 ppm and NO 250 ppm with 1% O_2 for the NH_3+O_2+NO reaction at a total flow rate 6.3-13.0 cm^3/s, 25 °C. The amounts of Na_2CO_3 ranged from 0.38-3.0±0.1 g and that of Na_2SO_4 were 3.0±0.1 g. The conclusions from the study are stated as follows:

1. The reactions of NH_3 consumption over Na_2CO_3 occurred significantly at 600-750 °C. In the presence of O_2, the highest NH_3 conversions of the reactions (NH_3+O_2 and NH_3+O_2+NO) were almost 100% at 750 °C, while the conversions were 26%, and 25-30% for those without O_2 (NH_3 and NH_3+NO).

2. The effect of Na_2SO_4 on the studied reactions was insignificant at the experimental conditions. So only the kinetics of the reactions over Na_2CO_3 were obtained.

3. The rate of NH_3 disappearance in the reaction NH_3+NO was the same as that of NH_3 decomposition.

4. The reaction order with respect to NH_3 concentration of the NH_3 decomposition and the reaction NH_3+NO was 0.53 and the activation energy was 98±3 kJ/mol at 95% confidence interval in the temperature range studied.

5. NO in the reaction NH_3+NO was also consumed (up to 18% at 750 °C). The NO conversion was increased by an increase of NH_3.

6. The first order reaction with respect to NH_3 concentration was accepted for the reaction NH_3+O_2 and the reaction NH_3+O_2+NO in the temperature range studied. The activation energies were 170±23 kJ/mol and 185±42 kJ/mol (95% confidence interval), respectively.

7. For the reactions in the presence of O_2, the rate of NH_3 disappearance was also promoted by the presence of NO.

8. NO was produced in the reaction NH_3+O_2. The average fraction of NH_3 reacted that formed NO was 0.28 at the temperature range 600-700 °C and 0.35 at 750 °C.

9. NO disappearance in the reaction NH_3+O_2+NO was highest at 650-700 °C. At 750 °C, the conversion decreased possibly due to an increase in NO production in the reaction.

10. A simple model for the estimation of the importance of the reactions gave an NH_3 conversion of 29%. This suggests that other reactions of NH_3 consumption maybe significant.

6.2 Recommendations for the Future Work

The recommendations for future studies are as follows:

- Study NH_3 oxidation over other catalysts found in recovery boilers such as black liquor char. Estimate the importance of the reactions in the recovery boiler.

- Study NH_3 oxidation by molten and gas phase fume compounds in laminar entrained flow reactor.

- Use of a computational fluid dynamics to predict the importance of the reactions in recovery boiler.

BIBLIOGRAPHY

Adams, T.N., Frederick, W.J., "Kraft Recovery Boiler Physical and Chemical Processes", American Paper Institute, NY, 1988.

Adams, T.N., Jones, A.K., and Stewart, R. I., Tappi 1993 Engineering Conference Proceedings, TAPPI PRESS, Atlanta, p.625.

Aho, K., Hupa, M., and Nikakanen, S., Tappi Engineering Conference, in press, 1994.

Aho, K., Hupa, M., and Nikakanen, S., "Fuel Nitrogen Release During Black Liquor Pyrolysis , Part II: Comparisons Between Different Liquors", Tappi Journal, Vol. 77, No.8, p.182, 1994.

"An Analysis of Kraft recovery Furnace NO_X Emissions and Related Parameters," NCASI Technical Bulletin NO.636, July, 1992.

Austin, G.T., "Shreve's Chemical Process Industries", 5th edition, Mc Graw Hill, p. 619,1984

Backman, R., Hupa, M., and Uusikartano,"Kinetic of Sulphation of Sodium Carbonate in Flue Gas", 1985 International Chemical Recovery, p445-450.

Boonsongsup, L., M.S. Thesis, Oregon State University, September, 1993.

Borg, A., Teder, A., and Warnqvist, B., Tappi Journal, Vol. 57, No.1, p.126-129, 1974.

Bowman, C.T., "Chemistry of Gaseous Pollutant Formation and Destruction.", Fossil Fuel combustion: A Source Book (W. Bartok and A.F. Sorofim, Eds.), John Wiley & Sons, NY, 1991.

Cameron, J.H., Clay, D.T., and Grace, T.M., "Oxidative fuming-the phenomenon and possible interpretations," Tappi/CPPA 1985 International Chemical Recovery Conference, p435-444, New Orleans, LA,1985.

Cameron, J.H.,"Fume generation in kraft recovery boilers," PIMA, p 32-34,1986, referenced by Adams, T.N., and Frederick, W.J., 1988.

Cameron, J.H., Chem. Eng. Comm., Vol. 59, p 243-257, 1988, referenced by Adams, T.N., and Frederick, W.J., 1988.

Cameron J.H., Vaporization from alkali carbonate melts," JPPS, in press, 1988, referenced by Adams, T.N., and Frederick, W.J., 1988.

Carangal A., M.S. Thesis, Oregon State University, September 1994.

Flagan, R.C., and Seinfeld J.H., "Fundamentals of Air Pollution Engineering, Prentice Hall, Inc., Englewood Cliffs, NJ, 1988, reference by Carangal, 1994.

Fogler, H.S., "Elements of Chemical Reaction Engineering", 2nd edition, Prentice Hall, NJ, p.625-635, 1992.

Forssen M., Hupa M., Pettersson R., and Martin D., 1995 International Chemical Recovery Conference,Toronto, Canada.

Frederick, W.J., and Hupa, M., Tappi Journal, Vol. 74, No. 11, p.192-194, 1991.

Grace, T.M., "A Critical Review of Computer Modeling of Kraft Recovery Boilers", Tappi 1995 Engineering Conference, TAPPI PRESS, Dallas.

Grace, T.M., Cameron, J.H., and Clay, D.T., "Char Burning", Project 3473-6 Report, The institute of Paper Chemistry, 1985, referenced by Adams, T.N., and Frederick, W.J., 1988.

Holland, C.D., and Anthony, R.G., "Fundamentals of Chemical Reaction Engineering", 2nd edition, Prentice-Hall International Series, p.51-52, 1989.

Iisa, K., Carangal, A., Scott, A., Pianpucktr, R., and Tangpanyapinit, V., International Chemical Recovery Furnaces, Toronto, Canada, 1995.

Kubota, H., and Ikeda, N., Kagaku Kagaku, Vol. 27, p.373, 1963.

Levenspiel, O., "Chemical Reaction Engineering", 2nd edition,Wiley International Edition, p.483-485, 1972.

Martin, D.M., Malcolm, E.W., Hupa, M., Eastern state sections, The Combustion Institue, Fall Technical Meeting Proceedings, FL, 1994.

McCabe, W.L., Smith, J.C., and Harriott, P., "Unit Operation of Chemical Engineering", 5th edition, Mc Graw Hill, p.670 and 672, 1993.

Mikkanen, E.I., Kaupinnen, Jokiniemi, J.K., Singquefield, S.A., Frederick, W.J., and Mäkinen, M., AIChe SYPOSIUM SERIES, Vol. 90, No. 302,1994

Nichols, K.M., Thompson, L.M., and Empie, H.J., "A Review of NO_X Formation Mechanisms in Recovery Furnaces", Tappi Journal, Vol. 76, No. 3, 1993.

Pianpucktr, R., M.S. Thesis, Oregon State University, September, 1995.

Rizhinshvili, G.V., and Kaplun, L.V., Bummazh. Prom. (Moscow), Vol. 1, p.26, Available Inst. Paper Chemical Translation No. T-2260 referenced by Cameron, J.H., Clay, D.T., and Grace, T.M., 1985.

Sarofim, A.F., and Beer, J.M., 17th Symposium (International) on Combustion, The Combustion Institute, Pittsburgh, PA, p.189, 1979, reference by Wu, S.L.,1994.

Seinfeld, J.H., "Air Pollution: Physical and Chemical Fundamentals", John Wiley & Son, NY, 1974.

Sricharoenchaikul, V., M.S. Thesis, Oregon State University, February, 1995.

Verrill, C.L., Grace, T.M., and Nichols K.M., J. Pulp Paper Sci. (in press), 1994.

Verrill, C.L., and Nichols, K.M., AIChE SYPOSIUM SERIES 1994, Vol.90, No. 302

Veverka P.J., Nichols K.M., Horton R.R., Adams T.N., 1993 Tappi Environmental Conference, Boston, MA., p.B239, reference by Forssen M., Hupa M., Pettersson R., and Martin D., 1995 International Chemical Recovery Conference,Toronto, Canada.

Wark, K., and Warner, C.F., "Air Pollution: Its Origin and Control, 2nd Edition. Harper and Row Publisher, Inc, NY, 1981.

Welty, J.R., Wicks, C.E., and Wilson, R.E., "Fundamentals of Momentum, Heat, and Mass Transfer", 3rd edition, Wiley International Edition, p.487-488, 1984.

Yoshida, F., Ramaswami, O., and Hougen, O.A., AIChe J., Vol. 8, No.1, p.5, 1962.

APPENDICES

APPENDIX A
FLOWMETER CALIBRATIONS

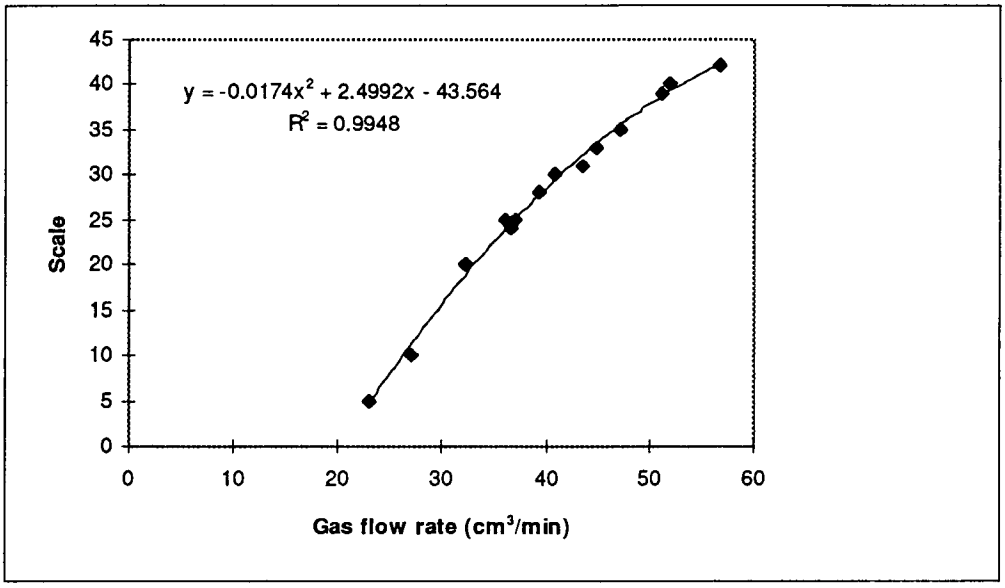

Figure A.1 N062-01 st Flowmeter Calibration curve (Air)

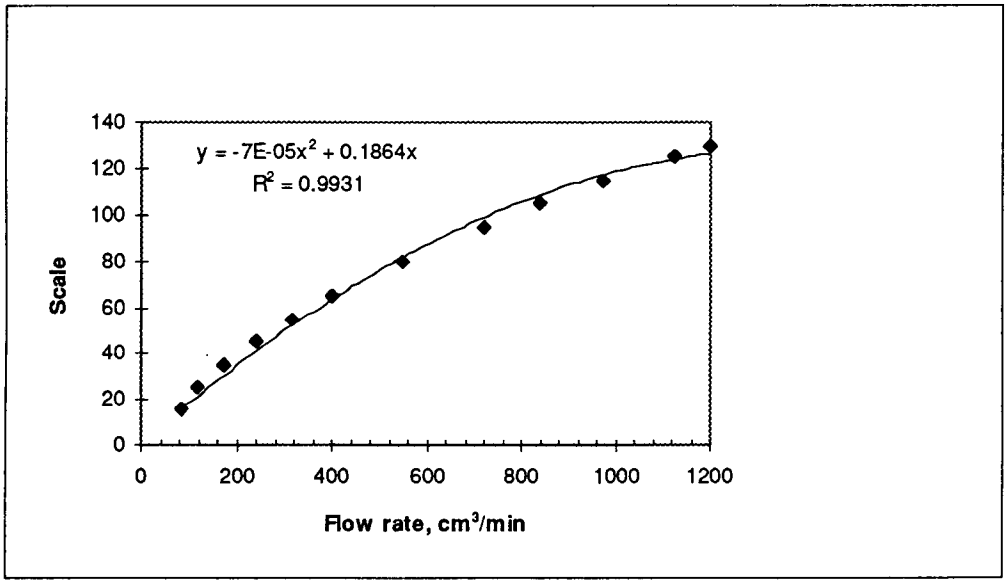

Figure A.2 N112-02 st Flowmeter Calibration curve (He)

APPENDIX B
FT-IR CALIBRATIONS

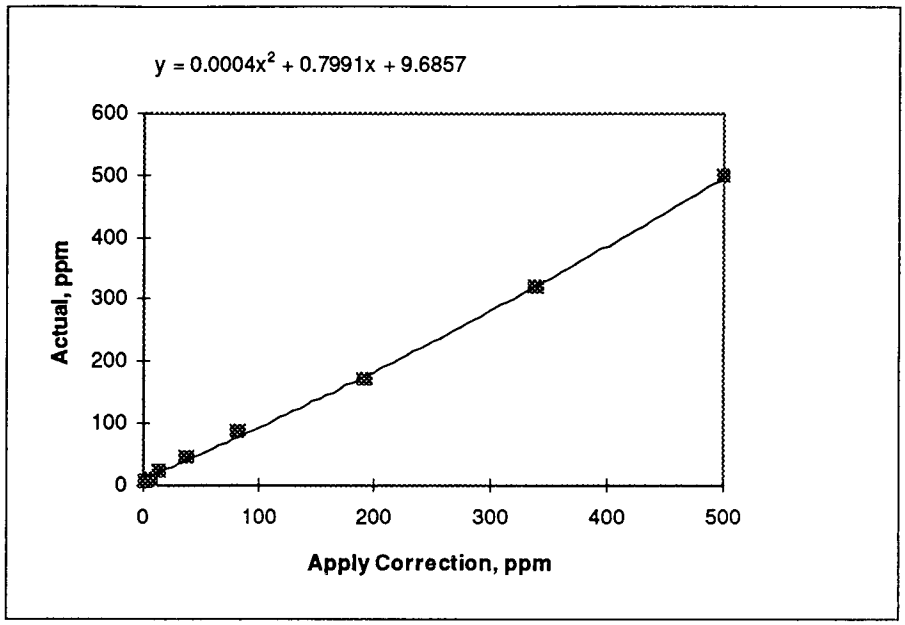

Figure B.1 NO FT-IR calibration curve

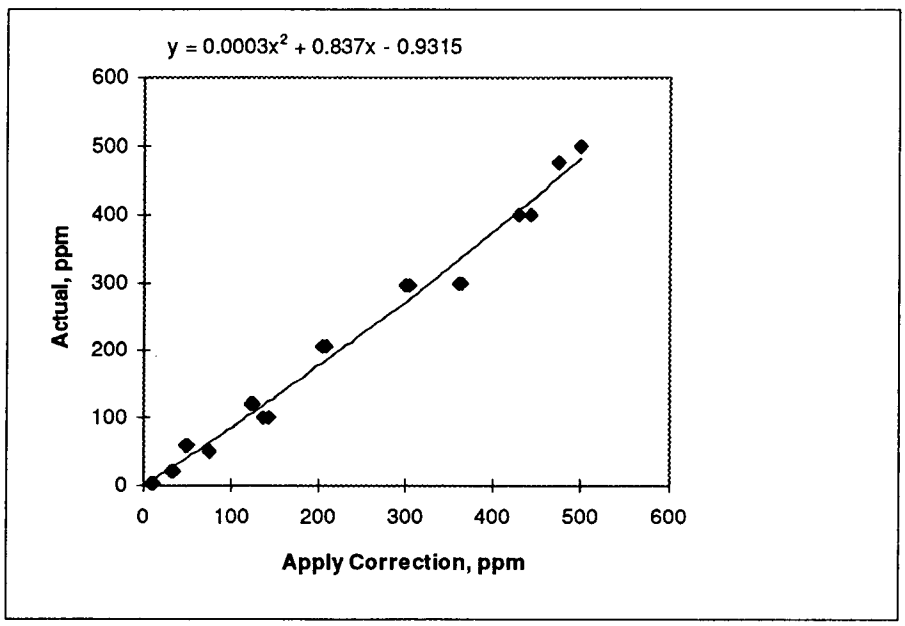

Figure B.2 NH_3 FT-IR calibration curve

The concentrations were measured by Apply Correction mode from FT-IR.

APPENDIX C
NH_3 REACTION RATE CALCULATION ($-r'_{NH3}$)

For a differential reactor, the NH_3 consumption rate can be calculated from

$$-r'_{NH3,ave} = F_{NH3,o} * X_{NH3} / W$$

where $-r'_{NH3,ave}$ = rate of reaction of NH_3, mol/gs

W = weight of the catalyst used in the fixed bed, g

$F_{NH3,o}$ = NH_3 feed rate, mol/s

$$= P*V'*C'_{NH3,o}*10^{-6}/(R*298\ K)$$

V' = total gas volumetric flow rate, cm^3/s at 25 °C

P = total pressure, atm

R = ideal gas constant = 82.05 cm^3.atm/(mol.K)

$C'_{NH3,o}$ = inlet concentration of NH_3, ppm

C'_{NH3} = outlet concentration of NH_3, ppm

X_{NH3} = NH_3 conversion

$$= (C'_{NH3,o} - C'_{NH3}) / C'_{NH3,o}$$

Data: from the reaction of NH_3

V' = 12.7 cm^3/s at 25 °C P = 1 atm

W = 3.08 g $C'_{NH3,o}$ = 453 ppm

C'_{NH3} = 340 ppm, at reaction temperature of 750 °C

So, $F_{NH3,o}$ = 1 atm *12.7 cm^3/s*453 ppm*10^{-6}

/(82.05 cm^3.atm/(mol.K)* 298 K)

= $2.35*10^{-7}$ mol/s

$X_{NH3} = 0.25$

$-r'_{NH3,ave} = 2.35*10^{-7}$ mol/s*0.25/3.08 g

$= 1.91*10^{-8}$ mol/gs

For integral reactor, observed rate reaction of NH_3 can be calculated from for first order reaction;

$-r'_{NH3,obs} = k'_{,obs}*C_{NH3}$, mol/gs

where

$k'_{,obs}$ = observed reaction rate constant, cm^3/s

C_{NH3} = concentration of NH_3, mol/cm^3

$= P*C'_{NH3}*10^{-6}/(R*T)$

T = temperature of experiment, °C

Data: for the reaction of NH_3+O_2

$k'_{,obs} = 64.5\ cm^3/s$ P = 1 atm T = 1023 K

$C'_{NH3,o} = 479$ ppm

So, $C_{NH3,o} = 1$ atm*479ppm*10^{-6}/(82.05 cm^3.atm/(mol.K)* 1023 K)

$= 5.7*10^{-9}$ mol/cm^3

$-r'_{NH3} = 64.5\ cm^3/s * 5.7*10^{-9}$ mol/cm^3

$= 3.68*10^{-7}$ mol/gs (this is an initial observed rate of reaction)

APPENDIX D
DIFFUSION COEFFICIENTS CALCULATION

1. Binary Gas Mixture Diffusivities

The diffusion of NH_3 in mixture gas is considered as the binary gas diffusion becasue of the dilute concentrations of all reactants in the inert gas (He). For the the diffusion of binary gas at low to moderate pressures, the Hirschfelder equation is a well known theoretical equation to estimate the diffusion coefficient for the system (Welty et al.,1984).

$$D_{NH3-He} = \frac{0.001858 * T^{\frac{3}{2}} * \left[\frac{1}{M_{NH3}} + \frac{1}{M_{He}}\right]^{\frac{1}{2}}}{P * \sigma^2_{NH3-He} * \Omega_D} \qquad (D.1)$$

Where D_{NH3-He} = diffusion coefficient, cm^2/s

M_{NH3} = molecular weight of NH_3 = 17

M_{He} = molecular weight of He = 4

P = absolute pressure, atm

T = temperature, K

σ_{NH3-He} = collision diameter or Lennard-Jones length, Å

Ω_D = collision integral*

Note (*) Ω_D is a function of $\kappa T/\varepsilon_{NH3-He}$

where κ = Boltzmann constant = $1.38*10^{-23}$ J/K

ε_{NH3-He} = the energy of molecular interaction for NH_3-He or Lennard-Jones energy, J

Both values of $\sigma_{NH3\text{-}He}$ and $\varepsilon_{NH3\text{-}He}$ are obtained empirically from the Lennard-Jones parameters of the pure component which are given by:

$$\sigma_{NH3\text{-}He} = (\sigma_{NH3}+\sigma_{He})/2,\ \varepsilon_{NH3\text{-}He} = (\varepsilon_{NH3}*\varepsilon_{He})^{1/2} \qquad (D.2)$$

2. Diffusivities in Porous Solids

2.1) Knudsen diffusion

Knudsen diffusion occurs when molecules of gas collide for more frequently with the walls of a porous solid than with other gas species. The diffusivity for Knudsen diffusion is described by Equation (D.3).

$$D_{NH3-K} = 9700 * r_e * \left(\frac{T}{M_{NH3}}\right)^{\frac{1}{2}} \qquad (D.3)$$

where $D_{NH3\text{-}K}$ = Knudsen diffusion coefficient, cm^2/s

r_e= average pore radius, cm

T = temperature, K

M_{NH3} = molecular weight of NH_3 = 17

2.2) Effective diffusivities in porous materials

For diffusion of gas in a porous material, the effective diffusion coefficient is defined by:

$$\frac{1}{D_{NH3-eff}} = \frac{\tau_m}{\varepsilon_a} * \left(\frac{1}{D_{NH3-He}} + \frac{1}{D_{NH3-K}}\right) \qquad (D.4)$$

where $D_{NH3\text{-}eff}$ = effective diffusion coefficient, cm^2/s

ε_a = total void fraction in packed bed

τ_m = average for the tortuosity of pores of variety of size

$= 1/\varepsilon_a$

Data: T = 1023 K P = 1 atm

$\sigma_{NH3} = 2.90$ Å $\sigma_{He} = 2.56$ Å

$\varepsilon_{NH3}/\kappa = 558.3$ K $\varepsilon_{He}/\kappa = 10.2$ K

$\varepsilon_a = 0.6$ $r_e = 52.3*10^{-8}$ cm

So, $\sigma_{NH3\text{-}He} = 2.73$ Å $\varepsilon_{NH3\text{-}He}/\kappa = 75.5$ K $\kappa T/\varepsilon_{NH3\text{-}He} = 13.5$

$\Omega_D = 0.719$, (Welty et al.,1984).

The results of diffusion coefficients obtained are:

$$D_{NH3\text{-}He} = 0.001858*(1023)^{3/2}*[1/17+1/4]^{1/2}/(1*2.73^2*0.719)$$

$$= 6.32 \text{ cm}^2/\text{s}$$

$$D_{NH3\text{-}K} = 9700*(52.3*10^{-8})*(1023/17)^{1/2}$$

$$= 0.039 \text{ cm}^2/\text{s}$$

$$D_{NH3\text{-}eff} = (0.6)^2/(1/6.32+1/0.039) = 0.0141 \text{ cm}^2/\text{s}$$

APPENDIX E
FILM MASS TRANSFER EFFECT

The significance of the film mass transfer effect to the rate of reaction can be tested by using the Mears' criterion (Fogler, 1992). The effect of film mass transfer can be neglected if

$$\frac{-r'_{NH3,obs} * \rho_b * R * n}{k_c * C_{NH3,o}} < 0.15 \qquad (E.1)$$

where $-r'_{NH3,obs}$ = observed rate of NH_3 consumption, mol/gs

ρ_b = bulk density of packed bed, g/cm^3

R = particle radius, cm

n = reaction order

k_c = mass transfer coefficient, cm/s

$C_{NH3,o}$ = concentration of NH_3 in bulk flow, mol/cm^3

The mass transfer coefficient (k_c) is calculated from the mass transfer correlation for packed bed (Yoshida et al., 1962):

$$Sh' = 0.84*(Re')^{0.49}*(Sc)^{1/3} \quad \text{for } 0.01<Re<50 \qquad (E.2)$$

Equation (E.2), when expaned is

$$\left[\frac{k_c * d_p}{D_{NH3-He}}\right] * \left(\frac{\varepsilon_b}{1-\varepsilon_b}\right) * \frac{1}{\gamma} = 0.84 * \left[\frac{U * d_p * \rho_{He}}{\mu_{He} * (1-\varepsilon_b) * \gamma}\right]^{0.49} * \left[\frac{\mu_{He}}{\rho_{He} * D_{NH3-He}}\right]^{\frac{1}{3}}$$

where $Re' = Re/[(1-\varepsilon_b)*\gamma]$

$Sh' = Sh*\varepsilon_b/[(1-\varepsilon_b)*\gamma]$

ε_b = macro void fraction of packed bed

k_c = mass transfer coefficient, cm/s

$D_{NH3\text{-}He}$ = diffusion coefficient, cm^2/s

γ = shape factor

U = superficial velocity of gas flow in packed bed, cm/s

= Vol. gas flow rate at 1073K/ A_c

A_c = cross sectional area of fixed bed = 1.33 cm^2

ρ_{He} = bulk density of gas, g/cm^3

μ_{He} = viscosity of gas, g/cms

d_p = diameter of particle,cm

Data: $\varepsilon_b = 0.6$ $D_{NH3\text{-}He} = 6.32\ cm^2/s$ $\gamma = 1$

$\rho_{He} = 4.79*10^{-5}\ g/cm^3$, $\mu_{He} = 4.1*10^{-4}$ g/cms, at 1atm 1073 K

$d_p = 1.08*10^{-2}$ cm $\rho_b = 0.97\ g/cm^3$ U = 31.7 cm/s

$C_{NH3,o} = 5.7*10^{-9}\ mol/cm^3$ $-r'_{NH3,obs} = 3.68*10^{-7}$ mol/gs

n = 1

Equation (E.2) yields:

k_c = 118 cm/s

So the Mears' criterion = $3.68*10^{-7}$ mol/gs*0.97g/cm^3*(1.08*10^{-2} cm)/2/118cm/s

/$5.7*10^{-9}\ mol/cm^3$

= 0.0028 < 0.15

APPENDIX F
PORE DIFFUSION EFFECT

The effect of pore diffusion can be tested by the Weisz-Prater criterion given by:

$$C_{wp} = \frac{-r'_{NH3,obs} * \rho_p * L^2}{D_{NH3,eff} * C_{NH3,s}} \qquad (F.1)$$

(Fogler et al., 1992)

where C_{wp} = Weisz-Prater criterion number

$D_{NH3\text{-}eff}$ = effective diffusivity , cm^2/s =0.0141 cm^2/s

$C_{NH3,s}$ = concentration of NH_3 at the external surface area of particle, mol/cm^3

L = characteristic length of particle, cm

= R/3 for spherical particle

R = radius of particle, cm

ρ_p = density of the particle, g/cm^3

$-r'_{NH3,obs}$ = observed reaction rate of NH_3 , mol/gs

The pore diffusion can be ignored if $C_{wp} << 1$

Data: $R = 54*10^{-4}$ cm $\rho_p = 2.53$ g/cm^3

$C_{NH3} = 5.7*10^{-9}$ mol/cm^3 $-r'_{NH3} = 3.68*10^{-7}$ mol/gs

$D_{NH3\text{-}eff} = 0.0141$ cm^2/s

So, $C_{wp} = 3.68*10^{-7}$ mol/gs$*2.53$ $g/cm^3*(54*10^{-4}$ cm$/3)^2/0.0141$ cm^2/s

$*5.7*10^{-9}$ mol/cm^3

$= 0.037 << 1$

APPENDIX G
THE ESTIMATION OF THE EFFECT OF Na_2CO_3 ON NH_3 OXIDATION IN A RECOVERY BOILER

The data (shown in Table G.1) of the general layout of a recovery boiler, typical operation conditions, and feeding materials were used in the estimation.

1. Average Residence Time of Flue Gas in the Reaction Zone

The reaction zone is defined from the char bed surface to the tertiary air port of the recovery boiler. Typically, the char bed height is 1-3 m from the furnace floor (average 2 m). So the average residence time(t_{ave}, s) in the reaction zone is obtained by:

$$t_{ave} = (h_{3rd\ air} - h_{char\ bed})/V_{F,ave}$$

$$= (8\text{-}2)\ m/4.7\ m/s = 1.3\ s$$

2. Fume Compounds Characteristics and Amount of Fume Formed

At the flue gas temperature of 1373 K, the fume compounds within the reaction zone are assumed to be molten droplets with a diameter of 0.7 μm. The surface area of one droplet (s_D) estimated from the surface of a sphere of the same size is $1.54*10^{-8}$ cm^2 /droplet and the volume of the droplet (v_D) is $1.8*10^{-13}$ cm^3/droplet.

If the fume droplets are composed of only Na_2CO_3, the weight per droplet can be calculated by:

$$w_{Na2CO3} = \rho_{Na2CO3} * v_D$$

where w_{Na2CO3} = weight per droplet of Na_2CO_3, g/droplet

Table G.1 Data of typical recovery boiler for the estimation (Adams and Frederick, 1988).

Recovery boiler General Layout		**Reference page**
Furnace height (h_F), m.	31	176
Furnace crossectional area (A_f), m^2	79	176
Tertiary air port height above floor, ($h_{3rd\ air}$), m.	8	18
Feeding materials		
1. Kraft Black Liquor (BL)		22
Dry solids (% of BL), (BLS)	65	
Na (% of BLS)	18.6	
N(% of BLS)	0.11	Nichols et al.,1993
2. Make-up Saltcake, kg/100 kg BLS	3	22
Na (%)	32.4	
3. Air (15% excess of stoichiometric air), kg/100 kg BLS	524	27
Operating conditions		
Hearth loading, (G_f/A_f), kg BLS/s.m^2	0.18	175
Black liqour firing rate, (G_f), kg BLS/s	14.22	
Flue gas produced, (M_F), kg/100 kg BLS	663.5	27
Flue gas molecular weight, (M_{wF}), g/mol	27.3	174
Furnace gas temperature, (T_F), K	1373	175
Stoichiometric air, (kg/ kg BLS)	4.56	175
Average furnace gas velocity, ($v_{F,ave}$), m/s	4.7	175

ρ_{Na2CO3} = density of molten Na_2CO_3

= 1.864 g/cm^3 at 1373 K (Janz et al.,1968)

So, $w_{Na2CO3} = 1.864\ g/cm^3 * 1.8*10^{-13}\ cm^3$

$= 3.36*10^{-13}$ g/droplet

Borg et al.(1974) suggested that approximately 9% of Na fired in the boiler contributes to fume formation.

Total Na input = the amount of Na in 100 kg BLS + the amount of Na in 3 kg Make-up salt cake

= 18.6 kg + 0.324*3 kg = 19.6 kg Na/100 kg BLS

Amount of Na contributed to fume = 0.09*19.6 kg Na/100 kgBLS

= 1.76 kg Na/100 kg BLS

Total amount Na input in a recovery boiler per second (Na_{fume})

= 1.76 kg Na/100 kg BLS*G_f = 1.76 kg Na/100 kg BLS*14.22 kg BLS/s

= 0.251 kg Na/s

In the reaction zone, the average fraction of Na_2CO_3 in fume was found to be 68%. So the fraction of Na_{fume} that is Na_2CO_3, is calculated as follows:

$Na_{fume,Na2CO3}$ = 0.68*0.251 kg Na/s= 0.171 kg Na/s

Molecular weight of Na (M_{Na}) = 22.99 kg/kmol

moles of $Na_{fume,Na2CO3}$ = 0.171 kg Na/s/22.99 kg/kmol Na

= 0.0074 kmol Na/s

moles of $Na_2CO_{3,fume}$ = 0.0074 kmol Na/s/2 kmol Na/kmol Na_2CO_3

= 0.0037 kmol Na_2CO_3/s

Molecular weight of Na_2CO_3 = 105.8 kg/kmol

Thus, the amount of Na_2CO_3 generated is:

W_{Na2CO3} = 0.0037 kmol Na_2CO_3/s*105.8 kg/kmol

= 0.391 kg/s or 391 g/s

Total number of droplets generated (no_{Na2CO3}) is equal to:

$$no_{Na2CO3} = W_{Na2CO3}/ w_{Na2CO3}$$

$$= 391 \text{ g/s}/3.36*10^{-13} \text{ g/droplet} = 1.164*10^{15} \text{ droplets/s}$$

Total surface area available (S_{Na2CO3}) is:

$$S_{Na2CO3} = s_D * no_{Na2CO3}$$

$$= 1.54*10^{-8} \text{ cm}^2/\text{droplet}*1.164*10^{15} \text{ droplets/s}$$

$$= 1.8*10^{7} \text{ cm}^2/\text{s}$$

3. NH_3 Concentration in the Reaction Zone

For 100 kg of black liquor solid (BLS) with 15% excess of stoichimetric air

Total moles of flue gas produced = M_F/ M_{wF}

= 663.5 kg flue gas/100kg BLS/27.3 kg flue gas/kmol

= 24.3 kmol/100 kgBLS

Total moles of flue gas produced per second = 24.3 kmol/100 kgBLS*14.22 kg BLS/s

= 3.46 kmol/s

Total volume of flue gas produced per second, V_F

= 3.46 kmol/s*82.05 L.atm/(kmol.K)*1373K/1 atm

= 390,000 L/s or 390 m^3/s

Typical average nitrogen content in BLS = 0.11 wt.% (Nichols et al.,1993)

So, N_{fuel} = 0.0011*100 kg BLS = 0.11 kg N/100 kg BLS

where N_{fuel} = nitrogen contained in the fuel (black liquor solid)

10-30 % of nitrogen in BLS will be transformed to NH_3 during pyrolysis in black liqour combustion (Aho et al.,1994).

With the 30% conversion; $N_{fuel} \rightarrow NH_3$ = 0.11 kg N/100 kg BLS*0.3

= 0.033 kg N/100 kg BLS

(Molecular weight of N = 14 kg/kmol)

or NH_3 produced = 0.033 kg N/100 kg BLS/14 kg/kmol

= 0.0024 kmol/100 kg BLS

With the 10% conversion; NH_3 produced = 0.0008 kmol/100 kg BLS

So the concentration of NH_3 formed (C'_{NH3}, ppm) will be:

C'_{NH3} = 0.0024 kmol NH_3/100 kg BLS/24.3 kmol flue gas/100 kg BLS *1*10^{-6}

= 99 ppm

to = 0.0008 kmol NH_3/100 kg BLS/24.3 kmol flue gas/100 kg BLS *1*10^{-6}

= 33 ppm

4. NH_3 Conversion in the Reaction Zone

4.1) The effect of mass trasfer rate in the reaction zone

First the condition within the reaction zone is tested for the effect of mass transfer to limit the rate of NH_3 comsumption.

Assumption: 1.The molten droplet is small enough to have the same coefficients for mass transfer as a solid particle.

2. The droplet is entrained in the flue gas and the terminal velocity of the droplet is zero.

For a solid particle in stagnant gas:

$$Sh = k_c D_p / D_V = 2$$

where Sh = Sherwood number

k_c = External mass transfer coefficient (m/s)

Dp = Droplet diameter (m)

D_V = Gas diffusivity (m^2/s)

(McCabe et al., 1993)

Data: $D_p = 0.7*10^{-6}$ m

D_V = approximate from $D_{NH3,AIR}$ at 1373 K

$= 3.3*10^{-4}$ m^2/s

(the method of calculation is the same as shown in Appendix E.)

So, $k_c = 2*3.3*10^{-4}$ $m^2/s / 0.7*10^{-6}$ m = 943 m/s

The rate of the NH_3+O_2 reaction with Na_2CO_3 is used to represent NH_3 oxidation in the reaction zone

Assumption 1.The reaction mechanism is the same at 1100 °C as at 600-750 °C

2.Activation energy(E) and frequency factor (k_o) change insignificantly from 550 °C to 1100 °C

At temperature = 1373 K,

the rate constant based on the weight of catalyst,

$$k' = 2.93*10^{10}\ cm^3/g_{cat}.s\ *EXP((-20400\ K)/T)$$

Dividing by the BET surface area of the Na_2CO_3 used in the experiments ($0.1808*10^4$ cm^2_{cat}/g_{cat}) gives the rate constant based on surface area of Na_2CO_3.

$$k'' = 2.93*10^{10}\ cm^3/g_{cat}.s\ *EXP((-20400\ K)/T)/0.1808*10^4\ cm^2_{cat}/g_{cat}$$

$$= 1.62*10^7\ cm/s*\ EXP((-20400\ K)/T)$$

$$= 5.72\ cm/s \quad \text{at } 1373\ K$$

Assuming the reaction occurs at the external surface area of the droplets only, we can directly compare k_c to k"

From the results of calculation:

$$k_c >> k"_{Na2CO3}$$

So the rate controlling step is the chemical reaction NH_3+O_2.

4.2) The conversion of NH_3 in the reaction zone

The rate of NH_3 comsumption by the NH_3+O_2 reaction at 1373 K based on the surface area of Na_2CO_3 ,$-r"_{NH3}$ is:

$$-r"_{NH3} = -1/S_{Na2CO3} * (dN_{NH3}/dt) = -V_F/S_{Na2CO3} * (dC_{NH3}/dt)$$

$$= k"_{Na2CO3}*C_{NH3} \quad , mol/cm^2\ s$$

Where (dN_{NH3}/dt) = rate of mole NH_3 change, mol/s

C_{NH3} = concentration of NH_3, mol/cm^3

V_F = total volume of flue gas = 390 m^3/s or $390*10^6$ cm^3/s

S_{Na2CO3} = total surface area of Na_2CO_3 = $1.8*10^7$ cm^2/s

Assumption 1.Cocurrent plug flow of solids and gas with residence time 1.3 s

2. at t = 0, $X_{NH3} = 0$

Integrating the reaction rate expression from t = 0 to t_{ave} and $C_{NH3} = C_{NH3,o}$ to C_{NH3} results:

$$-\ln(1-X_{NH3}) = k"* S_{Na2CO3}*t_{ave}/V_F$$

With the residence time of 1.3 s

$$-\ln(1-X_{NH3}) = 5.72\ cm/s*1.8*10^7 cm^2/s\ *1.3\ s/(390*10^6\ cm^3/s)$$

So, $X_{NH3} = 0.29$

The conversion of NH_3 by oxidation of NH_3 over Na_2CO_3 is 29% or 10 ppm to 29 ppm NH_3 is consumed in the reaction zone by the reaction.

APPENDIX H
MAXIMUM RELATIVE ERROR IN NH_3 DATA

1. Error in the Measurement of NH_3 Concentration

The inlet concentration of NH_3 is calculated by:

$$C_{NH3,o} = C_{NH3,cyd.} * R_2/R_T$$

Where $C_{NH3,o}$ = the inlet concentration of NH_3 , ppm

$C_{NH3,cyd.}$ = the standard concentration of NH_3 in gas cylinder, ppm

R_2 = NH_3 flow rate of rotameter#2, cm^3/min

R_T = Total gas flow rate, cm^3/min

= $R_1+...+R_n$ (n = rotameter#1, #2, #3, #4 depending on rotameter(s) used in each reaction): NH_3, $R_T = R_2$

NH_3+O_2, $R_T = R_2+R_3$

NH_3+NO, $R_T = R_1+R_2+R_4$

NH_3+O_2+NO, $R_T = R_1+R_2+R_3+R_4$

rotameter#1 : used for NO , rotameter#2 : used for NH_3

rotameter#3 : used for air , rotameter#4 : used for He

Data $C_{NH3,cyd}$ = 501 ppm

$\Delta C_{NH3,cyd}$ = absolute error of NH_3 concentration in gas cylinder (±1%)

= 5 ppm

ΔR_n = absolute error of gas flow rate caused by the rotameter used (±5%)

= $0.05*R_n$, cm^3/min where n =1,2,3,4

At standard conditions

NH_3 reaction

$C_{NH3,o}$ = 501 ppm

Absolute error of $C_{NH3,o}$ ($\Delta C_{NH3,o}$) is calculated by:

$$\Delta C_{NH3,o} = \Delta C_{NH3,cyd}$$

$$= 5 \text{ ppm}$$

NH_3+O_2 reaction

R_2 = 746 cm^3/min, ΔR_2 = 37 cm^3/min

R_3 = 37 cm^3/min, ΔR_3 = 2 cm^3/min

$R_T = R_2+R_3$ = 783 cm^3/min

$C_{NH3,o}$ = 501 ppm*746 cm^3/min/783 cm^3/min = 478 ppm

$$\Delta C_{NH3,o} = \left|\frac{R_2}{R_T}\right| * \Delta C_{NH3,cyd} + \left|\frac{C_{NH3,cyd} * (R_T - R_2)}{R_T^2}\right| * \Delta R_2 + \left|\frac{-C_{NH3,cyd} * R_2}{R_T^2}\right| * \Delta R_3$$

$$= \left|\frac{746\frac{cm^3}{min}}{783\frac{cm^3}{min}}\right| * 5ppm + \left|\frac{501ppm * (783-746)\frac{cm^3}{min}}{(783\frac{cm^3}{min})^2}\right| * 37\frac{cm^3}{min} + \left|\frac{-501ppm * 746\frac{cm^3}{min}}{(783\frac{cm^3}{min})^2}\right| * 2\frac{cm^3}{min}$$

$$= 7 \text{ ppm}$$

NH_3+NO reaction

R_1 = 91 cm^3/min, ΔR_1 = 5 cm^3/min

R_2 = 376 cm^3/min, ΔR_2 = 19 cm^3/min

R_4 = 285 cm^3/min, ΔR_4 = 14 cm^3/min

$R_T = R_1+R_2+R_4$ = 752 cm^3/min

$C_{NH3,o}$ = 501 ppm*376 cm^3/min/752 cm^3/min = 251 ppm

$$\Delta C_{NH3,o} = \left|\frac{R_2}{R_T}\right| * \Delta C_{NH3,cyd} + \left|\frac{C_{NH3,cyd} * (R_T - R_2)}{R_T^2}\right| * \Delta R_2 + \left|\frac{-C_{NH3,cyd} * R_2}{R_T^2}\right| * \Delta R_1$$

$$+ \left|\frac{-C_{NH3,cyd} * R_2}{R_T^2}\right| * \Delta R_4$$

$$= \left|\frac{376\frac{cm^3}{min}}{752\frac{cm^3}{min}}\right| * 5ppm + \left|\frac{501ppm * (752-376)\frac{cm^3}{min}}{(752\frac{cm^3}{min})^2}\right| * 19\frac{cm^3}{min} + \left|\frac{-501ppm * 376\frac{cm^3}{min}}{(752\frac{cm^3}{min})^2}\right| * 5\frac{cm^3}{min}$$

$$+ \left|\frac{-501ppm * 376\frac{cm^3}{min}}{(752\frac{cm^3}{min})^2}\right| * 14\frac{cm^3}{min}$$

$$= 16 \text{ ppm}$$

$$\Delta C_{NH3} = 0.05 * 251 \text{ ppm} = 13 \text{ ppm}$$

<u>NH_3+O_2+NO reaction</u>

$R_1 = 91$ cm^3/min, $\Delta R_1 = 5$ cm^3/min

$R_2 = 376$ cm^3/min, $\Delta R_2 = 19$ cm^3/min

$R_3 = 37$ cm^3/min, $\Delta R_3 = 2$ cm^3/min

$R_4 = 285$ cm^3/min, $\Delta R_4 = 14$ cm^3/min

$R_T = R_1+R_2+R_3+R_4 = 789$ cm^3/min

$C_{NH3,o} = 501$ ppm*376 cm^3/min/789 cm^3/min = 238 ppm

$$\Delta C_{NH3,o} = \left|\frac{R_2}{R_T}\right| * \Delta C_{NH3,cyd} + \left|\frac{C_{NH3,cyd} * (R_T - R_2)}{R_T^2}\right| * \Delta R_2 + \left|\frac{-C_{NH3,cyd} * R_2}{R_T^2}\right| * \Delta R_1$$

$$+ \left|\frac{-C_{NH3,cyd} * R_2}{R_T^2}\right| * \Delta R_3 + \left|\frac{-C_{NH3,cyd} * R_2}{R_T^2}\right| * \Delta R_4$$

$$= \left|\frac{376\frac{cm^3}{min}}{789\frac{cm^3}{min}}\right| * 5ppm + \left|\frac{501ppm*(789-376)\frac{cm^3}{min}}{(789\frac{cm^3}{min})^2}\right| * 19\frac{cm^3}{min} + \left|\frac{-501ppm*376\frac{cm^3}{min}}{(789\frac{cm^3}{min})^2}\right| * 5\frac{cm^3}{min}$$

$$+ \left|\frac{-501ppm*376\frac{cm^3}{min}}{(789\frac{cm^3}{min})^2}\right| * 2\frac{cm^3}{min} + \left|\frac{-501ppm*376\frac{cm^3}{min}}{(789\frac{cm^3}{min})^2}\right| * 14\frac{cm^3}{min}$$

$$= 15 \text{ ppm}$$

Absolute error of the outlet concentration of NH_3 (ΔC_{NH3}) is 5% of C_{NH3}:

$$\Delta C_{NH3} = 0.05* (1-X_{NH3})*C_{NH3,o}$$

2. Error in the NH_3 Conversion

Absolute error of NH_3 conversion is calculated by:

$$\Delta X_{NH3} = \left|\frac{(1-X_{NH3})}{C_{NH3,o}}\right| * \Delta C_{NH3,o} + \left|\frac{-1}{C_{NH3,o}}\right| \Delta C_{NH3}$$

Maximum relative error of NH_3 conversion is given by:

$$Error_{rel.} = \Delta X_{NH3}/X_{NH3}*100\%$$

<u>NH_3 reaction</u>

at 650 °C, $X_{NH3} = 0.06$ (which is the lowest conversion obtained)

ΔX_{NH3} = (1-0.06)/501ppm*5ppm+0.05*(1-0.06)*501ppm/501ppm = 0.06

$Error_{rel.}$ = 0.06/0.06*100% = 100%

at 750 °C, $X_{NH3} = 0.25$ (which is the highest concentration obtained)

ΔX_{NH3} = (1-0.25)/501ppm*5ppm+0.05*(1-0.25)*501ppm/501ppm = 0.05

$Error_{rel.}$ = 0.05/0.25*100% = 20%

<u>NH_3+O_2 reaction</u>

at 550 °C, X_{NH3} = 0.04

ΔX_{NH3} = (1-0.04)/478ppm*7ppm+0.05*(1-0.04)*478ppm/478ppm = 0.06

$Error_{rel.}$ = 0.06/0.04*100% = 150%

at 750 °C, X_{NH3} = 0.92

ΔX_{NH3} = (1-0.92)/478ppm*7ppm+0.05*(1-0.92)*478ppm/478ppm = 0.01

$Error_{rel.}$ = 0.01/0.92*100% = 1%

<u>NH_3+NO reaction</u>

at 550 °C, X_{NH3} = 0.02

ΔX_{NH3} = (1-0.02)/251ppm*16ppm+0.05*(1-0.02)*251ppm/251ppm = 0.11

$Error_{rel.}$ = 0.11/0.02*100% = 550%

at 750 °C, X_{NH3} = 0.30

ΔX_{NH3} = (1-0.30)/251ppm*16ppm+0.05*(1-0.30)*251ppm/251ppm = 0.08

$Error_{rel.}$ = 0.08/0.30*100% = 27%

<u>NH_3+O_2+NO reaction</u>

at 550 °C, X_{NH3} = 0.05

ΔX_{NH3} = (1-0.05)/238ppm*15ppm+0.05*(1-0.05)*238ppm/238ppm = 0.11

$Error_{rel.}$ = 0.11/0.05*100% = 220%

at 750 °C, X_{NH3} = 0.96

ΔX_{NH3} = (1-0.96)/238ppm*15ppm+0.05*(1-0.96)*238ppm/238ppm = 0.01

$Error_{rel.}$ = 0.01/0.96*100% = 1%

APPENDIX I
EXPERIMENTAL DATA

Experimental Condition			
Empty bed Reaction			
Reaction :	NH_3		
Total gas flow rate:		12.7	cm^3/s
Pressure:	1 atm		
$NH_{3,inlet}$ (ppm)	494		
Temperature	file.name	$NH_{3,outlet}$	
(°C)		ppm	
650	VT48	500	
750	VT47	469	

Experimental Condition			
Empty bed Reaction			
Reaction :	NH_3		
Total gas flow rate:		12.7	cm^3/s
Pressure:	1 atm		
$NH_{3,inlet}$ (ppm)	497		
Temperature	file.name	$NH_{3,outlet}$	
(°C)		ppm	
700	GT3	475	
	GT4	486	
750	GT5	476	

Experimental Condition			
Empty bed Reaction			
Reaction :	NH_3+NO		
Total gas flow rate:		12.5	cm^3/s
Pressure:	1 atm		
$NH_{3,inlet}$ (ppm)	233		
$NO_{,inlet}$ (ppm)	228		
Temperature	file.name	$NH_{3,outlet}$	NO_{outlet}
(°C)		ppm	ppm

550	VT63	232	206
	VT64	237	213
650	VT61	232	224
	VT62	232	226
750	VT59	210	218
	VT60	207	221

Experimental Condition			
Empty bed Reaction			
Reaction :	NH_3+O_2		
Total gas flow rate:		12.6	cm^3/s
Pressure:	1 atm		
$NH_{3,inlet}$ (ppm)	498		
O_2	1%		
Temperature	file.name	$NH_{3,outlet}$	NO_{outlet}
(°C)		ppm	ppm
550	VT55	513	-
	VT56	518	
650	VT53	498	-
	VT54	500	
750	VT51	471	-
	VT52	459	

Experimental Condition			
Empty bed Reaction			
Reaction :	NH_3+O_2+NO		
Total gas flow rate:		13.2	cm^3/s
Pressure:	1 atm		
$NH_{3,inlet}$ (ppm)	233		
$NO_{,inlet}$ (ppm)	274		
O_2	1%		
Temperature	file.name	$NH_{3,outlet}$	NO_{outlet}
(°C)		ppm	ppm
550	VT71	226	273
	VT72	235	274
650	VT69	228	274
	VT70	229	277
750	VT67	197	262
	VT68	197	255

Experimental Condition			
Material:	Na_2CO_3		
Weight =	3.07	g	
Particle size =	90-125 μm		
Reaction :	NH_3		
Total gas flow rate:		12.7	cm^3/s
Pressure:	1 atm		
$NH_{3,inlet}$ (ppm)	451		
Temperature	file.name	$NH_{3,outlet}$	
(°C)		ppm	
700	AK27	407	
	AK28	385	
750	AK29	342	
	AK30	338	

Experimental Condition			
Material:	Na_2CO_3		
Weight =	3.09	g	
Particle size =	90-125 μm		
Reaction :	NH_3		
Total gas flow rate:		12.7	cm^3/s
Pressure:	1 atm		
$NH_{3,inlet}$ (ppm)	455		
Temperature	file.name	$NH_{3,outlet}$	
(°C)		ppm	
550	KT3	450	
	KT4	457	
650	KT5	429	
	KT6	429	
750	KT7	336	
	KT8	336	

Experimental Condition			
Material:	Na_2CO_3		
Weight =	3.08	g	
Particle size =	90-125 μm		
Reaction :	NH_3		

Total gas flow rate:		12.6	cm^3/s
Pressure:	1 atm		
$NH_{3,inlet}$ (ppm)	243		
Temperature	file.name	$NH_{3,outlet}$	
(°C)		ppm	
750	KT10	161	
	KT11	160	

Experimental Condition			
Material:	Na_2CO_3		
Weight =	3.08	g	
Particle size =	90-125 μm		
Reaction :	NH_3		
Total gas flow rate:		12.7	cm^3/s
Pressure:	1 atm		
$NH_{3,inlet}$ (ppm)	115		
Temperature	file.name	$NH_{3,outlet}$	
(°C)		ppm	
750	KT13	66	
	KT14	60	

Experimental Condition			
Material:	Na_2CO_3		
Weight =	3.09	g	
Particle size =	90-125 μm		
Reaction :	NH_3		
Total gas flow rate:		12.6	cm^3/s
Pressure:	1 atm		
$NH_{3,inlet}$ (ppm)	274		
Temperature	file.name	$NH_{3,outlet}$	
(°C)		ppm	
750	HK25	205	
	HK26	196	

Experimental Condition			
Material:	Na_2CO_3		
Weight =	3.05	g	
Particle size =	90-125 μm		
Reaction :	NH_3+NO		
Total gas flow rate:		12.5	cm^3/s
Pressure:	1 atm		
$NH_{3,inlet}$ (ppm)	230		
$NO_{,inlet}$ (ppm)	261		
Temperature	file.name	$NH_{3,outlet}$	NO_{outlet}
(°C)		ppm	ppm
544	VT75	236	268
	VT76	237	269
594	VT77	233	262
	VT78	231	262
644	VT79	221	240
	VT80	215	243
694	VT81	200	239
	VT82	197	241
742	VT83	192	231
	VT84	192	232

Experimental Condition			
Material:	Na_2CO_3		
Weight =	3.07	g	
Particle size =	90-125 μm		
Reaction :	NH_3+NO		
Total gas flow rate:		12.5	cm^3/s
Pressure:	1 atm		
$NH_{3,inlet}$ (ppm)	228		
$NO_{,inlet}$ (ppm)	222		
Temperature	file.name	$NH_{3,outlet}$	NO_{outlet}
(°C)		ppm	ppm
700	V37	184	201
	V38	190	199
750	V39	169	180
	V40	170	185

Experimental Condition			
Material:	Na_2CO_3		
Weight =	3.09	g	
Particle size =	90-125 μm		
Reaction :	NH_3+NO		
Total gas flow rate:		12.5	cm^3/s
Pressure:	1 atm		
$NH_{3,inlet}$ (ppm)	242		
$NO_{,inlet}$ (ppm)	227		
Temperature	file.name	$NH_{3,outlet}$	NO_{outlet}
(°C)		ppm	ppm
750	zk3	173	187
	zk4	170	189

Experimental Condition			
Material:	Na_2CO_3		
Weight =	3.09	g	
Particle size =	90-125 μm		
Reaction :	NH_3+NO		
Total gas flow rate:		12.5	cm^3/s
Pressure:	1 atm		
$NH_{3,inlet}$ (ppm)	236		
$NO_{,inlet}$ (ppm)	212		
Temperature	file.name	$NH_{3,outlet}$	NO_{outlet}
(°C)		ppm	ppm
750	zk41	165	180
	zk42	165	179

Experimental Condition			
Material:	Na_2CO_3		
Weight =	3.09	g	
Particle size =	90-125 μm		
Reaction :	NH_3+NO		
Total gas flow rate:		12.6	cm^3/s
Pressure:	1 atm		
$NH_{3,inlet}$ (ppm)	344		
$NO_{,inlet}$ (ppm)	243		
Temperature	file.name	$NH_{3,outlet}$	NO_{outlet}
(°C)		ppm	ppm

750	zk7	265	185
	zk8	264	183
Experimental Condition			
Material:	Na_2CO_3		
Weight =	3.09	g	
Particle size =	90-125 μm		
Reaction :	NH_3+NO		
Total gas flow rate:		12.6	cm^3/s
Pressure:	1 atm		
$NH_{3,inlet}$ (ppm)	412		
$NO_{,inlet}$ (ppm)	226		
Temperature	file.name	$NH_{3,outlet}$	NO_{outlet}
(°C)		ppm	ppm
750	zk11	318	142
	zk12	312	141

Experimental Condition			
Material:	Na_2CO_3		
Weight =	3.09	g	
Particle size =	90-125 μm		
Reaction :	NH_3+NO		
Total gas flow rate:		12.6	cm^3/s
Pressure:	1 atm		
$NH_{3,inlet}$ (ppm)	159		
$NO_{,inlet}$ (ppm)	222		
Temperature	file.name	$NH_{3,outlet}$	NO_{outlet}
(°C)		ppm	ppm
750	zk49	100	225
	zk50	106	215

Experimental Condition			
Material:	Na_2CO_3		
Weight =	3.09	g	
Particle size =	90-125 μm		
Reaction :	NH_3+NO		
Total gas flow rate:		12.6	cm^3/s
Pressure:	1 atm		
$NH_{3,inlet}$ (ppm)	250		
$NO_{,inlet}$ (ppm)	322		
Temperature	file.name	$NH_{3,outlet}$	NO_{outlet}
(°C)		ppm	ppm

750	zk15	175	260
	zk16	175	262

Experimental Condition			
Material:	Na_2CO_3		
Weight =	3.09	g	
Particle size =	90-125 μm		
Reaction :	NH_3+NO		
Total gas flow rate:		12.6	cm^3/s
Pressure:	1 atm		
$NH_{3,inlet}$ (ppm)	248		
$NO_{,inlet}$ (ppm)	451		
Temperature	file.name	$NH_{3,outlet}$	NO_{outlet}
(°C)		ppm	ppm
750	zk19	167	399
	zk20	175	396

Experimental Condition			
Material:	Na_2CO_3		
Weight =	3.09	g	
Particle size =	90-125 μm		
Reaction :	NH_3+NO		
Total gas flow rate:		12.6	cm^3/s
Pressure:	1 atm		
$NH_{3,inlet}$ (ppm)	239		
$NO_{,inlet}$ (ppm)	1253		
Temperature	file.name	$NH_{3,outlet}$	NO_{outlet}
(°C)		ppm	ppm
750	zk45	160	1181
	zk46	156	1186

Experimental Condition			
Material:	Na_2CO_3		
Weight =	3.05	g	
Particle size =	90-125 μm		
Reaction :	NH_3+O_2+NO		
Total gas flow rate:		13.2	cm^3/s
Pressure:	1 atm		
$NH_{3,inlet}$ (ppm)	243		
$NO_{,inlet}$ (ppm)	247		
O_2	1%		
Temperature	file.name	$NH_{3,outlet}$	NO_{outlet}

(°C)		ppm	ppm
544	VT87	237	233
	VT88	235	234
594	VT89	206	222
	VT90	213	222
644	VT91	148	204
	VT92	144	204
694	VT93	48	210
	VT94	41	210
744	VT95	3	236

Experimental Condition			
Material:	Na_2CO_3		
Weight =	3.05	g	
Particle size =	90-125 μm		
Reaction :	NH_3+O_2+NO		
Total gas flow rate:		13.2	cm^3/s
Pressure:	1 atm		
$NH_{3,inlet}$ (ppm)	225		
$NO_{,inlet}$ (ppm)	196		
O_2	1%		
Temperature	file.name	$NH_{3,outlet}$	NO_{outlet}
(°C)		ppm	ppm
700	AK31	33	172
	AK32	33	173
750	AK33	0	195
	AK34	0	195

Experimental Condition			
Material:	Na_2CO_3		
Weight =	3.10	g	
Particle size =	90-125 μm		
Reaction :	NH_3+O_2+NO		
Total gas flow rate:		13.2	cm^3/s
Pressure:	1 atm		
$NH_{3,inlet}$ (ppm)	215		
$NO_{,inlet}$ (ppm)	206		
O_2	1%		
Temperature	file.name	$NH_{3,outlet}$	NO_{outlet}
(°C)		ppm	ppm
550	HK11	205	198

	HK12	205	198

Experimental Condition			
Material:	Na_2CO_3		
Weight =	1.54	g	
Particle size =	90-125 μm		
Reaction :	NH_3+O_2+NO		
Total gas flow rate:		13.2	cm^3/s
Pressure:	1 atm		
$NH_{3,inlet}$ (ppm)	223		
$NO_{,inlet}$ (ppm)	230		
O_2	1%		
Temperature	file.name	$NH_{3,outlet}$	NO_{outlet}
(°C)		ppm	ppm
751	ko19	8	233
	ko20	7	230

Experimental Condition			
Material:	Na_2CO_3		
Weight =	0.78	g	
Particle size =	90-125 μm		
Reaction :	NH_3+O_2+NO		
Total gas flow rate:		13.2	cm^3/s
Pressure:	1 atm		
$NH_{3,inlet}$ (ppm)	241		
$NO_{,inlet}$ (ppm)	236		
O_2	1%		
Temperature	file.name	$NH_{3,outlet}$	NO_{outlet}
(°C)		ppm	ppm
751	ko39	43	241
	ko40	38	241

Experimental Condition			
Material:	Na_2CO_3		
Weight =	0.78	g	
Particle size =	90-125 μm		
Reaction :	NH_3+O_2+NO		
Total gas flow rate:		26.0	cm^3/s
Pressure:	1 atm		
$NH_{3,inlet}$ (ppm)	235		
$NO_{,inlet}$ (ppm)	277		

O_2	1%		
Temperature	file.name	$NH_{3,outlet}$	NO_{outlet}
(°C)		ppm	ppm
751	ko43	66	286
	ko44	67	287

Experimental Condition			
Material:	Na_2CO_3		
Weight =	0.38	g	
Particle size =	90-125 μm		
Reaction :	NH_3+O_2+NO		
Total gas flow rate:		13.2	cm^3/s
Pressure:	1 atm		
$NH_{3,inlet}$ (ppm)	239		
$NO_{,inlet}$ (ppm)	217		
O_2	1%		
Temperature	file.name	$NH_{3,outlet}$	NO_{outlet}
(°C)		ppm	ppm
751	ko27	96	218
	ko28	80	218

Experimental Condition			
Material:	Na_2CO_3		
Weight =	3.09	g	
Particle size =	90-125 μm		
Reaction :	NH_3+O_2		
Total gas flow rate:		13.2	cm^3/s
Pressure:	1 atm		
$NH_{3,inlet}$ (ppm)	475		
O_2	1%		
Temperature	file.name	$NH_{3,outlet}$	NO_{outlet}
(°C)		ppm	ppm
550	VT15	455	4
	VT16	460	4
600	VT17	406	20
	VT18	402	19
650	VT19	292	54
	VT20	293	54
700	VT29	111	104
	VT30	113	108
750	VT31	8	159

	VT32	6	159

Experimental Condition			
Material:	Na_2CO_3		
Weight =	3.09	g	
Particle size =	90-125 μm		
Reaction :	NH_3+O_2		
Total gas flow rate:		13.2	cm^3/s
Pressure:	1 atm		
$NH_{3,inlet}$ (ppm)	503		
O_2	1%		
Temperature	file.name	$NH_{3,outlet}$	NO_{outlet}
(°C)		ppm	ppm
542	AK3	455	4
	AK4	479	4
642	AK7	356	46
	AK8	351	40
742	AK21	292	182
	AK22	293	186

Experimental Condition			
Material:	Na_2CO_3		
Weight =	3.09	g	
Particle size =	90-125 μm		
Reaction :	NH_3+O_2		
Total gas flow rate:		13.2	cm^3/s
Pressure:	1 atm		
$NH_{3,inlet}$ (ppm)	492		
O_2	1%		
Temperature	file.name	$NH_{3,outlet}$	NO_{outlet}
(°C)		ppm	ppm
542	BK1	478	4
	BK2	470	4
592	BK5	440	19
	BK6	440	19
642	BK7	344	50

Experimental Condition			
Material:	Na_2CO_3		
Weight =	3.07	g	
Particle size =	90-125 μm		
Reaction :	NH_3+O_2		

Total gas flow rate:		12.6	cm^3/s
Pressure:	1 atm		
$NH_{3,inlet}$ (ppm)	471		
O_2	1%		
Temperature	file.name	$NH_{3,outlet}$	NO_{outlet}
(°C)		ppm	ppm
750	AK43	6	163
	AK44	2	168

Experimental Condition			
Material:	Na_2CO_3		
Weight =	3.0	g	
Particle size =	90-125 μm		
Reaction :	NH_3+O_2		
Total gas flow rate:		12.8	cm^3/s
Pressure:	1 atm		
$NH_{3,inlet}$ (ppm)	494		
O_2	1%		
Temperature	file.name	$NH_{3,outlet}$	NO_{outlet}
(°C)		ppm	ppm
542	ko1	474	5
	ko2		
592	ko3	417	22
	ko4		
642	ko5	302	60
	ko6		
692	ko7	132	108
	ko8		
742	ko9	12	140
	ko10		

Experimental Condition			
Material:	Na_2CO_3		
Weight =	3.09	g	
Particle size =	90-125 μm		
Reaction :	NH_3+O_2		
Total gas flow rate:		13.2	cm^3/s
Pressure:	1 atm		
$NH_{3,inlet}$ (ppm)	256		
O_2	1%		
Temperature	file.name	$NH_{3,outlet}$	NO_{outlet}
(°C)		ppm	ppm

550	HK3	254	2
600	HK4	221	6
650	HK5	151	26
	HK6	143	28
700	HK7	46	55
	HK8	41	49
750	HK9	6	94
	HK10	2	98

Experimental Condition			
Material:	Na_2CO_3		
Weight =	3.09	g	
Particle size =	90-125 μm		
Reaction :	NH_3+O_2		
Total gas flow rate:		12.5	cm^3/s
Pressure:	1 atm		
$NH_{3,inlet}$ (ppm)	230		
O_2	1%		
Temperature	file.name	$NH_{3,outlet}$	NO_{outlet}
(°C)		ppm	ppm
642	AK15	145	22
	AK16	135	21

Experimental Condition			
Material:	Na_2CO_3		
Weight =	3.09	g	
Particle size =	90-125 μm		
Reaction :	NH_3+O_2		
Total gas flow rate:		12.5	cm^3/s
Pressure:	1 atm		
$NH_{3,inlet}$ (ppm)	495		
O_2	1%		
Temperature	file.name	$NH_{3,outlet}$	NO_{outlet}
(°C)		ppm	ppm
642	BK19	349	39
	BK20	351	38
	BK27	325	42

Experimental Condition		

Material:	Na_2CO_3		
Weight =	3.09	g	
Particle size =	90-125 μm		
Reaction :	NH_3+O_2		
Total gas flow rate:		12.5	cm^3/s
Pressure:	1 atm		
$NH_{3,inlet}$ (ppm)	224		
O_2	1%		
Temperature	file.name	$NH_{3,outlet}$	NO_{outlet}
(°C)		ppm	ppm
642	BK17	133	20
	BK18	135	20

Experimental Condition			
Material:	Na_2CO_3		
Weight =	1.53	g	
Particle size =	90-125 μm		
Reaction :	NH_3+O_2		
Total gas flow rate:		12.5	cm^3/s
Pressure:	1 atm		
$NH_{3,inlet}$ (ppm)	229		
O_2	1%		
Temperature	file.name	$NH_{3,outlet}$	NO_{outlet}
(°C)		ppm	ppm
642	OK9	120	31
	OK10	118	31

Experimental Condition			
Material:	Na_2CO_3		
Weight =	1.53	g	
Particle size =	90-125 μm		
Reaction :	NH_3+O_2		
Total gas flow rate:		12.5	cm^3/s
Pressure:	1 atm		
$NH_{3,inlet}$ (ppm)	494		
O_2	1%		
Temperature	file.name	$NH_{3,outlet}$	NO_{outlet}
(°C)		ppm	ppm
750	MK15	68	150
	MK16	67	148

Experimental Condition			
Material:	Na_2CO_3		
Weight =	1.54	g	
Particle size =	90-125 μm		
Reaction :	NH_3+O_2		
Total gas flow rate:		12.5	cm^3/s
Pressure:	1 atm		
$NH_{3,inlet}$ (ppm)	489		
O_2	1%		
Temperature	file.name	$NH_{3,outlet}$	NO_{outlet}
(°C)		ppm	ppm
751	ko17	43	143
	ko18	30	143

Experimental Condition			
Material:	Na_2CO_3		
Weight =	0.78	g	
Particle size =	90-125 μm		
Reaction :	NH_3+O_2		
Total gas flow rate:		12.5	cm^3/s
Pressure:	1 atm		
$NH_{3,inlet}$ (ppm)	479		
O_2	1%		
Temperature	file.name	$NH_{3,outlet}$	NO_{outlet}
(°C)		ppm	ppm
751	ko33	110	114
	ko34	113	116

Experimental Condition			
Material:	Na_2CO_3		
Weight =	0.38	g	
Particle size =	90-125 μm		
Reaction :	NH_3+O_2		
Total gas flow rate:		12.5	cm^3/s
Pressure:	1 atm		
$NH_{3,inlet}$ (ppm)	493		
O_2	1%		
Temperature	file.name	$NH_{3,outlet}$	NO_{outlet}
(°C)		ppm	ppm
751	ko25	221	95

	ko26	215	95

Experimental Condition			
Material:	Na_2CO_3		
Weight =	1.53	g	
Particle size =	90-125 μm		
Reaction :	NH_3+O_2		
Total gas flow rate:		6.3	cm^3/s
Pressure:	1 atm		
$NH_{3,inlet}$ (ppm)	488		
O_2	1%		
Temperature	file.name	$NH_{3,outlet}$	NO_{outlet}
(°C)		ppm	ppm
750	MK3	27	124
	MK4	29	126
750	MK5	17	137
	MK6	18	140

Experimental Condition			
Material:	Na_2SO_4		
Weight =	3.08	g	
Particle size =	90-125 μm		
Reaction :	NH_3		
Total gas flow rate:		12.7	cm^3/s
Pressure:	1 atm		
$NH_{3,inlet}$ (ppm)	475		
Temperature	file.name	$NH_{3,outlet}$	
(°C)		ppm	
550	CK1	478	
	CK2	478	
650	CK3	458	
	CK4	465	
750	CK5	447	
	CK6	445	

Experimental Condition			
Material:	Na_2SO_4		
Weight =	3.08	g	
Particle size =	90-125 μm		

Reaction :	NH_3+O_2		
Total gas flow rate:		12.6	cm^3/s
Pressure:	1 atm		
$NH_{3,inlet}$ (ppm)	484		
O_2	1%		
Temperature	file.name	$NH_{3,outlet}$	NO_{outlet}
(°C)		ppm	ppm
550	CK9	486	-
	CK10	476	-
600	CK11	488	-
	CK12	483	-
650	CK13	483	1
	CK14	462	1
700	CK15	457	2
	CK16	457	2
750	CK17	406	6
	CK18	398	6

Experimental Condition			
Material:	Na_2SO_4		
Weight =	3.08	g	
Particle size =	90-125 μm		
Reaction :	NH_3+NO		
Total gas flow rate:		12.5	cm^3/s
Pressure:	1 atm		
$NH_{3,inlet}$ (ppm)	234		
$NO_{,inlet}$ (ppm)	210		
Temperature	file.name	$NH_{3,outlet}$	NO_{outlet}
(°C)		ppm	ppm
550	CK21	220	210
	CK22	229	209
600	CK23	239	217
	CK24	236	219
650	CK25	233	216
	CK26	231	222
700	CK27	225	211
	CK28	224	213
750	CK29	218	215
	CK30	214	214

Experimental Condition		